

**Andalusite in the South Mountain Batholith contact
aureole, Halifax NS:
A tale of two isograds**

Glenn G. Hart

**Submitted in partial fulfillment of the requirements
for the Degree of Bachelor of Science, Honours
Department of Earth Sciences
Dalhousie University, Nova Scotia,
April 2006**

Andalusite in the South Mountain Batholith contact aureole, Halifax NS: A tale of two isograds

Glenn Hart

Department of Earth Sciences, Dalhousie University, Halifax, NS, B3H 4J1
<glenn@dal.ca>

The contact aureole of the South Mountain Batholith cuts the Halifax Formation in the area of the Halifax peninsula. Isograds have been mapped based on outcrops on the Dalhousie University campus, railroad cuts, Point Pleasant Park and scattered outcrops and construction sites throughout the peninsula. Within the study area two lithological units are recognized based on contrasts in lithology, bulk composition and contact metamorphic mineral assemblages. The Cunard member is an aluminous, graphitic black slate with sparse metasiltstone layers and characteristic rusty weathering, which extends from the southeast side of the Dalhousie campus north to the Fairview area. The “Bluestone” member (informal name), which stratigraphically overlies the Cunard member, is a blue-grey slate with abundant metasiltstone layers and local calcareous concretions. It is exposed from the vicinity of Oakland Road to Point Pleasant Park, and underlies the Williams Lake area on the west side of the Northwest Arm. Prior to the intrusion of the South Mountain Batholith, the Halifax Formation was regionally deformed into NE-SW trending upright folding with associated slaty cleavage and a chlorite zone regional metamorphic assemblage. Contact metamorphism overprinted the chlorite zone assemblage and progressively annealed the slaty cleavage proximal to the contact. The outer limit of the aureole, about two kilometers from the contact, is defined by sparse cordierite “spots” in both the Cunard and Bluestone members. The biotite isograd, which is continuous between the Cunard and Bluestone members is marked by nucleation of biotite within the muscovite/chlorite stacks inherited from the regional metamorphism. Between the biotite-in isograd and the contact, the modal abundances of both cordierite and biotite increase in both units. In contrast, there is a striking difference in the texture and first occurrence of andalusite between the Cunard and Bluestone members. In the Cunard member idioblastic chiastolite appears after cordierite, but before biotite. Its early appearance is attributed to the reaction $Pg + Qtz \rightarrow And + Ab + L$. Crystal size and modal abundance increase towards the contact. In the less aluminous Bluestone member andalusite first appears as ovoid xenoblastic aggregates within 300 metres of the contact, probably as a result of the reaction $Ms + Crd \rightarrow And + Bt + Qtz + L$. Adjacent to the contact the assemblage $And + Crd + Kfs + Bt + Qtz \pm Sil$ (*Fibrolite*) is present in both the Cunard and Bluestone members. ThermoCalc P-T estimates show a pressure of 3.3 kb \pm 2.2 kb and a temperature of 645°C \pm 16°C nearest the contact and 551°C \pm 6°C at approximately 2km from the contact.

Keywords: contact metamorphism, isograds, metamorphic, petrology, mineral assemblage, chiastolite, andalusite, Halifax Formation, Meguma

Table of Contents

	Page
Abstract	ii
Table of contents	iii
List of Figures and tables	v
Acknowledgements	ix
Chapter 1: Introduction	1
1.1 Introduction	1
1.2 Regional Geology	2
1.3 Study area	5
1.4 Transects	7
1.5 Previous work in study area	7
1.6 Objectives and approach	9
Chapter 2: Lithology and Structure	11
2.1 Introduction	11
2.2 Meguma Group	11
2.3 Halifax Formation	11
2.3.1 Cunard member	12
2.3.2 Bluestone member	12
2.4 South Mountain Batholith	15
2.5 Regional Deformation and metamorphism	15
2.6 Summary	15
Chapter 3: Petrography	17
3.1 Introduction	17
3.2 Pre-contact metamorphism assemblages and textures	19
3.3 Transect 1: Bluestone member, Oakland Road to Williams Lake	20
3.3.1 Biotite Zone (2km from contact)	20
3.3.2 Andalusite zone (<1km from contact, Williams Lake area)	21
3.4 Transect 2: Cunard member, Dalhousie University to Dingle Park	23
3.4.1 Andalusite-in isograd (2km from contact)	23
3.4.2 Biotite zone (1.2km from contact)	23
3.4.3 Between the biotite zone to the contact	25
3.5 Transect 3: Cunard member, Bayers Road	25
3.5.1 Andalusite-in isograd (2km from contact)	25
3.5.2 Biotite zone (1.6km from contact)	30
3.5.3 Between the biotite zone to the contact	30
3.6 Summary of isograd sequences	30

	Page
Chapter 4: Chemistry	31
4.1 Introduction	31
4.2 Whole rock geochemistry	31
4.3 Mineral chemistry (microprobe)	33
4.3.1 Muscovite, Cunard member, below biotite-in isograd	34
4.3.2 Muscovite, Cunard member, above biotite-in isograd	37
4.3.3 Muscovite, Bluestone member, below biotite-in isograd	38
4.3.4 Muscovite, Bluestone member, above biotite-in isograd	39
4.3.5 Chlorite	40
4.3.6 Biotite	41
4.3.7 Feldspar	44
4.3.8 Andalusite	46
4.3.9 Cordierite	46
4.4 Powder X-ray Diffraction results	48
Chapter 5: P-T conditions and metamorphic reactions	49
5.1 Introduction	49
5.2 Reactions and P-T Grid	50
5.2.1 Biotite in	50
5.2.2 Andalusite C-in	51
5.2.3 Andalusite B-in	52
5.2.4 P-T Grid	53
5.2.5 Summary of isograds and reactions	53
5.3 P-T conditions	57
5.3.1 Constraints from P-T grid	57
5.3.2 P-T estimates using ThermoCalc	57
Chapter 6: Discussion and conclusions	59
6.1 Discussion	59
6.2 Conclusions	61
6.3 Suggestions for further work	62
References	63
Appendices	
Appendix I: Microprobe data	I. 67
Appendix II: Microprobe BSE images	II. 97
Appendix III: Maps	III. 115

List of Figures and Tables

	Page
Fig. 1.1:	4
A. Schematic regional geology map of Nova Scotia. Meguma Zone (color) with Avalon Zone (white). Study area highlighted in red.	
B. Simplified regional geological history	
C. Schematic study area geology map. Contact aureole isograds show first appearance of mineral designated. High-grade side always towards the SMB. Andalusite C = below biotite, andalusite-in isograd in Cunard Member. Andalusite B = above biotite, andalusite-in isograd in Bluestone member.	
D. Simplified study area geological history.	
Fig 1.2: Satellite imagery of study area from Google Earth with study area highlighted within polygon. Width is approximately 10 km. Shows location of Bluestone Quarry.	6
Fig 1.3: Schematic geological map of study area with transects and study area labeled. Line shows cross section area for Fig 1.4.	8
Fig 1.4: Simplified schematic diagram of upright folds within study area across line A-B in Fig 1.3. modified from (Horne and Culshaw 2001).	8
Fig 2.1: Cunard Member in downtown Halifax (building site next to Brewery Market). Sample location KBM05. Fissile, black slate, with small upright syncline/anticline (center/right).	13
Fig 2.2: Bluestone member, Point Pleasant Park. Sample location PPP04-9 (Black Rock). Note abundant siltstone layers, shown here on cleavage plane surface.	13
Fig 2.3: Worm borrows from sample collected from Point Pleasant Park, summer 2004.	16
Fig 2.4: Picture of Mahone Bay area Feltzen Member. Sample from Blue- Rocks, near Lunenburg, N.S..	16
Fig 3.1: Sample locations and transects referred to in this thesis.	18
Fig 3.2: Muscovite/chlorite stack from sample IB05-1. Chlorite is green in XN.	19
Fig 3.3: Biotite/muscovite stacks from sample location RSR04 (Bluestone member) within the biotite zone of Transect 1. Shows biotite / muscovite with chlorite / muscovite stacks.	21

Fig. 3.4: Ovoid, xenoblastic cordierite rimmed by muscovite and minor biotite below andalusite-in isograd (Bluestone member). Sample location PCR-10 (Purcell's Cove Road)	22
Fig. 3.5: Xenoblastic andalusite and quartz rimmed by biotite and minor muscovite above andalusite - in isograd (Bluestone member). Sample location WL04-3 (Williams Lake).	22
Fig. 3.6: Biotite/muscovite stacks from sample location BSUB-1 (Cunard member). Shows biotite / muscovite with chlorite / muscovite stacks	24
Fig. 3.7: Chialstolite from sample location IWK03 (Cunard member), below the biotite zone of transect 2. Shows chlorite / muscovite stacks, biotite absent.	24
Fig 3.8: Biotite/muscovite stacks from sample location BSUB-1 (Cunard Member). Bt/Ms stacks can co-exist with Chl/Ms stacks close to the biotite-in isograd, however Chl/Ms stacks disappear within ~700m towards the contact.	26
Fig 3.9: Chialstolite from sample location DP-2 (Cunard Member, close to contact), Transect 2. Shows biotite with an absence of Bt/Ms stacks. Minor fine grained muscovite in matrix, K-feldspar present.	26
Fig 3.10a: Chialstolite from sample HSC05-1 (Cunard Member), below the biotite zone of Transect 3. Biotite absent, matrix is highly altered with no identifiable chlorite/muscovite stacks. Andalusite is well formed and identifiable, cm scale at outcrop level. Andalusite is highly altered similar to IWK05, Transect 2.	27
Fig. 3.10b: Large chialstolite crystals in outcrop at sample location HSC05-1.	27
Fig. 3.11: Picture of RP05-1, transect 3, shows chlorite/muscovite stacks, biotite/muscovite stacks present. Chialstolite does not appear in this thin section.	28
Fig. 3.12: Chialstolite from sample AR05-2 (Cunard member, close to contact), transect 3. Shows biotite outside stacks. Minor fine grained muscovite in matrix.	28
Fig 3.13: Map showing isograd distribution and mineral assemblages within study area. This information compiled into a modified GEOfield database (Lipovsky et al 2003).	29
Table 4.1: Whole rock geochemistry analyses of study area rocks. Note variations in Carbon, Sulpher, SiO ₂ , and Al ₂ O ₃ content between Cunard and Bluestone samples.	32

- Fig 4.2:** AFM diagram of bulk analysis of Halifax area rocks. Cunard samples include HH Dark, HH Light (silty Cunard) for comparison to Bluestone. Andalusite not present in Bluestone samples or HH Light. 32
- Fig. 4.3:** BSE image of sample MBd, Cunard Member, andalusite in isograd. Chlorite/muscovite intergrowths in a quartz/muscovite matrix. 33
- Fig 4.4:** Paragonite/muscovite solvus. 100% muscovite on right. Highlighted range of paragonite (8%-43% in Cunard). Horizontal line marks maximum temperatures within contact aureole. Vertical lines lie on range of temperatures which would allow for Pa content present (600°C-1050°C). (Modified from Eugster et al 1972) 35
- Fig. 4.5:** Paragonite content vs. distance from contact approximate isograd locations overlain. Distances in km are relative to the nearest surface expression of the SMB. Average paragonite content is higher within Cunard samples in vicinity of Andalusite C and drops towards contact. $Mol\% Pa = Na/(Na+K+Ca)$ 36
- Fig. 4.6:** False colour BSE image of sample AR05-1, Cunard Member, close to contact. Muscovite shows large idioblastic crystals with little to no intergrowths. Chlorite is not present. 37
- Fig 4.7:** False colour BSE image of sample IB04-1, Bluestone member, low grade zone (> 2km from contact). Chlorite/muscovite intergrowths in a quartz/muscovite matrix. Similar to low grade Cunard samples. 38
- Fig 4.8:** False colour BSE image of sample WL05-4, Bluestone member, high grade zone (< 500 m from contact). Symplectic intergrowth between muscovite and K-feldspar located near point 258. 39
- Fig. 4.9:** False colour BSE image LSCN, Cunard member, Dalhousie campus (2000 m from contact). Intergrowths of biotite with chlorite and muscovite. 42
- Fig. 4.10:** Biotite rims around andalusite in high-grade WL04-3, Bluestone member. 42
- Fig. 4.11:** Graph showing Mg/Mg+Fe vs. distance from contact. Distances in km are relative to the nearest surface expression of the SMB. Mg/Mg+Fe is content higher within Bluestone samples with no difference proximal to the contact. 43
- Fig 4.12:** BSE image of sample W105-4, Bluestone member, above andalusite B-in isograd, (<500 m from contact). K-feldspar, biotite symplectic texture highlighted in box indicating a Bt \leftrightarrow Kfs reaction. 44

Fig 4.13: Feldspar composition and distribution in study area. Orthoclase shows no variation proximal to contact. Plagioclase shows an increase in An content towards the contact.	45
Fig. 4.15: Idioblastic chiastolite in low grade, sample LSCN, biotite zone, Cunard member.	47
Fig. 4.16: Spongy andalusite/quartz in high grade Bluestone member, sample WL05-12.	47
Table 5.2.1: Mineral assemblages below and above biotite-in isograd.	50
Table 5.2.2: Mineral assemblages below and above Andalusite C-in isograd (Cunard member only).	51
Table 5.2.3: Mineral assemblages below and above Andalusite B-in isograd.	52
Fig. 5.1: Muscovite with minor biotite rims around cordierite in sample PCR-10, below andalusite B-in isograd.	54
Fig. 5.2: Biotite rims around andalusite in high-grade WL04-3, above andalusite B-in isograd.	54
Fig. 5.3: Sample WL05-15. False color BSE image showing muscovite (green) between cordierite (rose) below andalusite B-in isograd.	55
Fig. 5.4: Sample WL05-12 False color BSE image showing biotite (blue) with minor muscovite (green) surrounding andalusite/quartz (brown)	55
Fig. 5.5: P-T grid of likely reactions and their distribution in P-T space. Calculated using PTXSS (Berman 1988,1991) using ideal solutions and Mg end members (biotite, chlorite, and cordierite). A=S is modified Al_2SiO_5 triple point and corresponding higher temperature location of the andalusite/sillimanite reaction as proposed by Pattison (1992). P-T estimates at 3 kb from sample location LSCN (biotite zone), $T=551^{\circ}C \pm 6^{\circ}C$ and AR05-5 (close to contact), $T=645^{\circ}C \pm 16^{\circ}C$ calculated by ThermoCalc.	56
Fig 5.6: Andalusite apparently without biotite from sample GA06-1 (Cunard Member) ~2.5 km from contact in Glen Arbour. This indicates that andalusite appears before biotite in other parts of the Cunard Member. More work is needed.	60

Acknowledgements

I would like to express my enduring gratitude to the entire geology department at Dalhousie University who helped get me to this point. I am deeply indebted to my supervisor Dr. Rebecca Jamieson whose help, suggestions and encouragement during the writing of this thesis. I would also like to thank Emma Kirsten, Jacob and Jennifer for being there when needed (and not when not).

Chapter 1 Introduction

1.1 Introduction

Halifax is located on the perimeter of the South Mountain Batholith, which has produced a contact metamorphic aureole in the Halifax Formation country rocks. Within the aureole an unusual isograd sequence, in which andalusite appears at lower temperature than biotite, has developed in graphitic slates of the Cunard Member. In contrast, siltier slates of the previously undefined Bluestone member contain the normal isograd sequence. This report is an examination of the effects of contact metamorphism within the Halifax area.

In particular, this thesis is about the lithological and geochemical differences and similarities that have led to the rare isograd sequence of:

cordierite > andalusite > biotite

Previously reported only as a single unit (Cunard Member), clear differentiation of the Cunard Member into two units is essential to understanding the distribution of the mineral assemblages in the Halifax peninsular area.

On the eastern edge of the exposed portion of the South Mountain Batholith (SMB) in Halifax, a well developed, high-temperature, low-pressure contact aureole has developed within the pelitic rocks of the Halifax Formation. Two distinctly different sequences of isograds have been documented in rocks of differing bulk compositions. In the Bluestone member, the isograds follow a typical “textbook” pattern, with increasing temperature, of:

(distal) cordierite > biotite > andalusite (proximal)

Within the Cunard Member, however an atypical pattern is developed:

(distal) cordierite > andalusite > biotite (proximal)

The previously undocumented appearance of andalusite below biotite is present in the Cunard Member. This study attempts to determine the reasons for the formation of andalusite at such low temperatures, with a focus on mineral assemblage variations between the Bluestone and Cunard Members.

1.2 Regional Geology

The City of Halifax is underlain by Cambrian-Ordovician deep-water turbidites of the Meguma Group, which were deposited along the slope and rise of Gondwanaland (Schenk 1982). The lower unit is the quartzo-feldspathic Cambrian Goldenville Formation greywacke with minor interbedded slate and local calcareous nodules (Schenk 1997) (Fig 1.1). The base of the Goldenville Formation is not exposed, but the formation has a maximum estimated thickness of 5600m (Faribault 1914). Conformably overlying the Goldenville is the Early Ordovician Halifax Formation, consisting of graphitic slate with siltstone and minor calcareous units. The Halifax Formation has a thickness between 500m and 8000m (Schenk 1982). Variation in graphite, sulphide, quartz and sheet silicate distribution result in highly variable mineralogical and colour layering related to bedding.

During the Acadian Orogeny (410-370 Ma), the Meguma Terrane collided with the Avalon Terrane during the final stages of accretion of the Appalachian Orogen (Williams 1979). The Meguma Group was deformed into regional-scale, upright, tight, northeast-trending folds (Fig 1.4) with a well developed axial planar slaty cleavage. Regional greenschist to amphibolite facies metamorphism accompanied deformation. Meguma Group units (Halifax and Goldenville Formations) in this study area were affected by chlorite zone (greenschist facies) regional metamorphism. Higher grade metamorphism occurs farther to the northeast and southwest of the study area.

In southwestern Nova Scotia and the Annapolis Valley, Silurian-Devonian sedimentary rocks of the Annapolis Group, also affected by the Acadian deformation, overlie the Meguma Group. Post-Acadian Carboniferous sedimentary rocks of the Horton and Windsor Groups unconformably overlie these rocks.

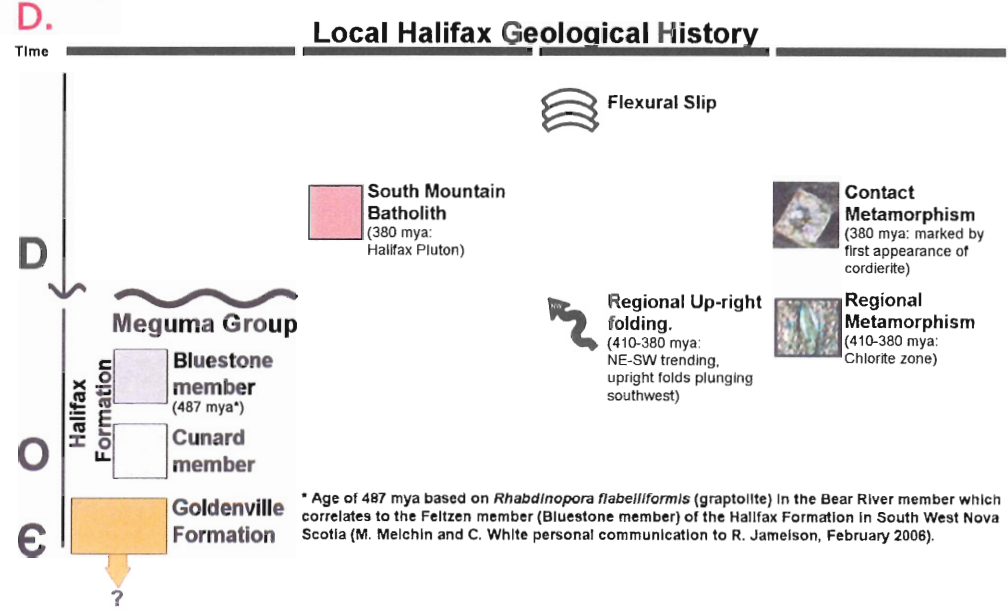
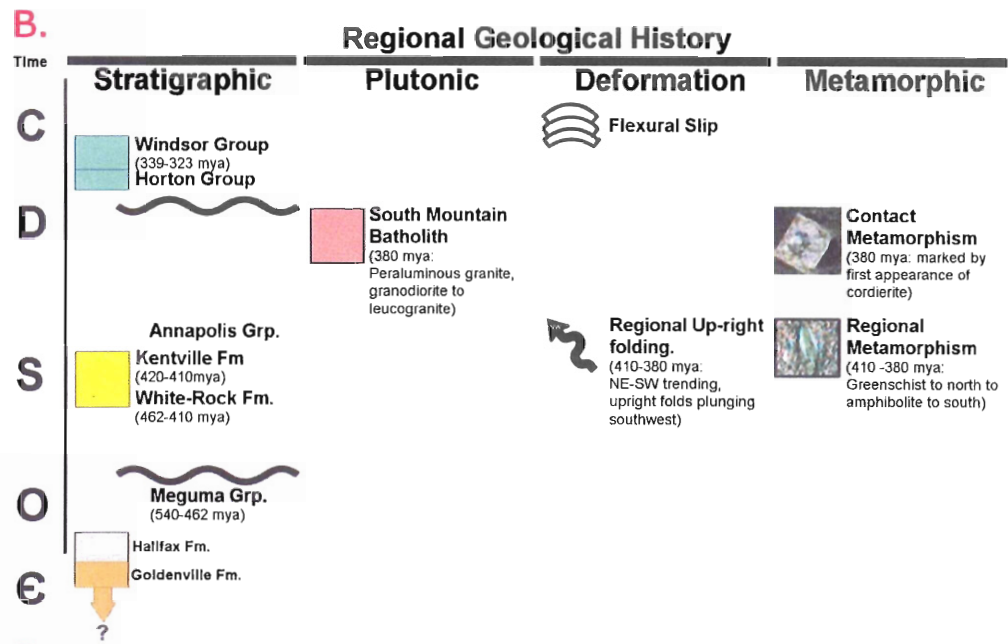
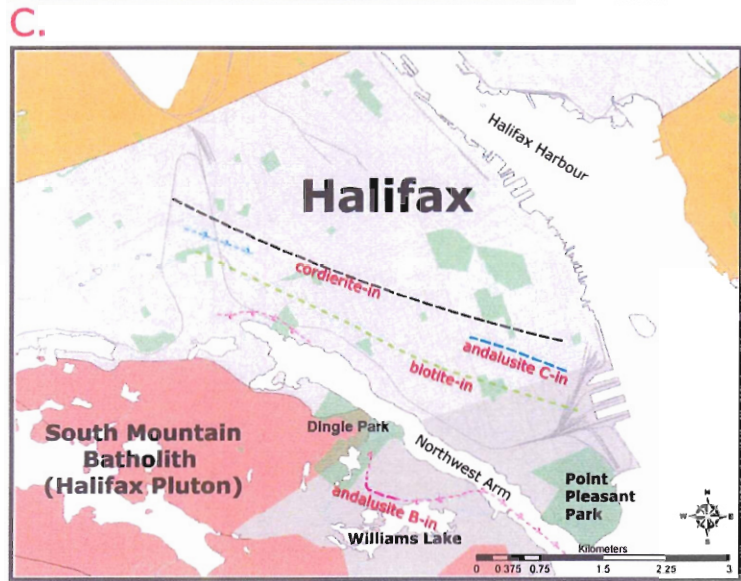
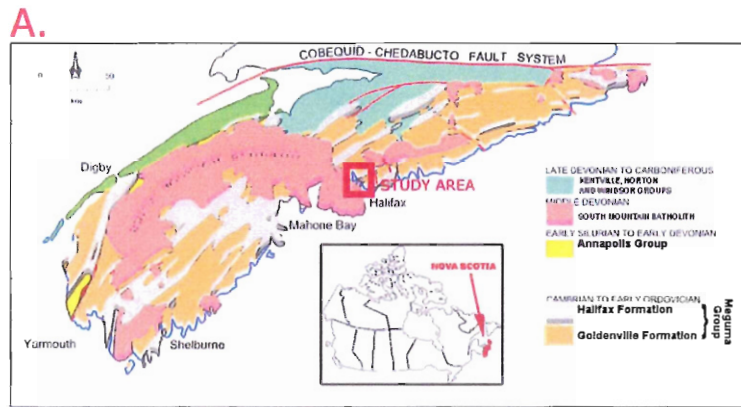
Intrusion of the Meguma Group by the ca. 380 Ma South Mountain Batholith (Macdonald 2001) caused high temperature overprinting of the chlorite zone mineralogy in the immediate vicinity of the contact. The intrusion truncated regional folds and caused annealing of slaty cleavage. The outer limit of the contact aureole within the study area is defined by the first appearance of cordierite.

The last glaciation period, which ended ca. 13000 years ago (Stea 1998), resulted in exposure of new outcrops and burial of other outcrops under thick layers of glacial till. Features of glacial origin, such as striations and chatter marks, are still visible throughout the study area.

1.3 Previous Work

Meguma Group rocks have been studied since the early 1800's. Jackson and Alger (1828-1829) first described the geology of southeastern Nova Scotia, including much of what is known today as the Meguma Group. In 1855 Dawson determined that the Meguma Group was distinguishable (and mappable) from Silurian and Devonian rocks in Nova Scotia. Faribault mapped the area for the Geological Survey of Canada between 1899 and 1929 and described three main lithological units, the lowest of which he called 'gold bearing series', which was later renamed the Goldenville Formation by Woodman (1904a,b).

Ami (1900) named the Halifax Formation, which overlies what is now the Goldenville. Woodman (1904a,b) grouped the Goldenville and Halifax Formations and called them the Meguma Series, which was later renamed to the Meguma Group by Stevenson (1965).



* Age of 487 mya based on *Rhabdinopora flabelliformis* (graptolite) in the Bear River member which correlates to the Feltzen member (Bluestone member) of the Halifax Formation in South West Nova Scotia (M. Melchior and C. White personal communication to R. Jamieson, February 2008).

Fig 1.1
 A. Schematic regional geology map of Nova Scotia. Meguma Zone (color) with Avalon Zone (white). Study area highlighted in red.
 B. Simplified regional geological history
 C. Schematic study area geology map. Contact aureole isograds show first appearance of mineral designated. High-grade side always towards the SMB. Andalusite C = below biotite, andalusite-in isograd in Cunard Member. Andalusite B = above biotite, andalusite-in isograd in Bluestone member.
 D. Simplified study area geological history.

Schenk (1970, 1971, 1973, 1983, 1991, 1997), whose efforts were directed at testing his hypothesis that the Meguma Group sediments originated from the North African craton (Schenk 1970, Schenk 1995), studied the sedimentology of Meguma Group extensively. Other studies of the Meguma Group have focused on gold mineralization within the Meguma terrane (e.g. Graves 1976, Graves and Zentilli 1982).

The Halifax Formation has recently been dated as Early Ordovician (ca. 487 Ma) with the identification of *Rhabdinopora flabelliformis* (graptolite) in the Bear River member of the Halifax Formation in southwest Nova Scotia (M. Melchin and C. White, personal communication to R. Jamieson, February 2006). The Bear River member correlates with the Feltzen (Bluestone) Member, the upper unit in the Halifax Formation, as described in more detail below.

The South Mountain Batholith has been studied extensively (Macdonald 2001) as it is the largest intrusive granitic complex in the Appalachians (Abbot 1989).

1.3 Study area

This study encompasses the peninsular area of Halifax (Fig 1.3), from Point Pleasant Park in the southeast to Highway 102 in the northwest and Halifax Harbour in the northeast, and extends across the North West Arm to Herring Cove Road to the southwest. The SMB contact is to the southwest, approximately parallel to the Herring Cove Road, and the contact aureole extends to the northeast through the central Halifax Peninsula. Three transects (Fig 1.3) across the study area were chosen perpendicular to the contact. These were based on availability of outcrop and previously known mineral assemblages (Jamieson et al. 2005).

Permanent outcrops within the study area exist along the railway cut running northwest along the North West Arm side of peninsular Halifax. Although outcrop coverage within the railway cut is near complete, the rocks are highly weathered and the railway is private property with

limited access. Some accessible railway outcrops were sampled. Shoreline outcrop is accessible within Point Pleasant Park and the Dingle Park. Shoreline access outside the parks is sparse due to limited public access to the shoreline of the Halifax peninsula.

Commercial and residential development in Halifax has resulted in temporary, fresh, bedrock exposure at building sites. Samples for this study came from outcrops within road cuts and construction sites. There are significant gaps in coverage in older residential areas and in central Halifax where bedrock is buried beneath the till blanket associated with the Citadel Hill drumlin.

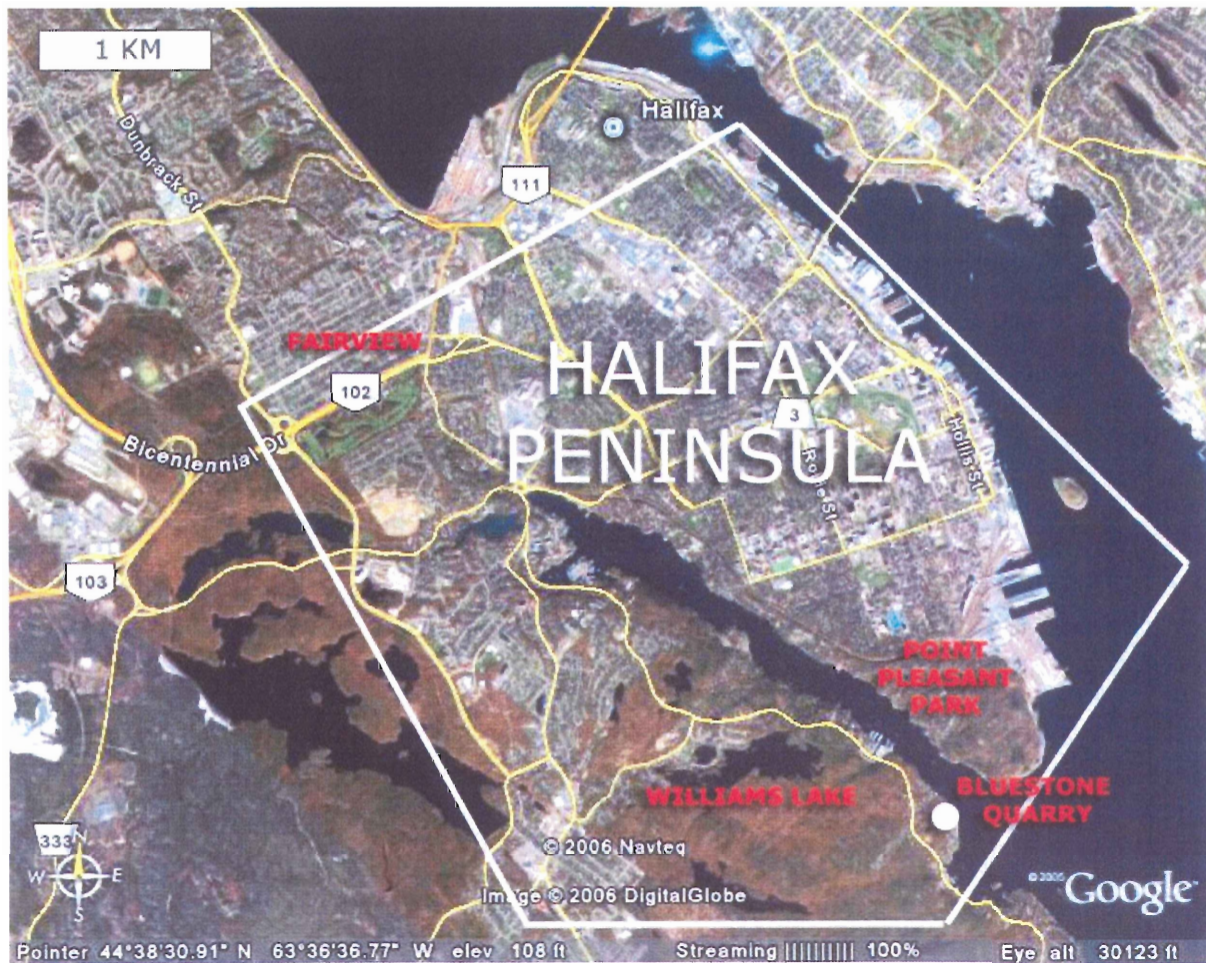


Fig 1.2: Satellite imagery of study area from Google Earth with study area highlighted within polygon. Width is approximately 10 km. Shows location of Bluestone Quarry.

1.4 Transects

Transect 1, Oakland Road to Williams Lake (Fig 1.3), extends from south end Halifax (Inglis Street - Saint Mary's University) to the Williams Lake area. This transect is entirely underlain by Bluestone member lithologies and contains the "normal" isograd sequence.

Transect 2, Dalhousie University to the Dingle (Fig 1.3), lies northwest of Transect 1, and extends from Halifax Harbour, southwest along University Avenue to the North West Arm, and includes outcrops at the Dingle Park. Transect 2 is underlain by the graphitic black slate of the Cunard Member and displays the "anomalous" isograd sequence.

Transect 3, Bayers Road to Fairview, northeast of Transect 2, (Fig 1.3) extends from Halifax Harbour to the Fairview area. Transect 3 was chosen in order to extend the mapped isograds further to the north and to determine which, if either, of the two isograd sequences is present in the contact aureole where it overprints the Halifax Formation in the northwest part of the city (Fig 1.4).

1.5 Previous work in study area

Dalhousie and Saint Mary's Universities, from mapping projects in Point Pleasant Park and Bluestone quarry (Fig 1.2) to mineralogical studies in various Earth Science classes, have long used rocks and outcrops within the study area as teaching tools. Mahoney (1996) studied the entire contact aureole in terms of general geochemistry and isograd structure. She determined P-T estimates, which show the eastern end of the pluton (Mount Uniacke-Halifax), intruded at higher pressure (3.5 kb to 3.8 kb) than the western end (3.0 kb). This corresponds to a 1 to 2 km burial depth difference between the eastern and western ends of the pluton. Calculated temperatures by Mahoney (1996) range from 460°C to 590°C within 5m of the contact. These P-T conditions have been plotted in Fig 5.5 along with results from this study.

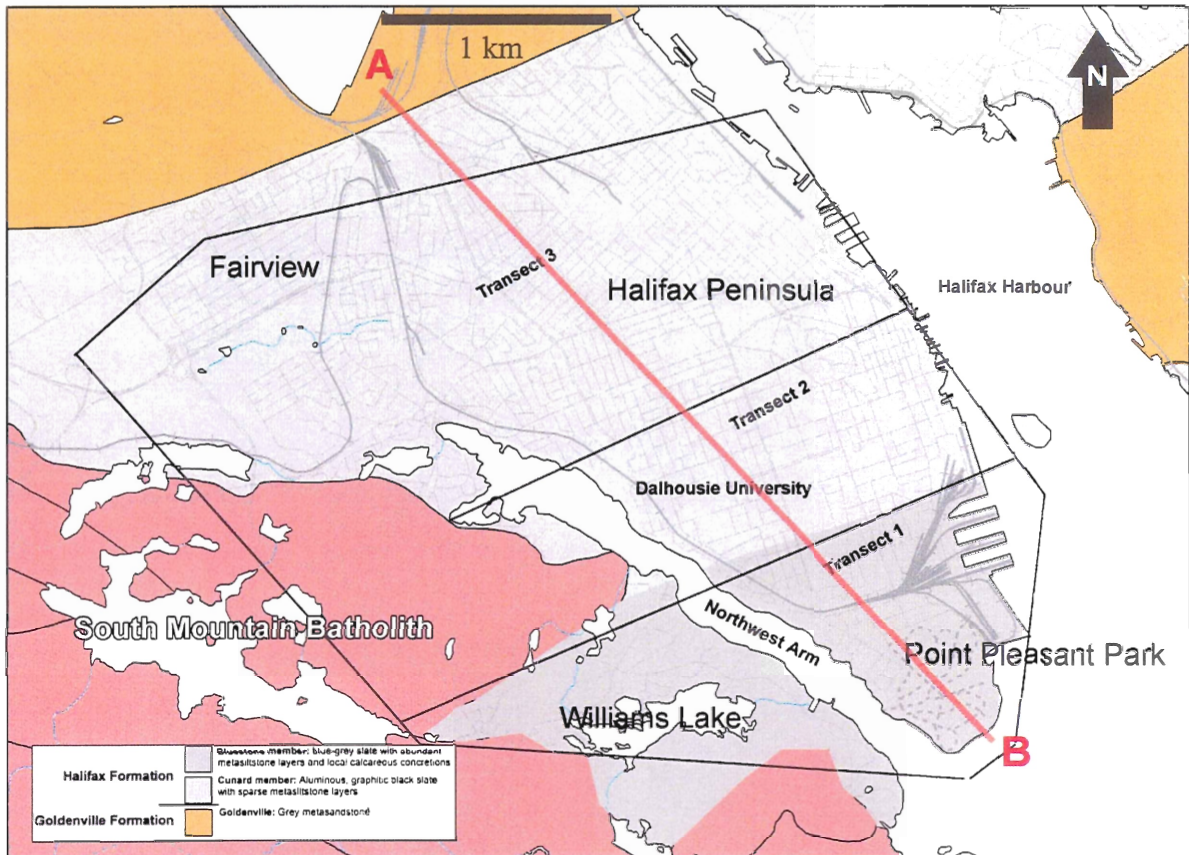


Fig 1.3: Schematic geological map of study area with transects and study area labeled. Line shows cross section area for Fig 1.4.

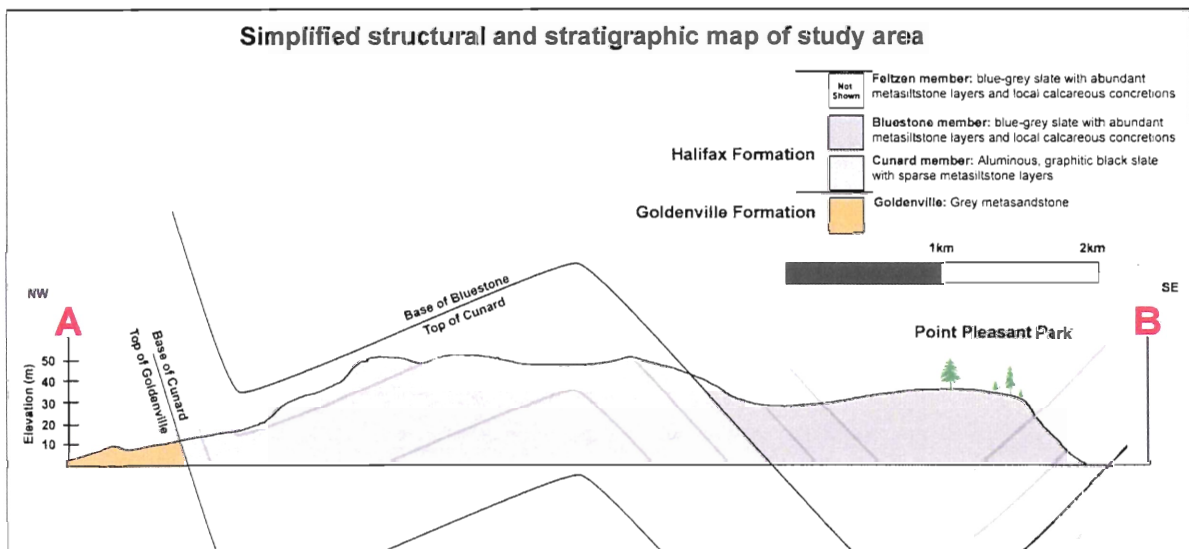


Fig 1.4: Simplified schematic diagram of upright folds within study area across line A-B in Fig 1.3. modified from (Home and Culshaw 2001).

Hicks (1996) studied the low-grade metamorphism of the Halifax Formation in the Mahone Bay area, outside the contact aureole. She analyzed multiple samples from various lithologies including Cunard Member rocks. Using XRD she was able to confirm the presence of paragonite within Cunard Member samples from Mahone Bay.

In a related, concurrent study, Neil Tobey is investigating the geology, including metamorphic geology, of Point Pleasant Park. Metamorphic petrology (ERTH 3020) classes made preliminary observations within the study area in 2002, 2004, and 2005. Jared Butler as part of his 2005 NSERC USRA project analyzed sulphides and oxides from Transect 2.

The zoned, peraluminous Halifax pluton has been studied extensively (e.g. MacDonald and Horne 1988; MacDonald 2001). MacDonald and Horne (1988) studied the petrology and zoning within the Halifax Pluton, and Clarke and Muecke (1985) reviewed the petrochemistry and hydrothermal circulation associated with its emplacement.

1.6 Objectives and approach

The primary objective of this study is to determine the reason for the anomalous early appearance of andalusite in the Cunard Member of the contact aureole. A more comprehensive list of objectives of this study is as follows:

1. To determine the distribution of mineral assemblages in the contact aureole in the city of Halifax.
2. To account for observed differences in isograd sequences between central and southern Halifax
3. To test the hypothesis that two lithologically and geochemically distinctive units are present within the Halifax Formation in the study area.
4. To determine the metamorphic reactions and P-T conditions associated with the contact metamorphism in the study area.

Methods included field mapping and microscopic petrology of mineral assemblages and rock types within the contact aureole. Microprobe data from selected samples were used to help determine reactions as well as P-T conditions and to identify sub-optical scale textures within the samples. Computer programs (ThermoCalc, PTXSS) were used to determine P-T conditions as well as to calculate positions of reactions in P-T space.

A database was created to compile and display data from this study, and others, for future reference.

Chapter 2

Lithology and Structure

2.1 Introduction

The geology of the Halifax area has been documented at a large-scale level (e.g. Schenk 1982), as well as in a number of M.Sc. (Horne 1998, Hicks 1996, Mahoney 1996) and B.Sc. theses (e.g. Bhatnagar 1998, Betts-Robertson 1998, Tobey 2006). This chapter describes the geology at the smaller scale in the Halifax peninsula and adjacent areas. Two main lithological units, the Halifax Formation and the South Mountain Batholith, are represented, with two subdivisions of the Halifax Formation recognized.

2.2 Meguma Group

Meguma Group rocks within the study area include the Goldenville Formation, which is conformably overlain by the Halifax Formation. Goldenville outcrops only to the northwest of the study area and is not part of this study, which deals only with contact metamorphism of the Halifax Formation.

2.3 Halifax Formation

The Halifax Formation is an early Ordovician sequence of graphitic shales/slates with minor (10%-15%) siltstones. In the Mahone Bay area, conformable units within the Halifax Formation include (from oldest to youngest), the Mosher's Island, Cunard and Feltzen Members (Fig 1.1, Schenk 1991). For the purposes of this thesis, I have distinguished an informal unit in the Halifax area referred to as the Bluestone member, which stratigraphically overlies the Cunard Member and which may correlate with the Feltzen Member.

2.3.1 Cunard Member

The Cunard Member (Fig 2.1) is a 1000m (Schenk 1991), fine-grained, sulfide-rich (40%), black graphitic slate interbedded with thin siltstone layers (< 5%). Bedding is finely laminated with well-preserved sedimentary structures (cross bedding, starved ripples), particularly in the low- grade areas (Hicks 1996). Slaty cleavage is strong in most places, but becomes annealed proximal to the contact with the SMB.

In the study area, the transition from the Cunard to the Bluestone member is gradational, associated with increasing siltstone content, as observed in the region between the Dalhousie campus and Point Pleasant Park (between Transect 1 and 2 in this study area).

2.3.2 Bluestone member

The Bluestone member is distinguished from the Cunard Member based on outcrop appearance, bulk chemistry and mineralogical assemblage (Fig 2.1, Fig 2.2). Bluestone slates are blue/grey with abundant (relative to Cunard Member) interbedded siltstone layers (15%-20%). Sedimentary structures (cross bedding, scour surfaces) are easily identifiable within coarser-grained layers.

The name “Bluestone” is taken from the Bluestone Quarry near Purcell’s Cove Road (Fig 1.2). This quarry operated in the 19th and early to mid 20th centuries. Older Dalhousie University buildings contain stone derived from this quarry. The Bluestone member conformably overlies the Cunard Member with a gradational contact marked by increasing siltstone content.

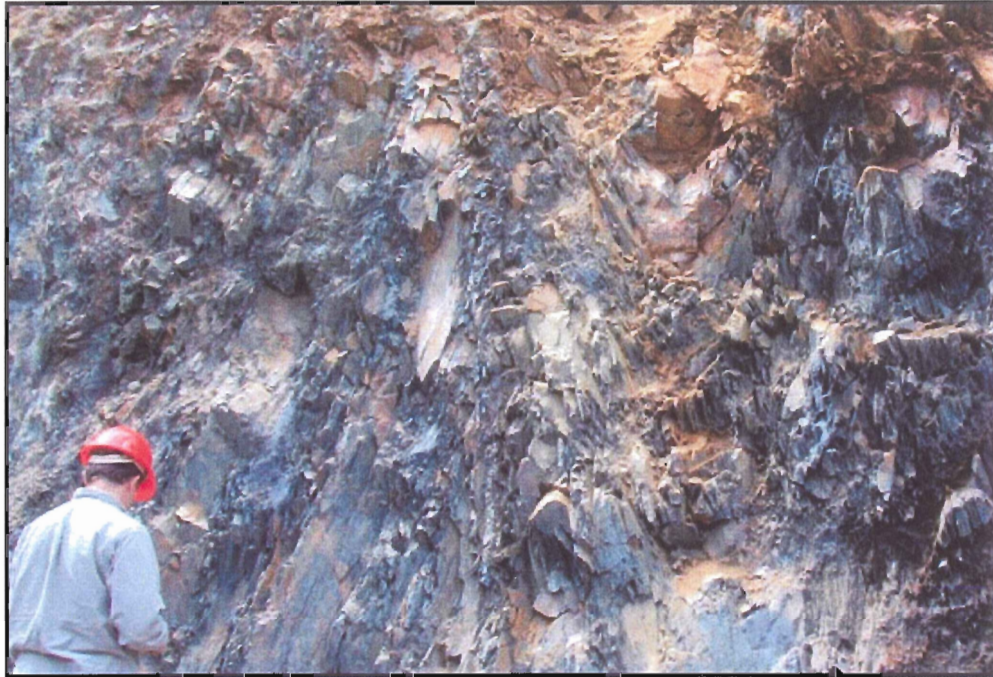


Fig 2.1: Cunard Member in downtown Halifax (building site next to Brewery Market). Sample location KBM05. Fissile, black slate, with small upright syncline/anticline (center/right).



Fig 2.2: Bluestone member, Point Pleasant Park. Sample location PPP04-9 (Black Rock). Note abundant siltstone layers, shown here on cleavage plane surface.

Rocks within this unit are recognized by a blue-grey color (Fig 2.2) in contrast to the black, graphitic Cunard Member. Slaty layers are dark blue/grey and typically show laminar bedding or are homogeneous. Interbedded siltstone layers comprise up to 20% or more of the outcrop. Sedimentary features within the siltstone layers are well preserved throughout Bluestone member, with cross ripples, scour surfaces and some soft sediment deformation easily identified in low-grade outcrops. Worm burrows were found in a loose sample taken in 2004, near sample location PPP04-13, in central Point Pleasant Park (Fig 2.3). Although the sample was not taken from bedrock, the presence of cordierite and its identical appearance to local outcrop suggest that it is locally derived.

In Point Pleasant Park, the lower Bluestone member (Unit A, Tobey 2006) contains calcareous concretions that are exposed from Battery Point (PPP04-8) to Cable Rock (PPP04-3). If the Bluestone member overlies the Cunard Member, the concretions within the lower Bluestone member on the southeast limb (Fig 1.4) of the Point Pleasant Park syncline should be present where the same stratigraphic layer re-emerges on the northwest limb of this syncline in the Bluestone – Cunard Member transition zone. They have not yet been observed. The apparent absence of concretions within the transition zone may indicate a lateral facies change, an additional structure that cuts out the concretion-bearing horizon, or a lack of outcrops within the transition zone.

Similar concretions within the Feltzen Member (O'Brien 1986) and other lithological similarities suggest that the Bluestone member in the Halifax area may correlate with the Feltzen Member in the Mahone Bay area (Fig 2.4)

2.4 South Mountain Batholith

The SMB is a peraluminous granitic intrusion (Clarke et al 1988) of approximately 380 ± 3 Ma based on zircon and monazite U-Pb crystallization ages (Carruzzo et al 2003). The SMB was intruded into the Meguma Group at an estimated depth of ~10 km (MacDonald et al 1992). The contact aureole surrounding the intrusion ranges from 400m to 3 km wide (Mahoney 1996). Intrusive contacts have been inferred to vary from vertical to shallow dipping within the Halifax area.

2.5 Regional deformation and metamorphism

On a regional scale, the Meguma Group was folded into NE-SW trending, upright anticlines and synclines plunging to the southwest. In the Halifax area, two synclines with an intervening anticline extend across the study area from the SMB contact to Halifax Harbour. The folds are cut by the pluton in the study area, but may be deflected further north (Bhatnagar 1998). Transects 1 and 2 lie on the SW- dipping limb of an anticline, Transect 3 lies within the hinge of the anticline and extends into the NW- dipping limb. The Bluestone member occupies the core of the Point Pleasant Park syncline with the Cunard Member occupying the flank and hinge of the anticline and the core of the syncline to the northwest. Post-SMB flexural slip folding (Horne 1998) has slightly affected the study area rocks, as evident from offsets in some cordierite crystals and retrogression associated with some post-contact metamorphic fabrics.

2.6 Summary

The Halifax Formation underlying the Halifax peninsula can be separated into two easily distinguishable units, the Cunard Member and the Bluestone member, the latter of which may correlate with the lower Feltzen Member of the Halifax Formation. Lithological differences are easy to identify at the outcrop level. The same deformation and metamorphic processes affected the two units.

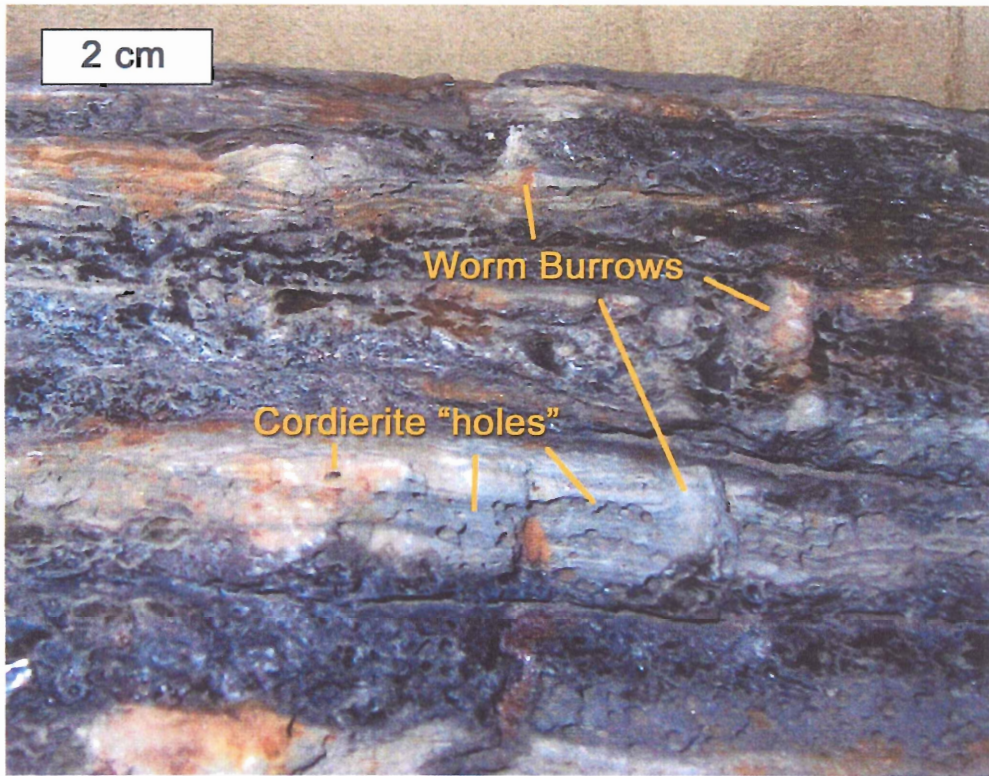


Fig 2.3: Worm burrows from sample collected from Point Pleasant Park, summer 2004.

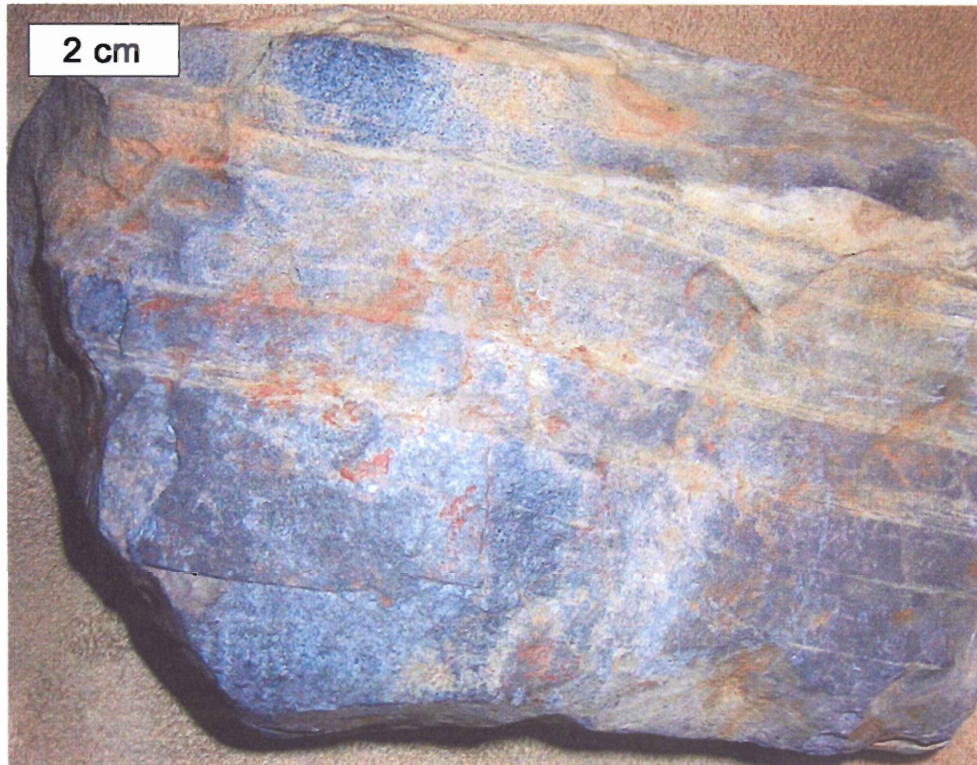


Fig 2.4: Picture of Mahone Bay area Feltzen Member. Sample from Blue-Rocks, near Lunenburg, N.S..

Chapter 3 Petrography

3.1 Introduction

The study area comprises two lithological units, which contain varied lithologies, bulk compositions and metamorphic assemblages, from which numerous samples have been taken (Fig 3.1). Folding, slaty cleavage development, and regional chlorite zone metamorphism prior to intrusion by the SMB affected the two identifiable lithological units, the Cunard and the overlying Bluestone member. Hicks (1996) observed a pre-contact metamorphic mineral assemblage in the Mahone Bay area of chlorite, white mica, quartz, albite, Fe-Ti oxides and sulfides.

Within the study areas, both units contain varying amounts of muscovite, albite, quartz, graphite, and Fe-sulphides (pyrite, pyrrhotite, sphalerite, and chalcopyrite) and Fe-Ti oxides (rutile and/or ilmenite). Mineral assemblages developed during contact metamorphism include some or all of the silicate minerals andalusite, biotite, cordierite, and K-feldspar with rare sillimanite. Figure 3.13 shows the distribution of mineral assemblages.

The first appearance of cordierite marks the outer limit of the contact aureole in both units. Modal percentages of cordierite and grain size both increase towards the contact. A distinctive feature of the low-grade rocks is the presence of muscovite/chlorite stacks (Fig 3.2) that are gradually replaced by biotite/muscovite stacks towards the contact. Proximal to the contact, the muscovite/chlorite and biotite/muscovite stacks are replaced by more idioblastic muscovite, and biotite, and chlorite disappears altogether. Modal abundance and grain size of biotite increase towards to the contact. Muscovite decreases in modal abundance but increases in grain size proximal to the contact. Andalusite increases in abundance towards the contact and K-feldspar only appears in close proximity (500m) to the contact.

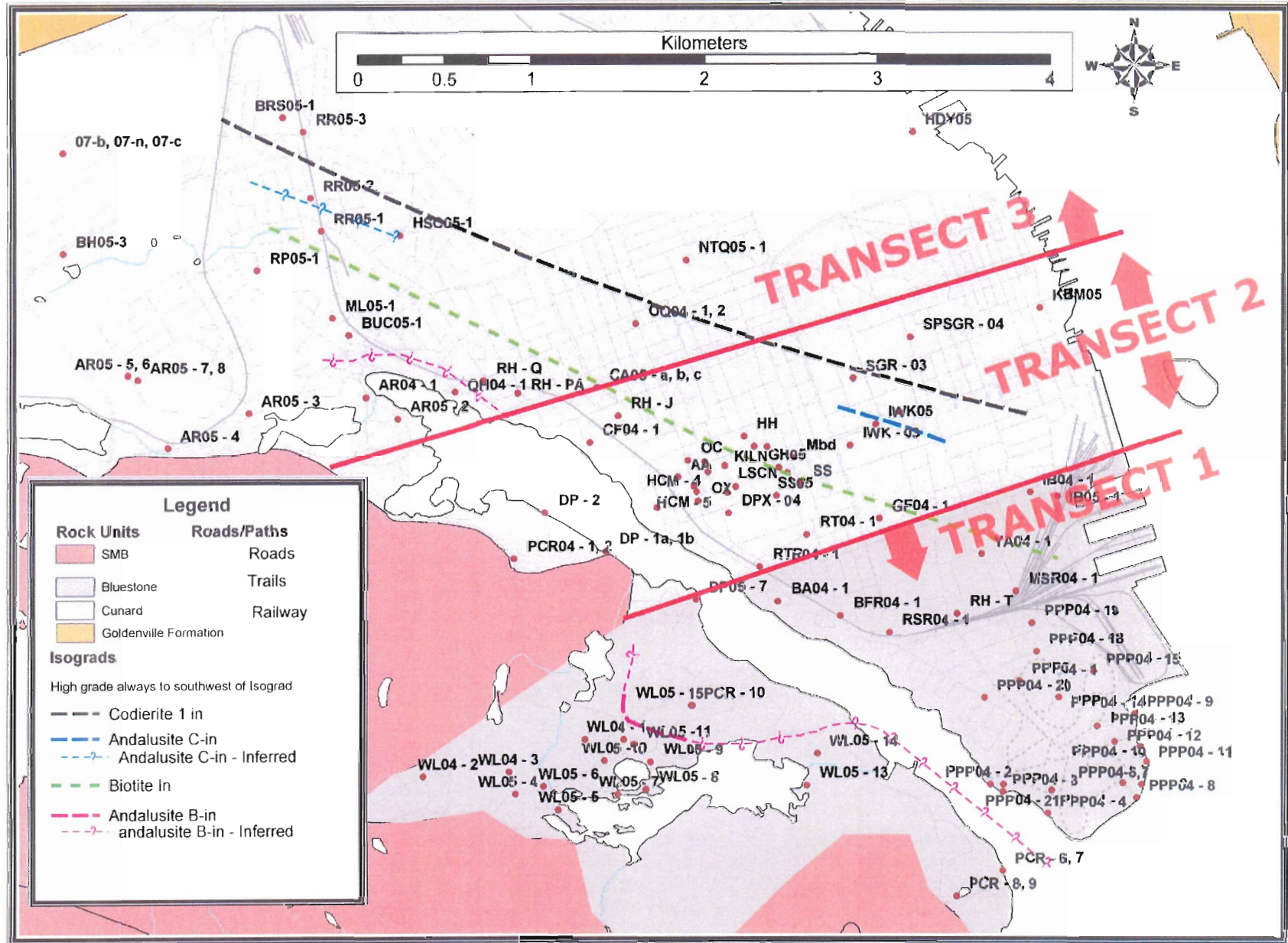


Fig 3.1: Sample locations and transects referred to in this thesis.

3.2 Pre-contact metamorphism assemblages and textures

Outside the contact aureole (Hicks 1996), chlorite zone metamorphism in both units produced varying amounts of quartz, muscovite, and graphite, as fine-grained to medium-grained typically xenoblastic crystals. Sulphides (pyrite/pyrrhotite/arsenopyrite) occur as idioblastic and xenoblastic, 1-10mm, porphyroblasts, commonly elongated parallel to slaty cleavage. Ilmenite and rutile occur as small (<1mm) crystals throughout the matrix and some may be detrital in origin. A characteristic feature of the mineral assemblage is muscovite/chlorite stacks (Fig 3.2). These are interpreted as pre-tectonic chlorite grains, later deformed and split with muscovite filling fractures in the chlorite grains (van der Pluijm and Kaars-Sijpesteijn 1984, Hicks 1996).

In hand sample, slaty cleavage is obvious and relict bedding is preserved in most samples. Slaty cleavage within the thin sections is defined by alignment of platy minerals, primarily muscovite and graphite, within the matrix,.

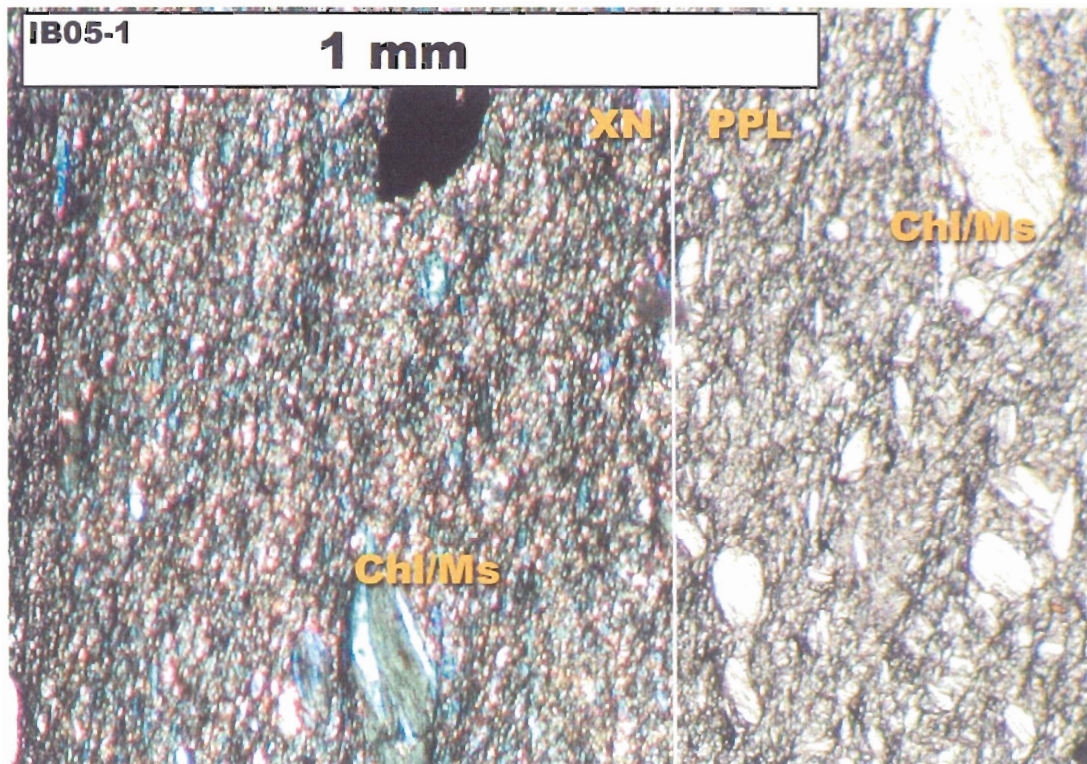


Fig 3.2: Muscovite/chlorite stack from sample IB05-1. XN on left, PPL on right.

3.3 Transect 1: Bluestone member, Oakland Road to Williams Lake

Transect 1 (Fig 1.3) lies wholly within the Bluestone member and encompasses the region east of Oakland Road to Point Pleasant Park and southwest to Williams Lake. This transect was chosen to exemplify the lithological and mineralogical differences between the Bluestone and Cunard Members. Outcrops comprise mainly railroad cuts and building sites on the Halifax peninsula and scattered outcrops throughout the Williams Lake area (Fig 3.1).

3.3.1 Biotite zone (2 km from contact)

The first appearance of cordierite defines the onset of contact metamorphism, which in this transect occurs outside the study area. With increasing proximity to the contact, the first appearance of biotite occurs with a reduction in modal percentage of chlorite. The creation of biotite/muscovite stacks from the pre-existing (pre-contact metamorphism) muscovite/chlorite stacks (Fig 3.3) defines the biotite-in isograd. Biotite appears within the chlorite/muscovite stacks before it does in the matrix.

The best-defined relict bedding occurs within Point Pleasant Park samples. Sedimentary structures (cross bedding, rhythmic layering) are easily recognizable by varying concentration and orientation of quartz-rich and mica-rich layers. The darker, slaty layers contain more graphite, muscovite, chlorite, and biotite than the lighter siltstone layers, which are quartz-rich and contain the majority of the sulphides. Biotite/muscovite stacks are concentrated within the darker, more graphitic, slaty layers.



Fig 3.3: Biotite/muscovite stacks from sample location RSR04 (Bluestone member) within the biotite zone of Transect 1. Shows biotite / muscovite with chlorite / muscovite stacks.

3.3.2 Andalusite zone (< 1 km from contact, Williams Lake area)

Between the biotite-in and andalusite-in isograds, the metamorphic assemblage undergoes an increase in grain size, increase in abundance and freshness of cordierite, and reduction/elimination of chlorite.

Within 1 km of the contact, the andalusite-in isograd is marked by the introduction of ovoid xenoblastic aggregates of quartz + andalusite rimmed (encircled) by biotite (Fig 3.5). Below the isograd, muscovite rims xenoblastic cordierite (Fig 3.4). Above the isograd (Fig 3.5), the abundance of biotite increases, particularly within the rims encircling xenoblastic andalusite + quartz cores. K-feldspar appears proximal to the contact (<500m) with a single sample (PCR-10), outside the andalusite zone containing K-feldspar. This sample location may be within the andalusite zone and further investigation is needed. Cleavage is fully annealed by mica and cordierite growth as well as random growth of sheet silicates across the cleavage surfaces in outcrops close to the contact (<500m).

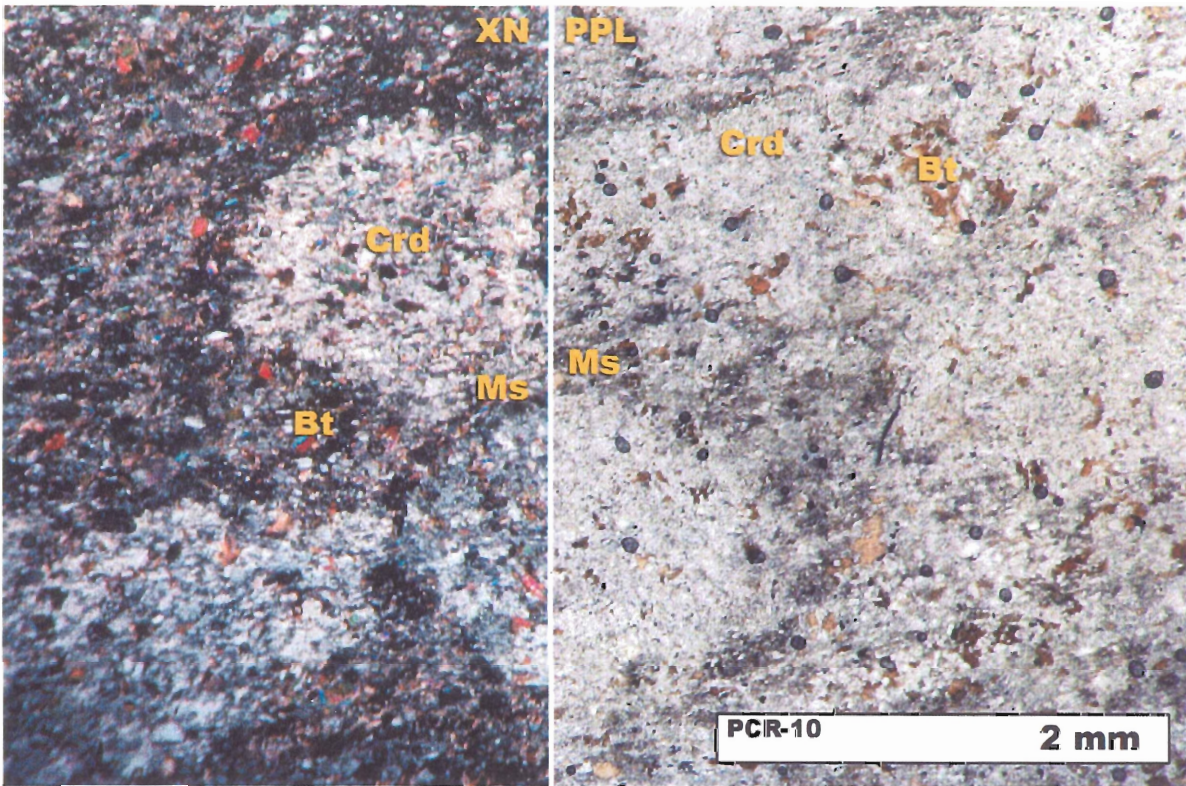


Fig 3.4: Ovoid, xenoblastic cordierite encircled by muscovite and minor biotite below andalusite-in isograd (Bluestone member). Sample location PCR-10 (Purcell's Cove Road). XN on left, PPL on right.

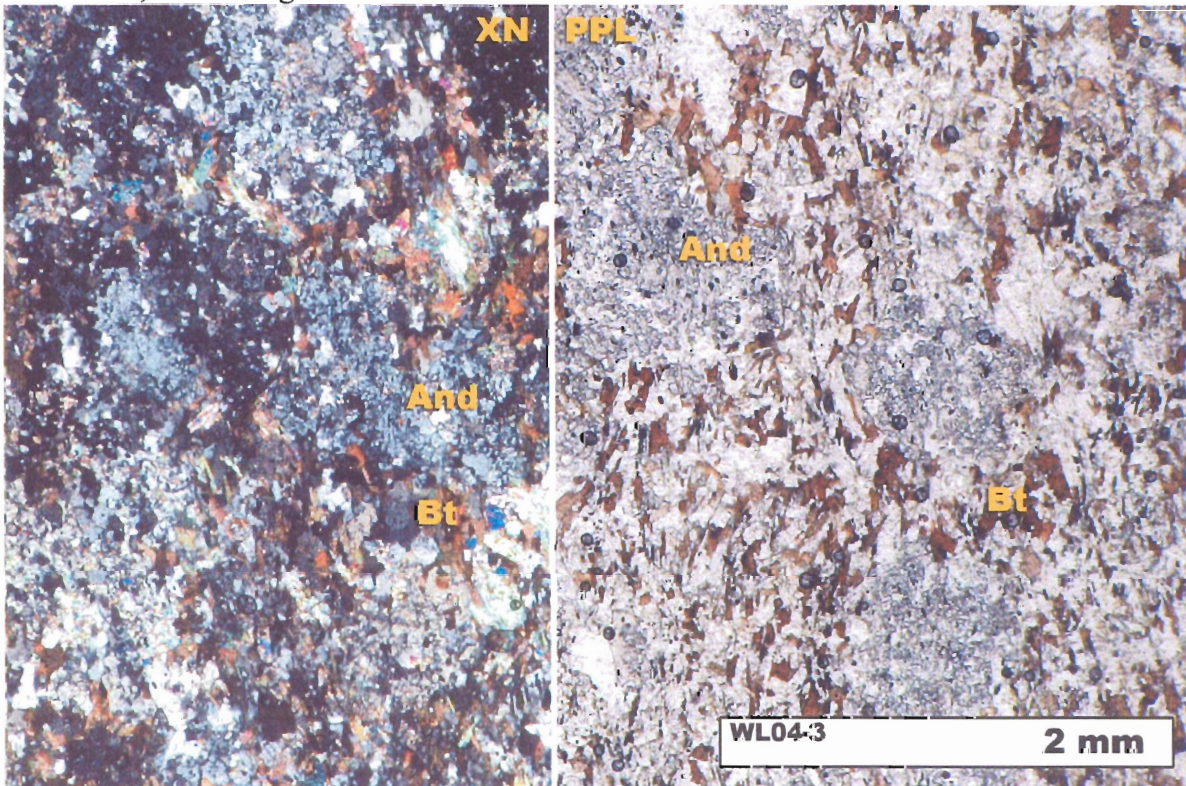


Fig 3.5: Xenoblastic andalusite and quartz encircled by biotite and minor muscovite above andalusite - in isograd (Bluestone member). Sample location WL04-3 (Williams Lake). XN on left, PPL on right.

3.4 Transect 2: Cunard Member, Dalhousie University - Dingle

Transect 2 (Fig 1.3) lies within the central Halifax peninsula along University Avenue and extends across the North West Arm to the Dingle Park. Transect 2 lies wholly within the Cunard Member and is the most intensively sampled transect within this study area. Outcrops include building sites, railway cuts, and other scattered outcrops. Recent construction on and around the Dalhousie campus has exposed new sample locations.

3.4.1 Andalusite-in isograd (2 km from contact)

Below the andalusite-in isograd, rocks contain a chlorite zone mineral assemblage. Xenoblastic cordierite appears as “spots” (0.5-2mm) within the fine-grained matrix comprising primarily fine-grained muscovite. Large (0.5mm -2mm) idioblastic chiastolite (Fig 3.7), randomly oriented in the fine matrix, first appears ~500m closer to the contact, near the corner of University Ave and Summer Street; there is no other change in the mineral assemblage. Chiastolite crystals increase in abundance and size and become less idioblastic in some samples proximal to the contact (Fig 3.8, Fig 3.9). In some locations, chiastolite can exceed 1 cm in length. Bedding is not easily detected in some samples and cleavage is well defined.

3.4.2 Biotite zone (1.2 km from contact)

Biotite first appears ~ 800m closer to the contact, with the isograd trending obliquely across the Dalhousie campus. Biotite first nucleates within the chlorite/muscovite stacks, and is limited to these biotite/muscovite stacks before it appears in the matrix closer to the contact. As in Transect 1, biotite modal abundance increases proximal to the contact.

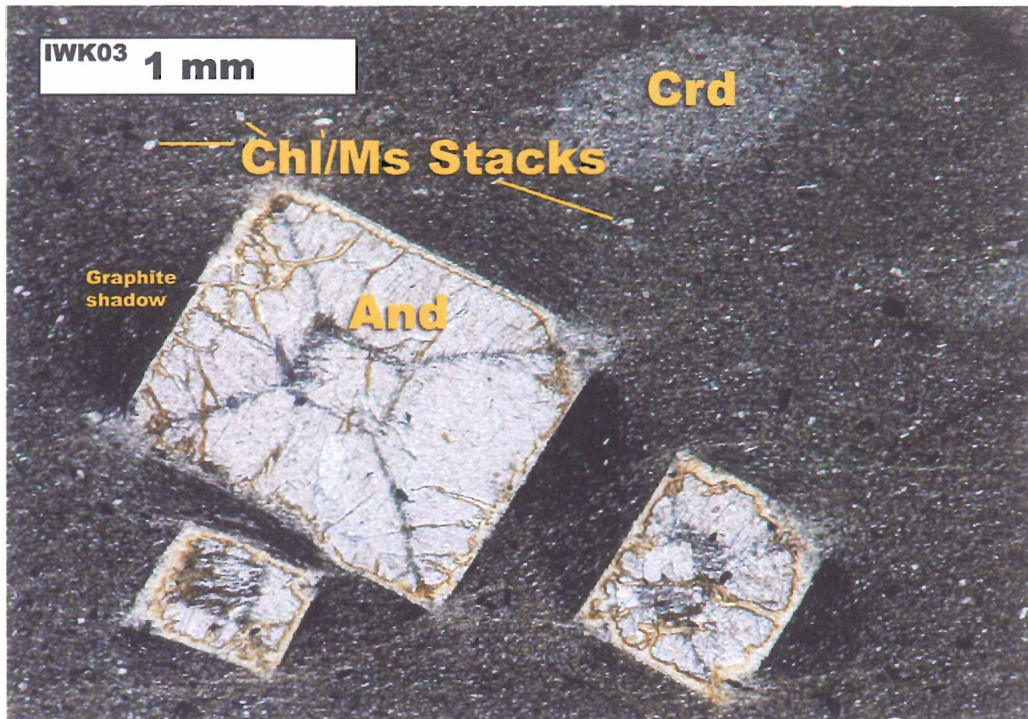


Fig 3.6: Chiastolite from sample location IWK03 (Cunard Member), below the biotite zone of Transect 2. Shows chlorite / muscovite stacks, biotite absent.

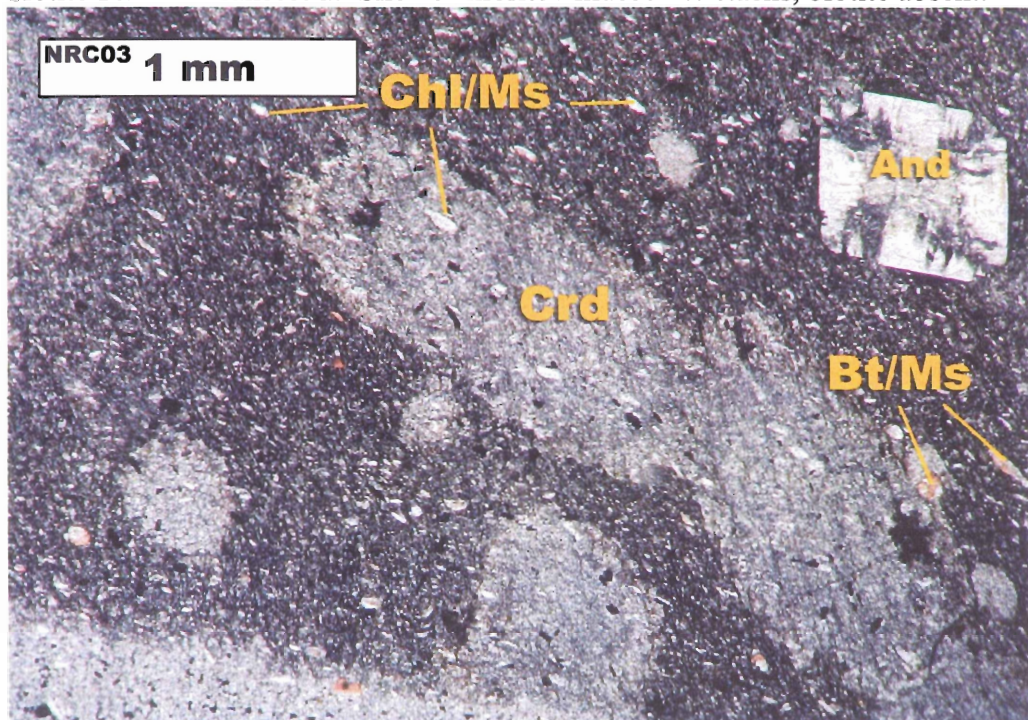


Fig 3.7: Chiastolite from sample location NRC03 (Cunard Member), above the biotite zone of Transect 2. Shows chlorite / muscovite stacks, biotite present.

3.4.3 Biotite zone to the contact

Idioblastic chiastolite persists to the contact, with an increase in modal abundance close to the contact. Chiastolite crystal size increases proximal to the contact and becomes visible in outcrop in samples closest to the contact. Cordierite increases in size, abundance and freshness proximal to the contact, with samples being “spotted” with millimeter-scale cordierite. Cleavage is fully annealed close to the contact with the growth of mica and cordierite across the cleavage surfaces.

3.5 Transect 3: Cunard Member, Bayers Road

Transect 3 (Fig 1.3), selected for comparison with Transect 2 and to determine the westward lateral continuation of the biotite and andalusite isograds, has fewer samples, owing to a lack of accessible outcrops. Lithologically, Transect 3 rocks are part of the Cunard Member and closely resemble Transect 2 rocks. They are black graphitic slates with a strong slaty cleavage and are highly weathered.

3.5.1 Andalusite-in isograd (2km from contact)

As in Transect 2, andalusite (chiastolite) first appears before biotite. Andalusite forms large, (≥ 0.5 mm) idioblastic crystals within a fine-grained graphitic slate. Chiastolite is not as idioblastic as in Transect 2, possibly due to weathering of exposed outcrop. Cruciform textures within the chiastolite are well developed (Fig 3.12).

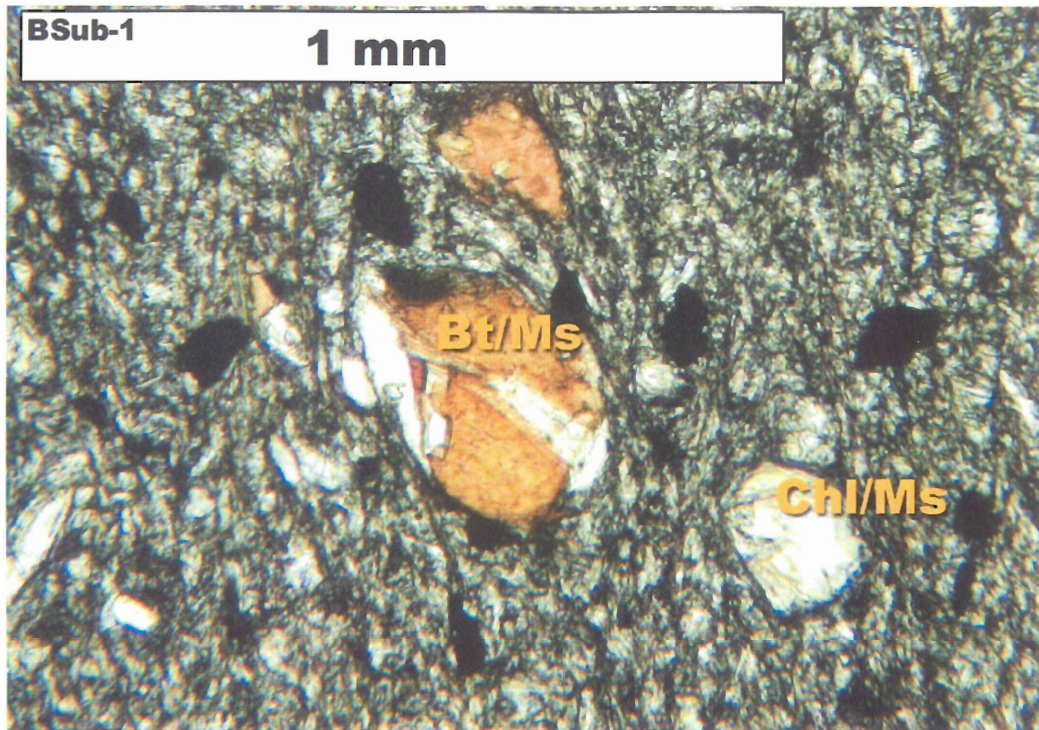


Fig 3.8: Biotite/muscovite stacks from sample location BSub-1 (Cunard Member). Bt/Ms stacks can co-exist with Chl/Ms stacks close to the biotite-in isograd, however Chl/Ms stacks disappear within ~700m towards the contact.

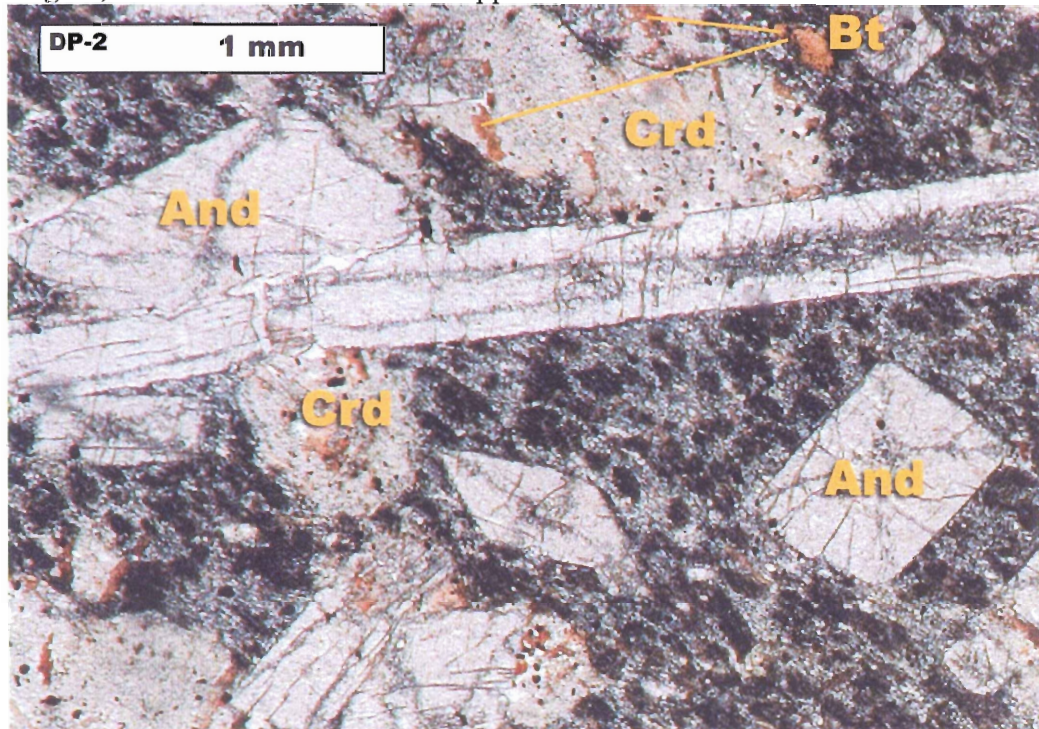


Fig 3.9: Chiastolite from sample location DP-2 (Cunard Member, close to contact), Transect 2. Shows biotite with an absence of Bt/Ms stacks. Minor fine grained muscovite in matrix, K-feldspar present.

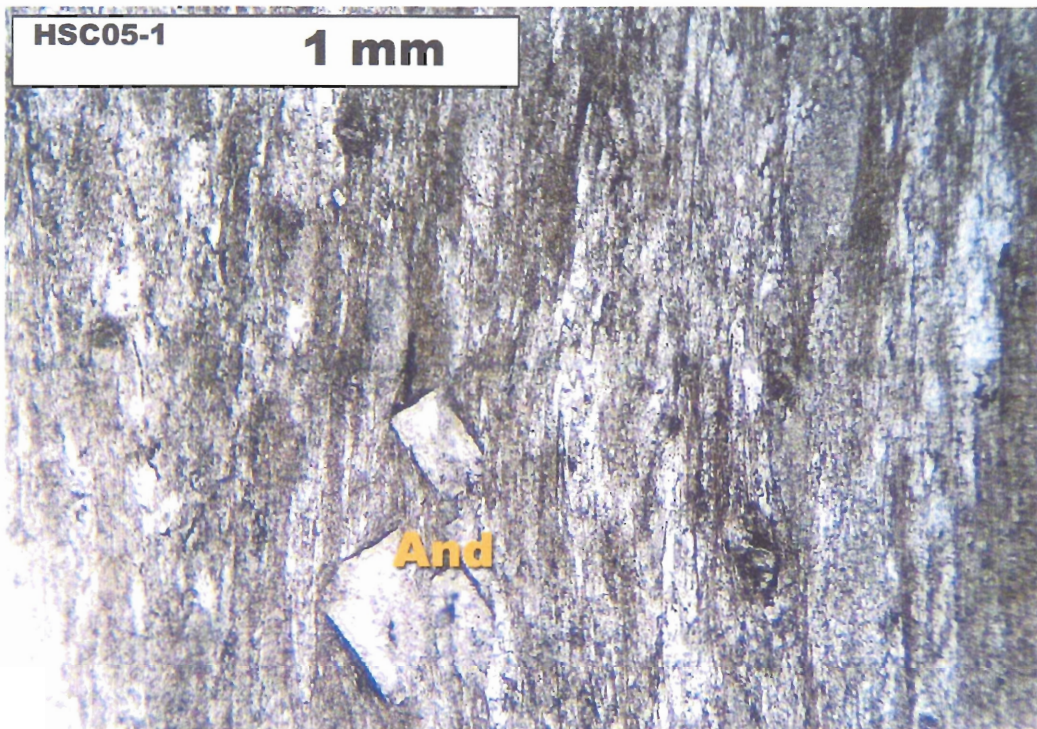


Fig 3.10a: Chiastolite from sample HSC05-1 (Cunard Member), below the biotite zone of Transect 3. Biotite absent, matrix is highly altered with no identifiable chlorite/muscovite stacks. Andalusite is well formed and identifiable, cm scale at outcrop level. Andalusite is highly altered similar to IWK05, Transect 2.



Fig 3.10b: Large andalusite (var. chiastolite) crystals in outcrop at sample location HSC05-1. (Halifax Shopping Centre)

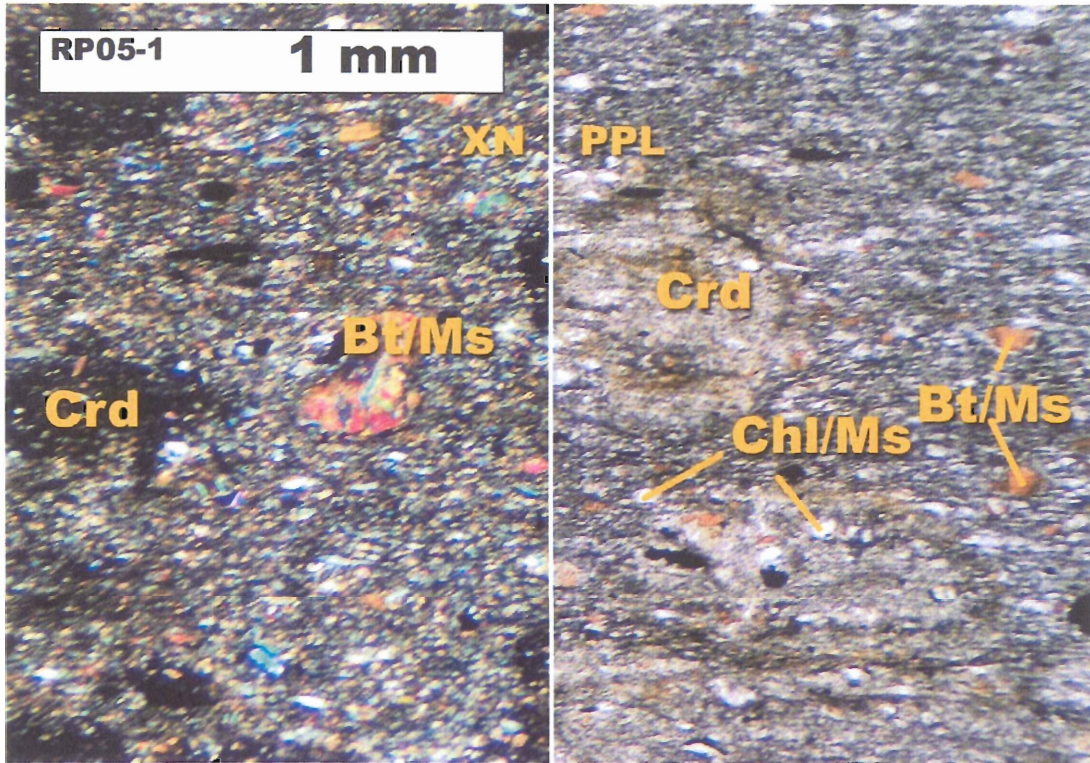


Fig 3.11: RP05-1, Transect 3, shows chlorite/muscovite stacks with biotite present. Chiasmolite is not present in this thin section. XN on left, PPL on right.

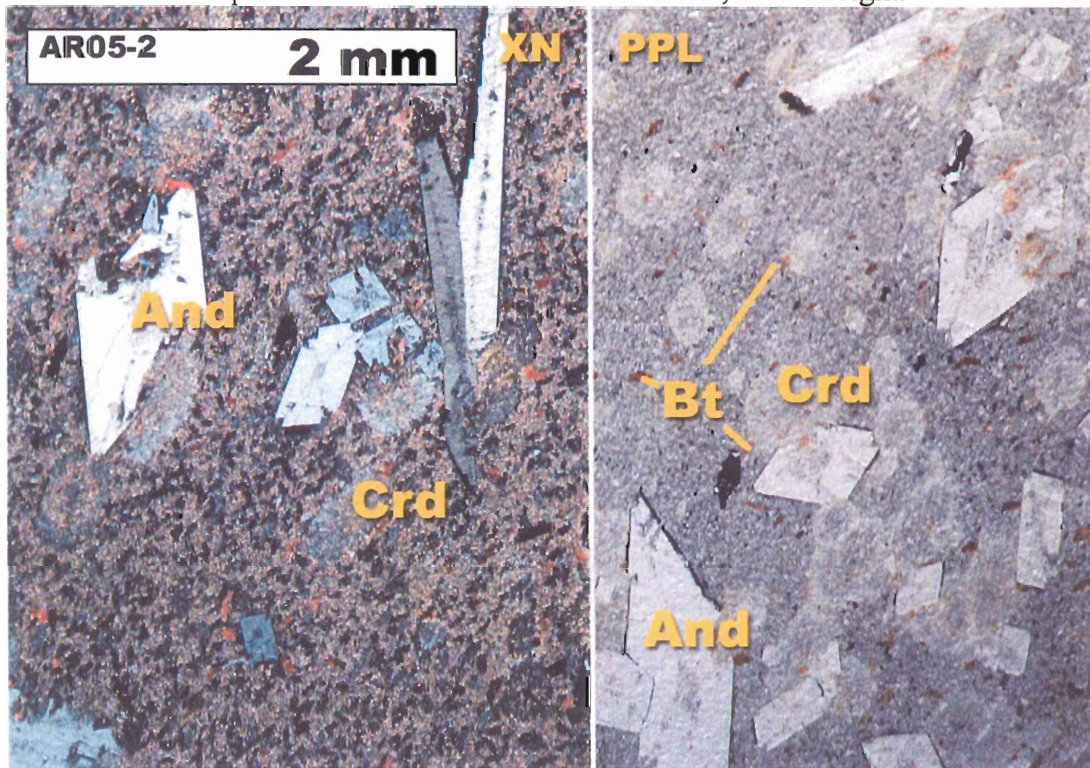


Fig 3.12: Chiasmolite, sample AR05-2 (Cunard Member, within 200m of contact), Transect 3. Biotite and minor fine-grained muscovite in matrix. Fresh cordierite and K-feldspar present. XN on left, PPL on right.

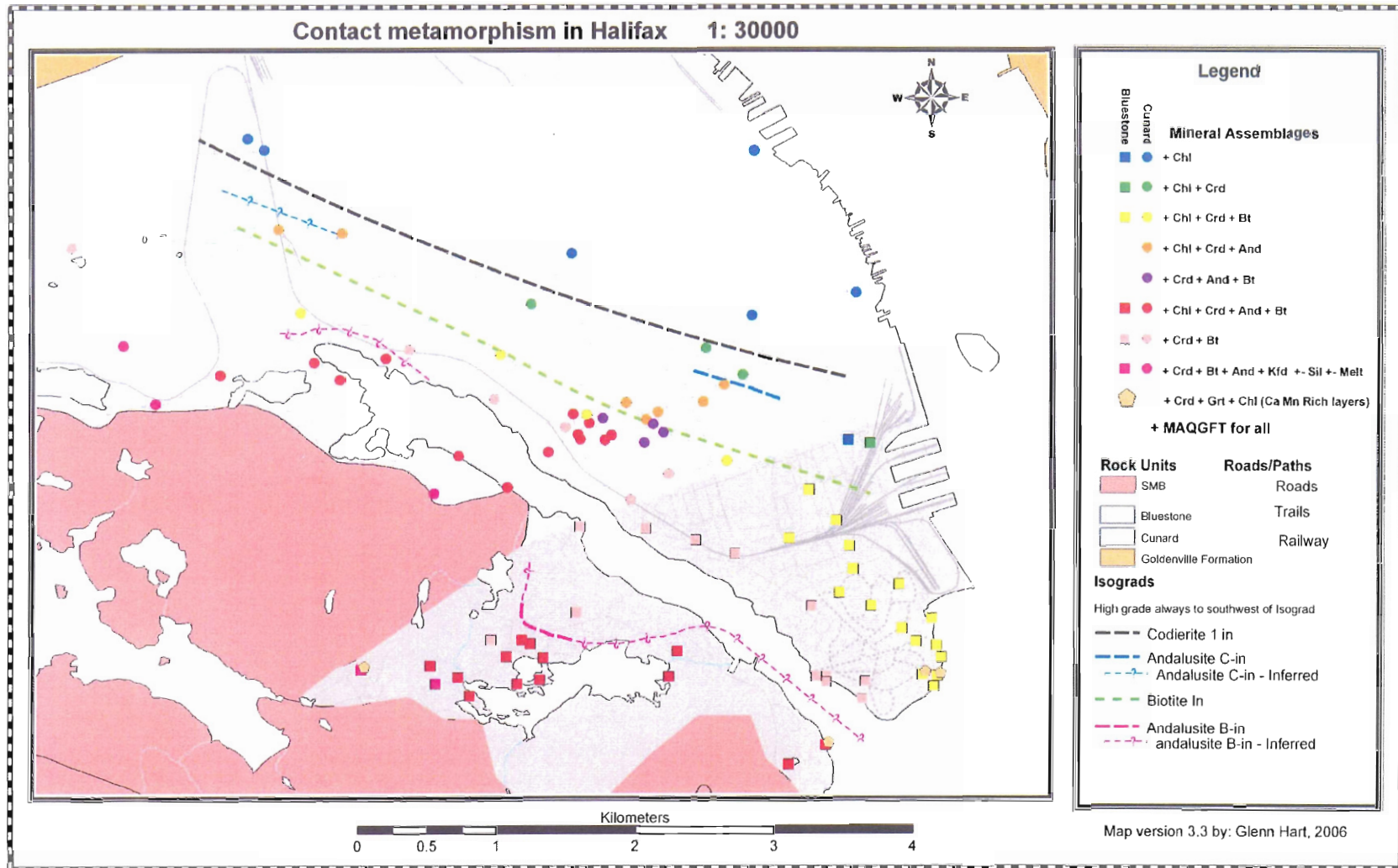


Fig 3.13: Map showing isograd distribution and mineral assemblages within study area. This information has been compiled into a modified GEOfield database (Lipovsky et al 2003).

3.5.2 Biotite zone (~1.6 km from contact)

The biotite-in isograd is not well located due to lack of samples. Biotite/muscovite stacks appear after chlorite/muscovite (Fig 3.11) as in Transect 2. Biotite/muscovite stacks increase in modal abundance towards the contact as Chl/Ms stacks disappear.

3.5.3 Between the Biotite zone to the contact

As with Transect 1 and 2, Transect 3 shows a large increase in abundance and size of andalusite adjacent to the contact in the Fairmount subdivision. Andalusite, biotite, and cordierite increase in size and abundance proximal to the contact and chlorite/muscovite stacks disappear within 400m. Annealed slaty cleavage occurs nearest the contact in Transects 1 and 2. This area was studied by Betts-Robertson (1998).

3.6 Summary of isograd sequences

The contact aureole, defined by the first appearance of cordierite, is approximately 3 km wide. It overprints the regional chlorite zone metamorphism in both the Bluestone and Cunard Members.

Within the Bluestone member, with increasing proximity to contact, the abundance of cordierite increases. The first appearance of biotite in chlorite/muscovite stacks marks the biotite-in isograd. Muscovite rims form around xenoblastic cordierite closer to the contact (~800m). The appearance of xenoblastic andalusite and quartz aggregates rimmed by biotite marks the andalusite-in isograd in the Williams Lake area, less than 1km from the contact.

Within the Cunard Member, in contrast to the Bluestone member, idioblastic chiastolite appears below the biotite-in isograd. The chiastolite shows cruciform texture. The biotite-in isograd occurs closer to the contact with nucleation of biotite in chlorite/muscovite stacks. Chiastolite increases in abundance towards the contact.

Chapter 4 Chemistry

4.1 Introduction

For a given set of P-T conditions, mineral assemblages and associated reactions depend on bulk composition. The contrast in isograd sequences between the Bluestone member and Cunard Member suggests a contrast in bulk composition.

To determine the likely reactions necessary to produce the early andalusite C-in isograd of the Cunard Member, whole rock, trace element and microprobe data representing a range of lithologies from the Cunard and Bluestone members within the study area were obtained to understand better the effect of bulk composition on mineral assemblage and isograds.

4.2 Whole-rock geochemistry

Whole-rock and trace element analyses representing a range of lithologies were obtained in 2004 (Table 4.1). X-Ray fluorescence (XRF) analyses performed at Saint Mary's University Regional Geochemistry Laboratory show elevated C and S in Cunard Member samples relative to Bluestone samples. Bluestone samples have elevated SiO₂, likely due to high quartz content in siltstone, and Cunard samples show higher Al₂O₃ relative to Bluestone samples. Elevated Al₂O₃ content can greatly influence mineral stability and assemblage in metapelitic rocks (Tinkham 2003).

An AFM ternary plot showing bulk composition variations relative to Al, Fe and Mg content shows a significant difference between Bluestone and Cunard Member rocks (Fig 4.2).

Major elements (wt % oxides)	Cunard			IWK 03	Mbe	Bluestone		HH LIGHT
	SS DARK	SS LIGHT	HH DARK			PPP04- 5A	PPP04- 5B	
SiO ₂	59.76	61.05	57.26	57.88	54.81	75.42	61.34	53.80
TiO ₂	0.99	0.95	0.98	0.97	1.01	0.56	0.99	0.76
Al ₂ O ₃	21.87	21.64	23.22	23.46	25.29	12.23	20.11	21.92
Fe ₂ O _{3t}	4.31	4.09	4.94	5.52	4.52	5.10	5.37	8.61
FeOt	3.88	3.68	4.45	4.97	4.07	4.59	4.83	7.75
MnO	0.04	0.04	0.05	0.05	0.06	0.08	0.06	0.04
MgO	0.91	0.98	1.86	1.79	1.32	1.15	1.20	2.26
CaO	0.48	0.50	0.22	0.15	0.23	0.33	0.16	0.19
Na ₂ O	1.20	1.12	0.95	1.18	1.47	1.55	1.21	0.84
K ₂ O	3.71	3.66	4.15	3.87	4.11	2.01	4.69	3.91
P ₂ O ₅	0.07	0.07	0.15	0.09	0.06	0.11	0.08	0.13
LOI	5.63	5.45	5.56	4.86	6.31	1.56	3.81	6.54
Carbon	0.49	0.45	0.52	0.46	0.46	0.04	0.07	0.25
Sulphur	0.36	0.81	0.71	1.12	0.14	0.25	0.11	3.66
Total (FeOt, LOI)	98.54	99.14	98.84	99.27	98.73	99.58	98.48	98.14

Table 4.1: Whole rock geochemical analyses of study area rocks. Note variations in C, S, SiO₂, and Al₂O₃ content between Cunard and Bluestone samples.

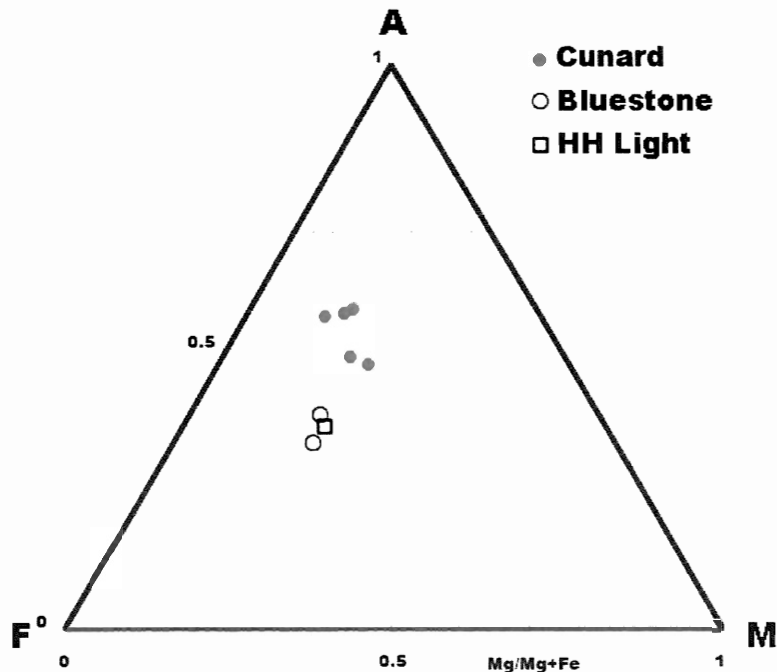


Fig 4.2: AFM diagram of bulk analysis of Halifax area rocks. Cunard samples include HH Dark, HH Light (silty Cunard) for comparison to Bluestone. Andalusite not present in Bluestone samples or HH Light.

4.3 Mineral Chemistry

Thirty polished thin sections representing a range in mineral assemblages and textures on all three transects were analyzed at Dalhousie Regional Electron Microprobe Laboratory. The instrument is a JEOL JXA-8200 microprobe with acceleration voltage 15 kV, spot size minimum 2 μm , and beam current 20 nA. For this study only silicate minerals were analyzed. All mineral analyses are reported in Appendix 3.

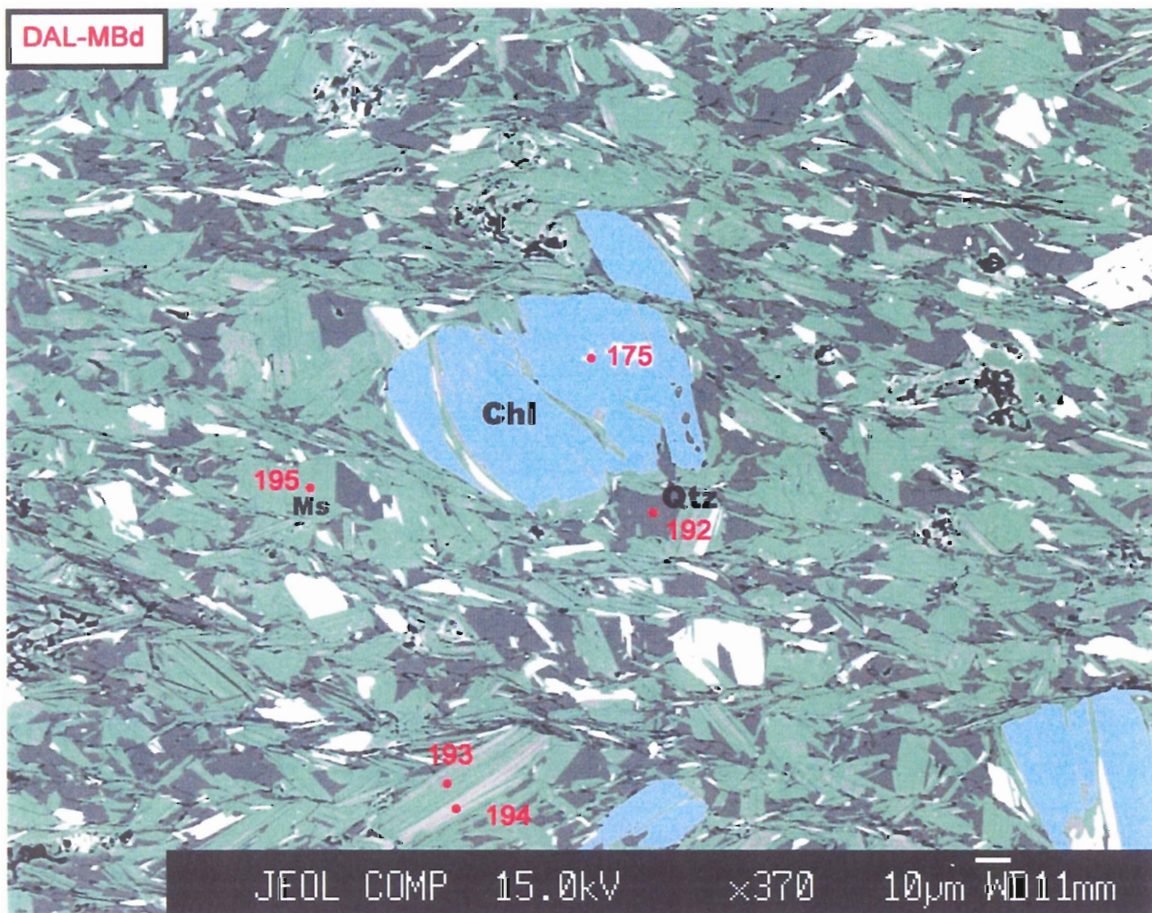


Fig 4.3: BSE image of sample MBd, Cunard Member, andalusite-in isograd. Chlorite/muscovite intergrowths in a quartz/muscovite matrix.

4.3.1 Muscovite, Cunard Member, below biotite-in isograd

Muscovites in low-grade zones (cordierite, chlorite and andalusite) are small idioblastic to xenoblastic aggregates within the matrix and larger, ovoid structures of interlayered muscovite and chlorite (Fig 3.2). Muscovite has an ideal composition of $\text{KAl}_2(\text{AlSi}_3\text{O}_{10})(\text{F}, \text{OH})_2$ (Deer et al. 1992). The average composition of muscovite in Cunard Member low-grade samples is $\text{K}_{0.8}\text{Na}_{0.2}\text{Al}_2(\text{AlSi}_3\text{O}_{10})(\text{F}, \text{OH})_2$. The most significant feature of analyzed muscovite is the anomalous Na, reflecting high paragonite ($\text{NaAl}_2(\text{AlSi}_3\text{O}_{10})(\text{F}, \text{OH})_2$) content. Expected values of paragonite in muscovite at low temperature are $\leq 5\%$ (Fig 4.4). Measured values are between 2% and 50% (Appendix I, Table A). The elevated Na content is interpreted to represent paragonite, likely interlayered with the muscovite, which is too small to be separately detected by the microprobe. Microprobe X-ray mapping for Na was attempted to locate paragonite but was unsuccessful. However, Hicks (1996) reported paragonite in Cunard Member samples from the Mahone Bay area.

Further analysis across lithologies was done to determine the extent of the paragonite distribution and its possible role in the formation of the andalusite C-in isograd. Paragonite content within the Cunard Member peaks at 63% with an average of 19%. Paragonite content >1 km from the contact averages 23%. Paragonite content drops proximal to the contact to between 2% and 8% (Fig 4.5).

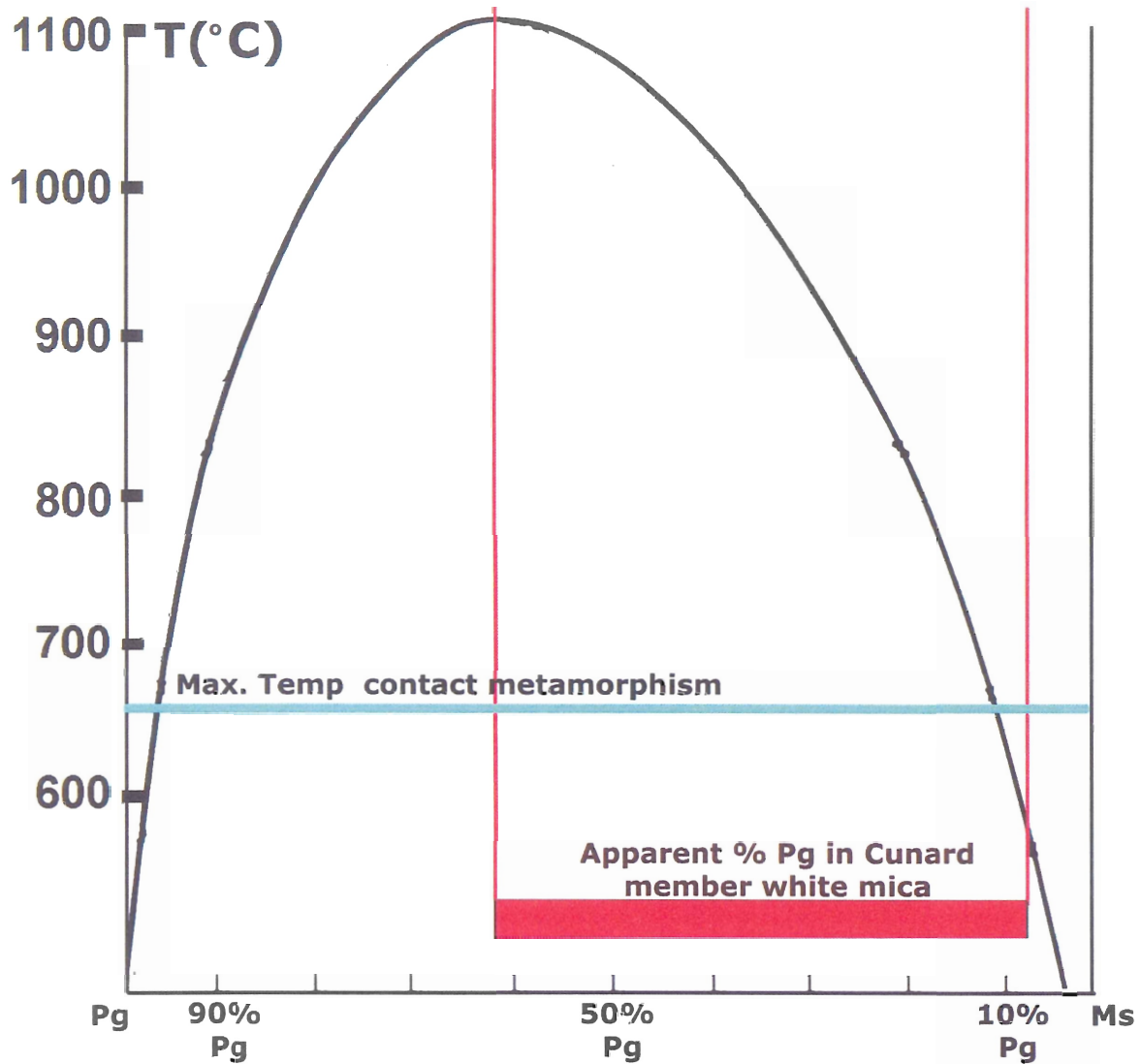


Fig 4.4: Paragonite/muscovite solvus. 100% muscovite on right. Highlighted range of paragonite (8%-43%) in Cunard). Horizontal line marks maximum temperatures within contact aureole. Vertical lines lie on range of temperatures which would allow for Pa content present (600°C-1050°C). (Modified from Eugster et al 1972)

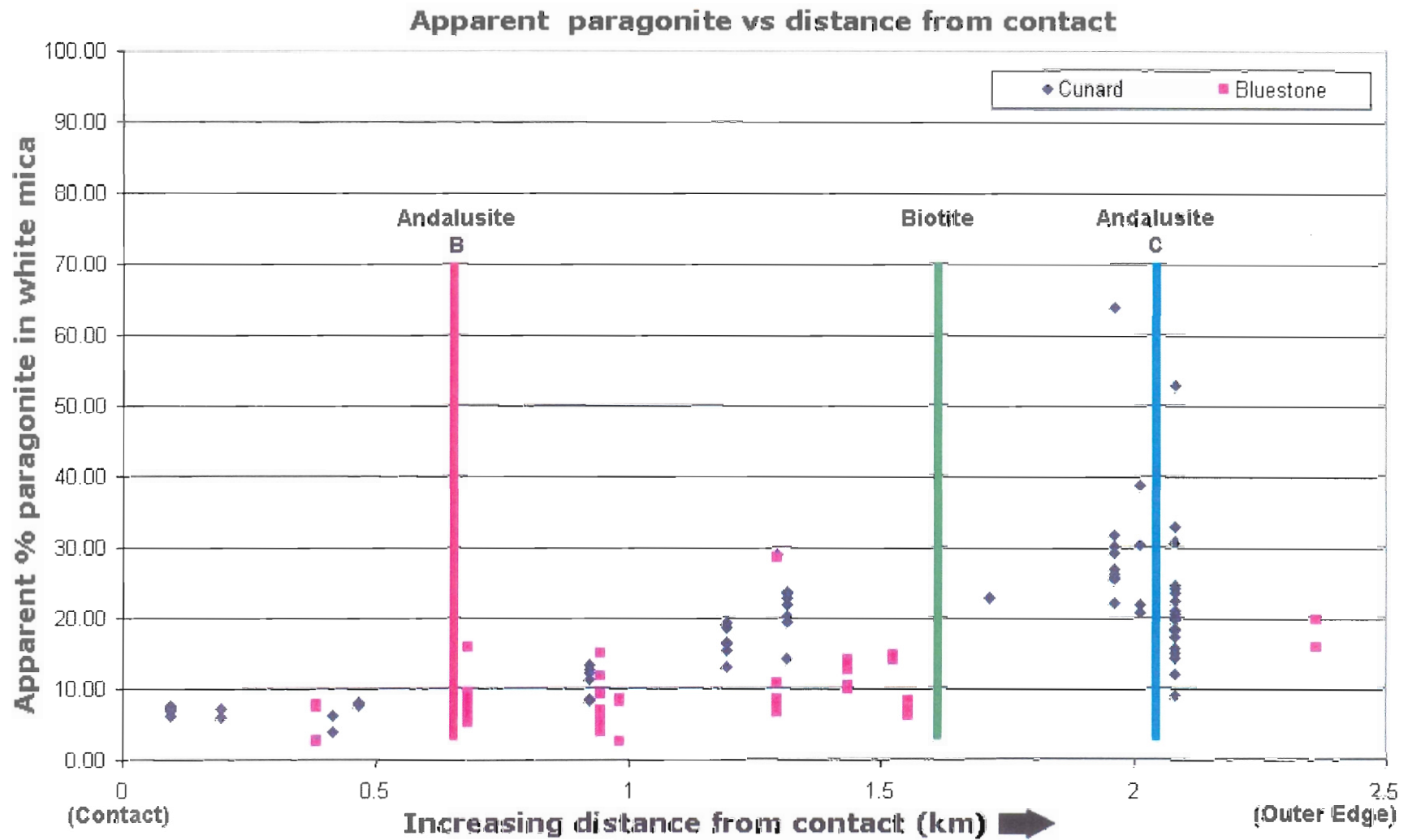


Fig 4.5: Paragonite content vs. distance from contact; approximate isograd locations within Transect 2 shown. Distances in km are relative to the nearest surface expression of the SMB. Average paragonite content is higher within Cunard samples in vicinity of Andalusite C and drops towards contact. $\text{Mol\% Pa} = \text{Na}/(\text{Na}+\text{K}+\text{Ca})$

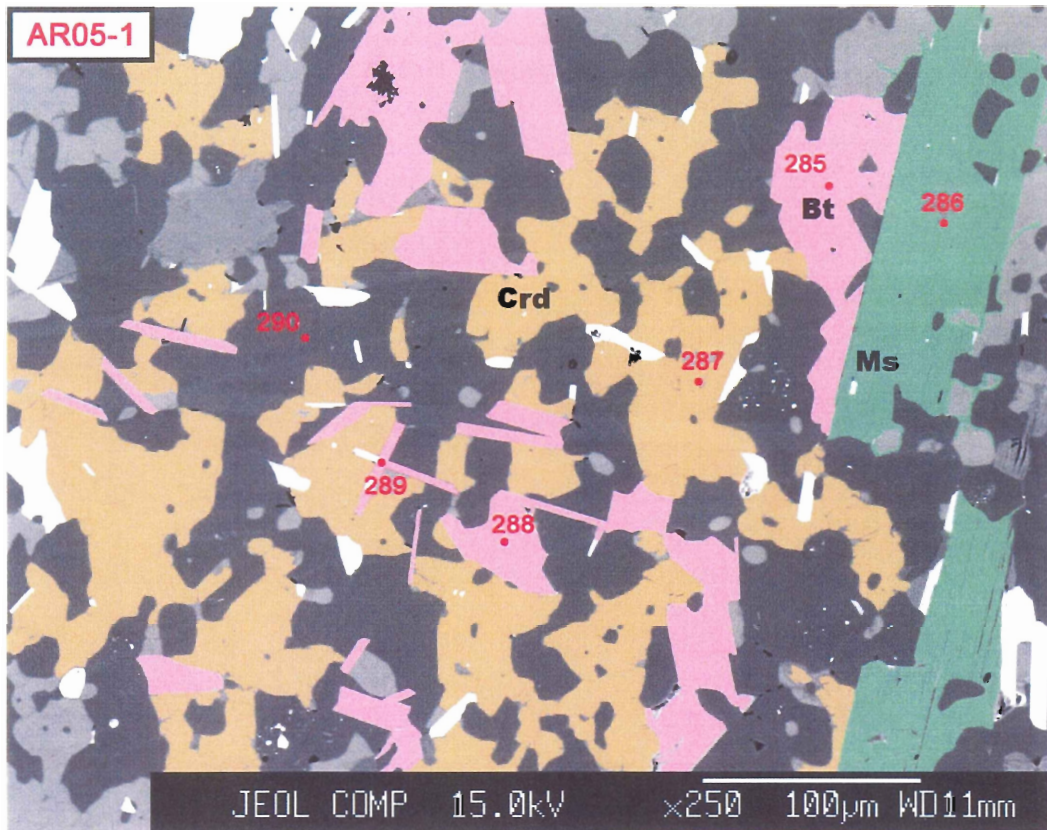


Fig 4.6: False colour BSE image of sample AR05-1, Cunard Member, close to contact. Muscovite forms large idioblastic crystals with little to no intergrowths. Chlorite is not present.

4.3.2 Muscovite, Cunard Member, above biotite-in isograd

In the Cunard Member above the biotite-in isograd, the mineral assemblage of cordierite, andalusite, and biotite, muscovite forms larger idioblastic crystals with no noticeable intergrowths, and chlorite is minimal (Fig 4.6). Muscovite is less abundant compared with lower grade Cunard Member samples (Fig 4.3). Paragonite content in muscovite within the high-grade zone (< 1 km of contact) averages 8%.

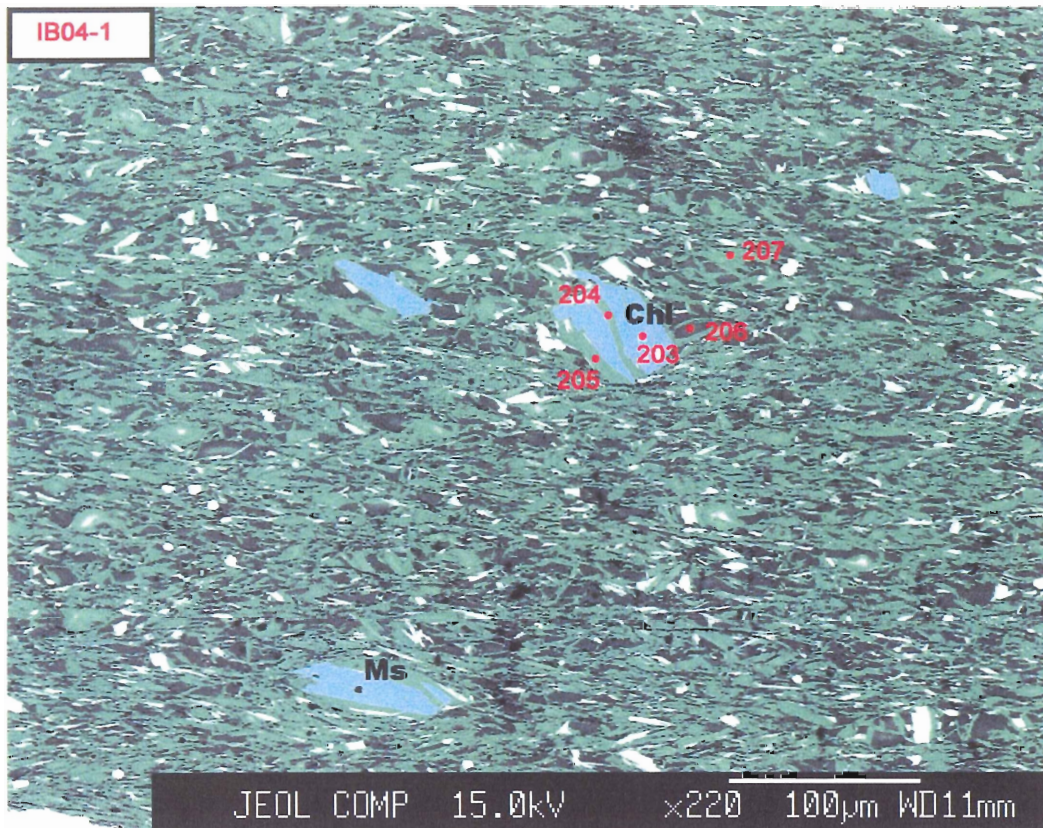


Fig 4.7: False colour BSE image of sample IB04-1, Bluestone member, low-grade zone (> 2km from contact). Chlorite/muscovite intergrowths in a quartz/muscovite matrix. Similar to low-grade Cunard samples.

4.3.3 Muscovite, Bluestone Member, below biotite-in isograd

Chlorite/muscovite stacks in the Bluestone member are identical to those in similar grade Cunard samples. However, Bluestone member muscovites contain less paragonite (avg. 8%) than Cunard Member muscovites, with only slight increases with distance from the contact (Fig 4.5). Paragonite content varies greatly between the two units, both in amount and distribution relative to the contact.

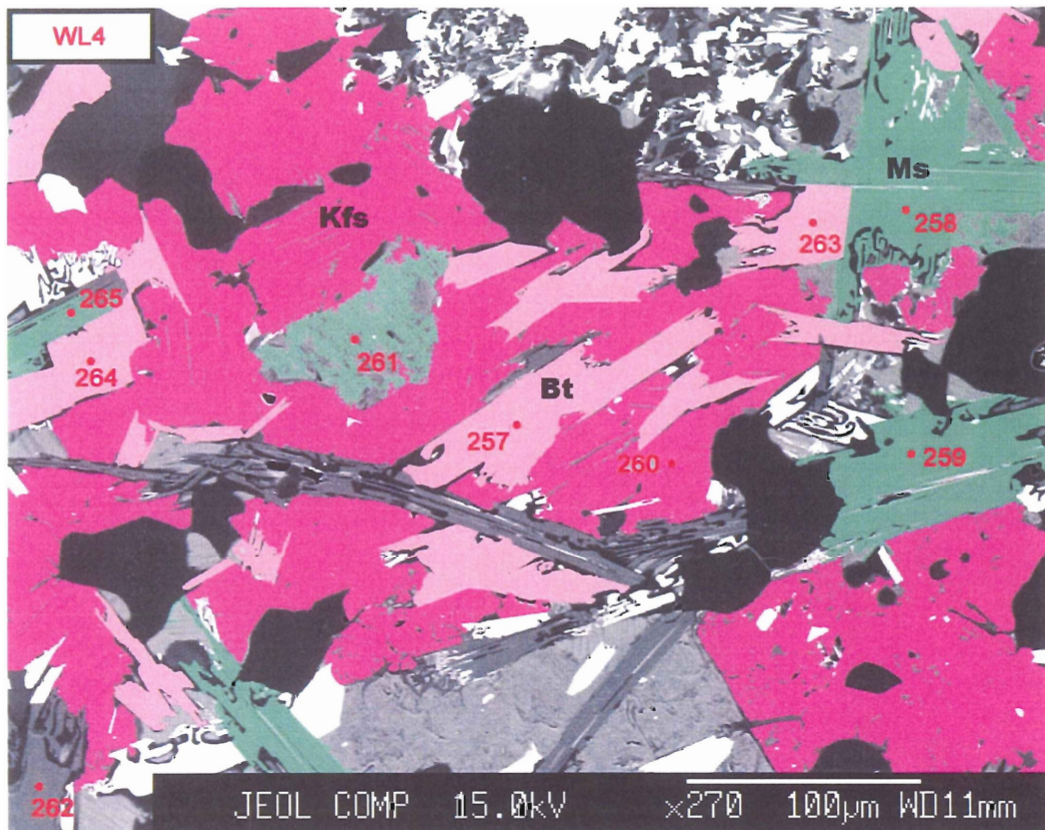


Fig 4.8: False colour BSE image of sample WL05-4, Bluestone member, high grade zone (< 500 m from contact). Symplectic intergrowth between muscovite and K-feldspar located near point 258.

4.3.4 Muscovite, Bluestone Member, above andalusite-in isograd

Muscovite forms idioblastic to xenoblastic crystals associated with biotite and K-feldspar. Muscovite forms a symplectic intergrowth with K-feldspar suggesting that K-feldspar replaces muscovite (Fig 4.8). Paragonite content in muscovite is between 7% and 8%, within the average range for all Bluestone samples, and compatible with a temperature of 600°C-650°C (Fig 4.4).

4.3.5 Chlorite

Chlorite, in both Bluestone and Cunard Member rocks, exists outside the contact aureole as ovoid aggregates interlayered with muscovite (Fig 4.3, Fig 4.7), remnants of the regional metamorphic assemblage (Hicks 1996). Chlorite Fe and Mg contents are approximately equal in Bluestone and Cunard Member samples, with average X_{Fe} of 0.54 and average X_{Mg} of 0.48. At the biotite-in isograd, biotite nucleates within and replaces chlorite within the muscovite/chlorite stacks (Fig 3.6, Fig 4.9).

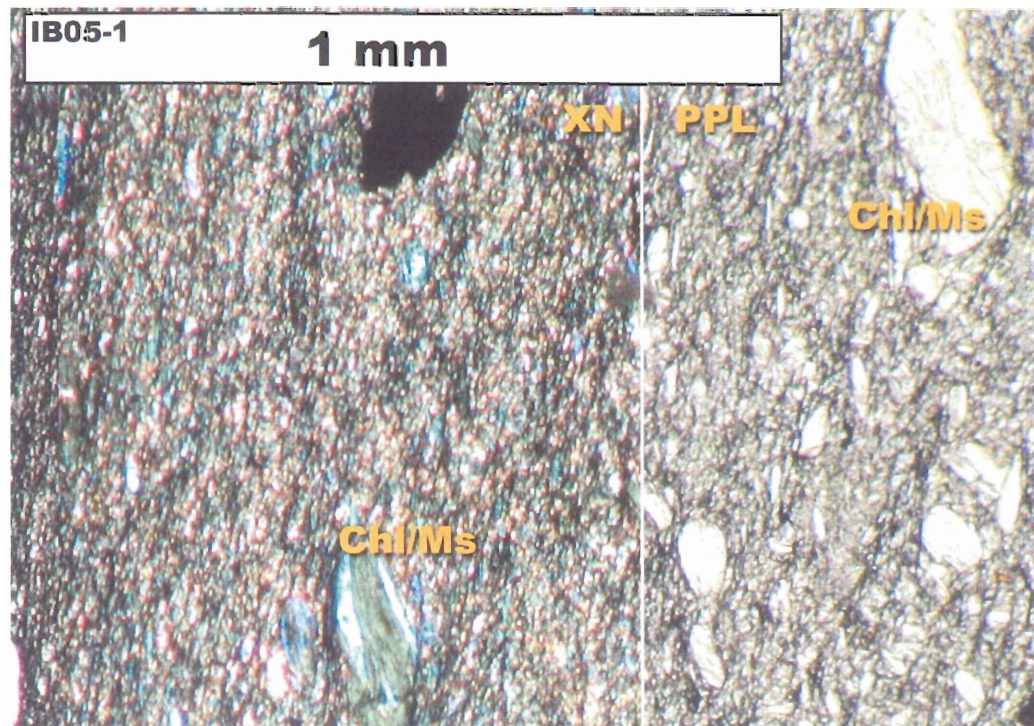


Fig 3.2: Muscovite/chlorite stacks from sample IB05-1. XN on left, PPL on right.

4.3.6 Biotite

Biotite within both the Cunard and Bluestone members first appears within chlorite/muscovite stacks (Fig 3.2,3.6). Biotite increases in modal abundance, grain size increases, and crystals become more idioblastic proximal to the contact (Fig 4.6, 4.8, 4.9) in both units.

Biotite ($\text{K}(\text{Fe}, \text{Mg})_3 \text{AlSi}_3 \text{O}_{10} (\text{OH})_2$), can be considered in terms of two end members: phlogopite ($\text{K Mg}_3 \text{AlSi}_3 \text{O}_{10} (\text{OH})_2$) and annite ($\text{K Fe}_3 \text{AlSi}_3 \text{O}_{10} (\text{OH})_2$). For a given bulk composition, X_{phl} typically increases with increasing metamorphic grade. Cunard samples have higher X_{phl} contents compared with Bluestone samples. Bluestone biotite composition averages $X_{\text{ann}} = 71\%$ and $X_{\text{phl}} = 29\%$. Cunard samples composition averages $X_{\text{ann}} = 57\%$, $X_{\text{phl}} = 43\%$. No systematic variation occurs in biotite composition in either unit with distance to the contact (Fig 4.11). The difference in biotite composition between the two members probably reflects bulk chemistry variations between the Bluestone and Cunard Members. Biotite above the andalusite B-in isograd within the Bluestone member encircles xenoblastic andalusite (Fig 4.10), possibly after muscovite and cordierite. The composition of this biotite ranges from $X_{\text{ann}} = 67\%$ to $X_{\text{ann}} = 78\%$.

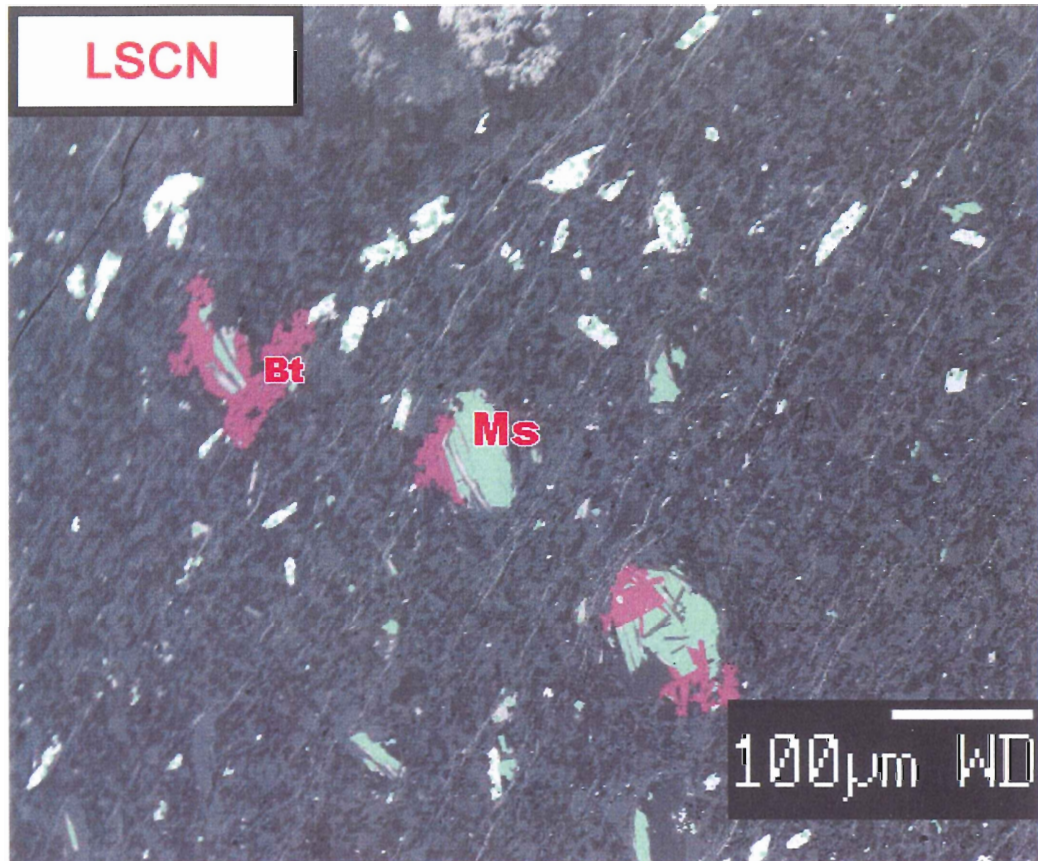


Fig 4.9: False colour BSE image LSCN, Cunard Member, Dalhousie campus (2000 m from contact). Intergrowths of biotite with chlorite and muscovite.

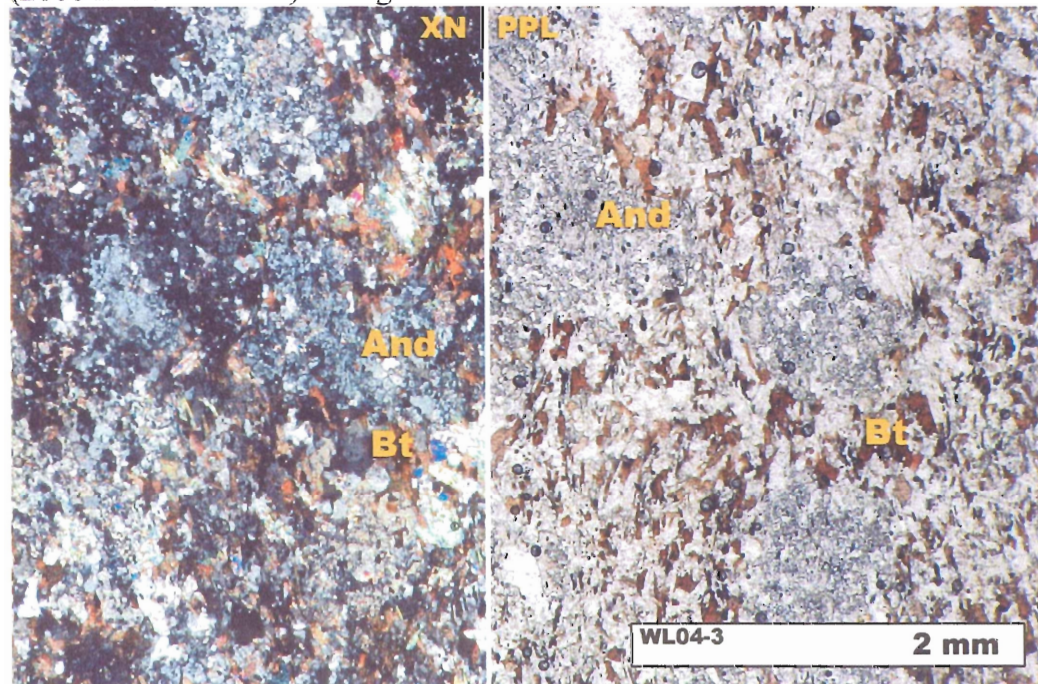


Fig 4.10: Biotite rims around andalusite in high-grade sample WL04-3, Bluestone member. XN on left, PPL on right.

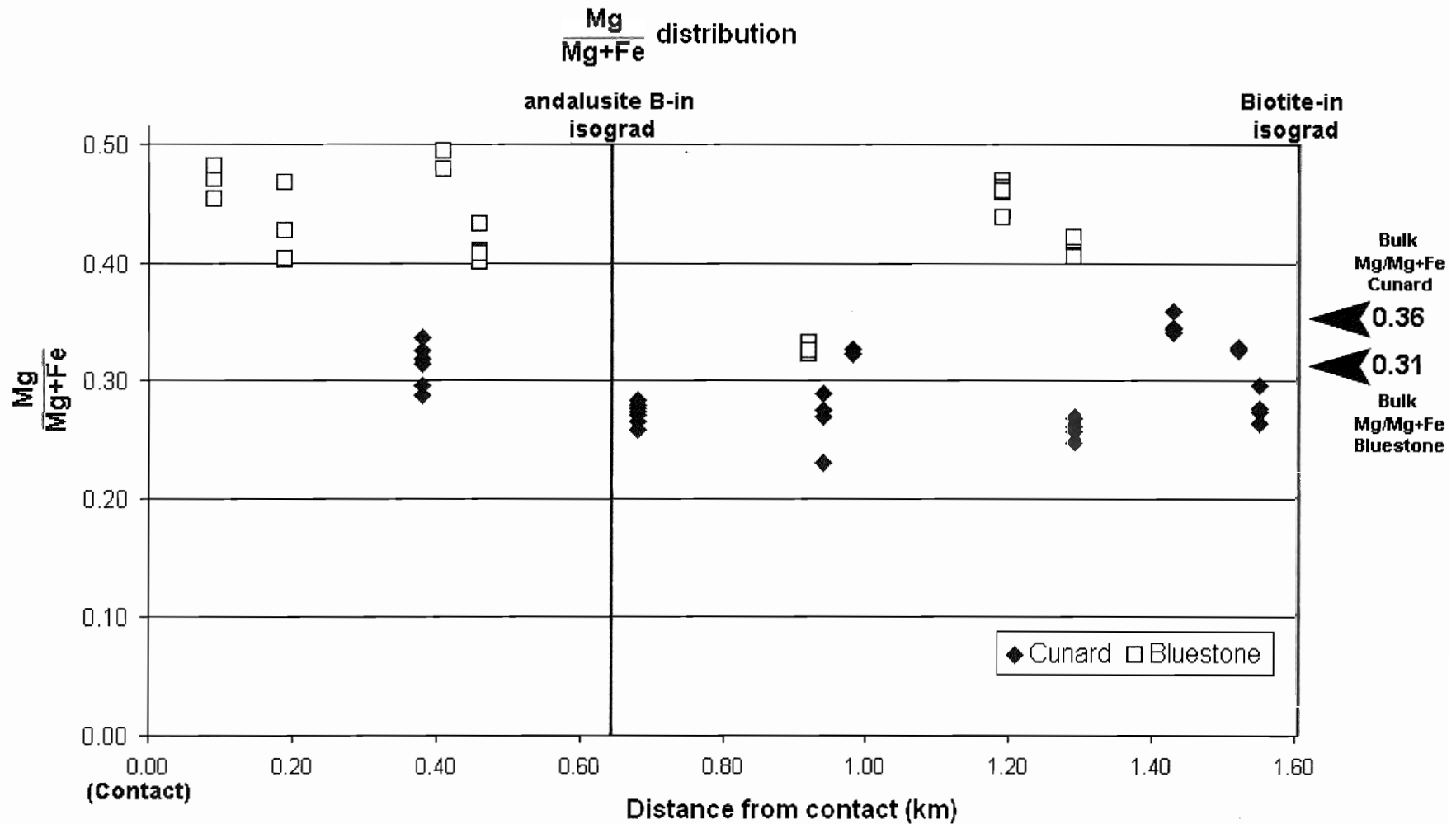


Fig 4.11: Mg/(Mg+Fe) in biotite vs. distance from contact. Distances in km are relative to the nearest surface expression of the SMB. Mg/(Mg+Fe) content is higher within Bluestone samples, but does not vary with distance from contact.

4.3.7 Feldspar

Plagioclase, in the form of An_0 to An_{20} (albite to oligoclase), is present throughout both the Cunard and Bluestone members, with %An increasing from albite at the outer edges of the aureole to oligoclase nearest the contact. K-feldspar appears as larger crystals typically associated with biotite (Fig 4.13) proximal to the contact. As discussed below, it may have formed in conjunction with the andalusite B-in isograd. K-feldspar appears further from the contact in the Bluestone member than in the Cunard Member (Fig 4.14). A symplectitic texture (Fig 4.8) is present between K-feldspar and biotite close to the contact, indicating a reaction between the two minerals.

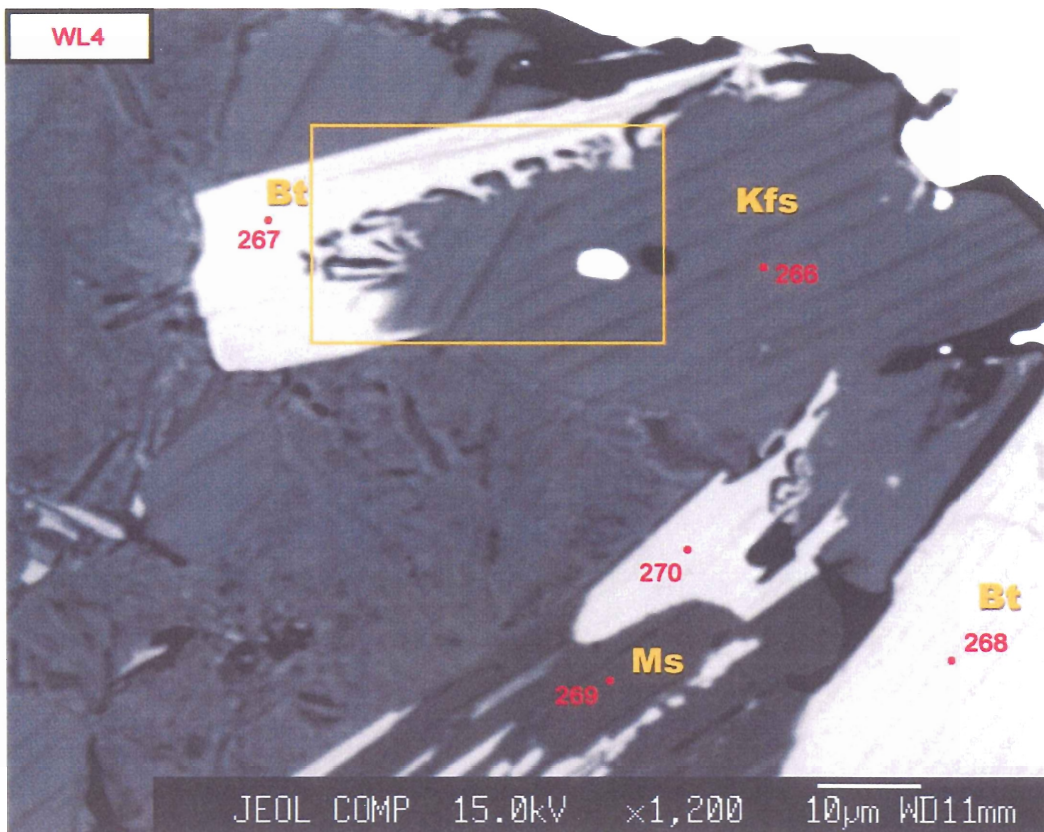


Fig 4.12: BSE image of sample W105-4, Bluestone member, above andalusite B-in isograd, (<500 m from contact). K-feldspar, biotite symplectitic texture highlighted in box indicating a Bt ↔ Kfs reaction.

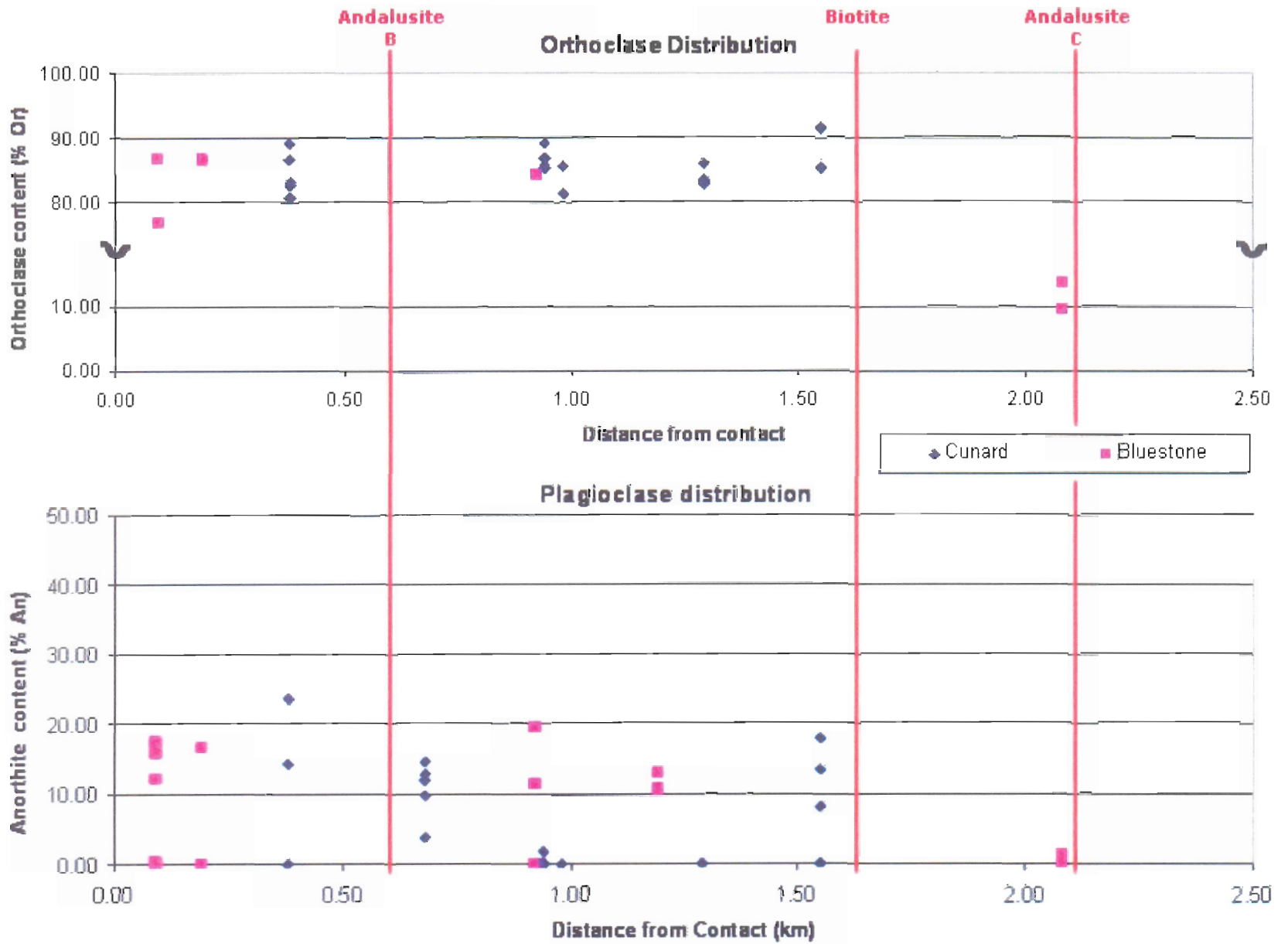


Fig 4.13: Feldspar composition and distribution in study area. K-feldspar shows no variation proximal to contact. Plagioclase shows an increase in An content towards the contact.

4.3.8 Andalusite

The composition of andalusite within the study area does not change. Modal abundance increases in both the Cunard and Bluestone members proximal to the contact as discussed in chapter 3. The first appearance and texture of andalusite varies between the Cunard and Bluestone members, but this is not associated with any detectable compositional variation.

4.3.9 Cordierite

Cordierite defines the extent of contact metamorphism in both units. Pristine cordierite is rare in the outer part of the aureole, where muscovite, chlorite and other fine-grained sheet silicates commonly replace it. Average Fe/Fe+Mg ratio in Cunard Member cordierite is 0.55 and in the Bluestone member is 0.45. This may reflect different bulk compositions but more data are needed to understand the significance of this variation. Cordierite appears to be involved in the reaction at the andalusite B-in isograd (Ch. 5), and may be involved in other reactions within the contact aureole. This problem deserves further study but is beyond the scope of this project.

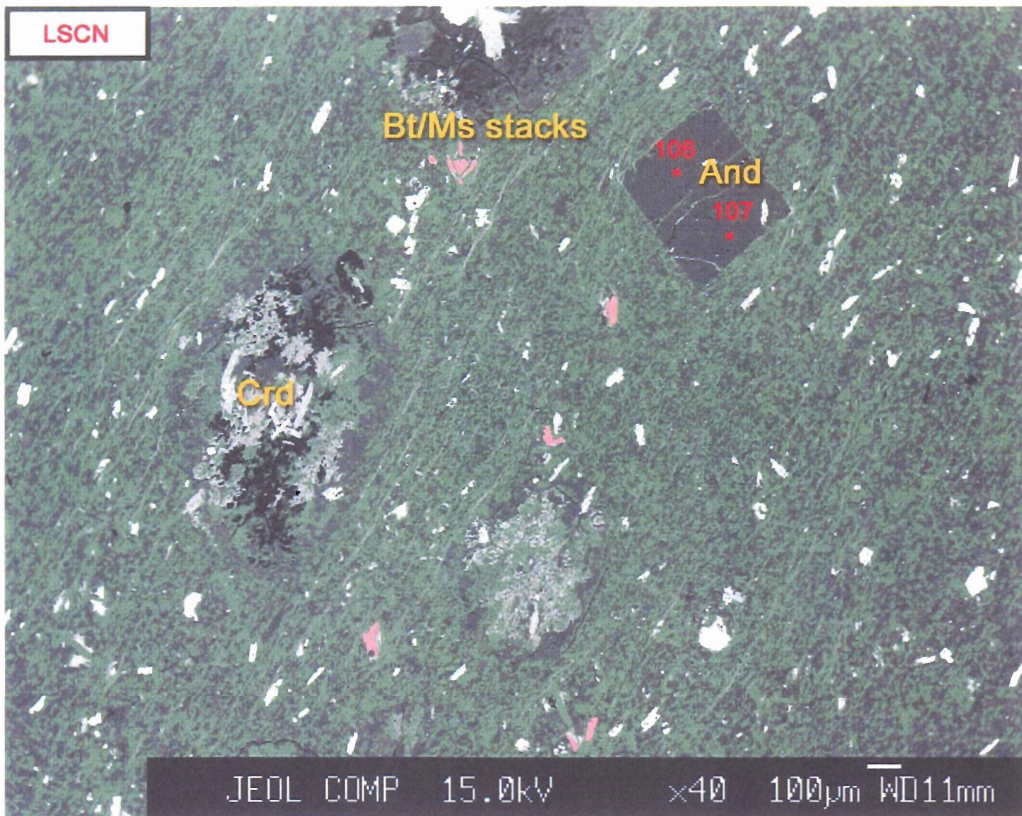


Fig 4.15: Idioblastic chiasolite in low-grade, sample LSCN, biotite zone, Cunard Member.

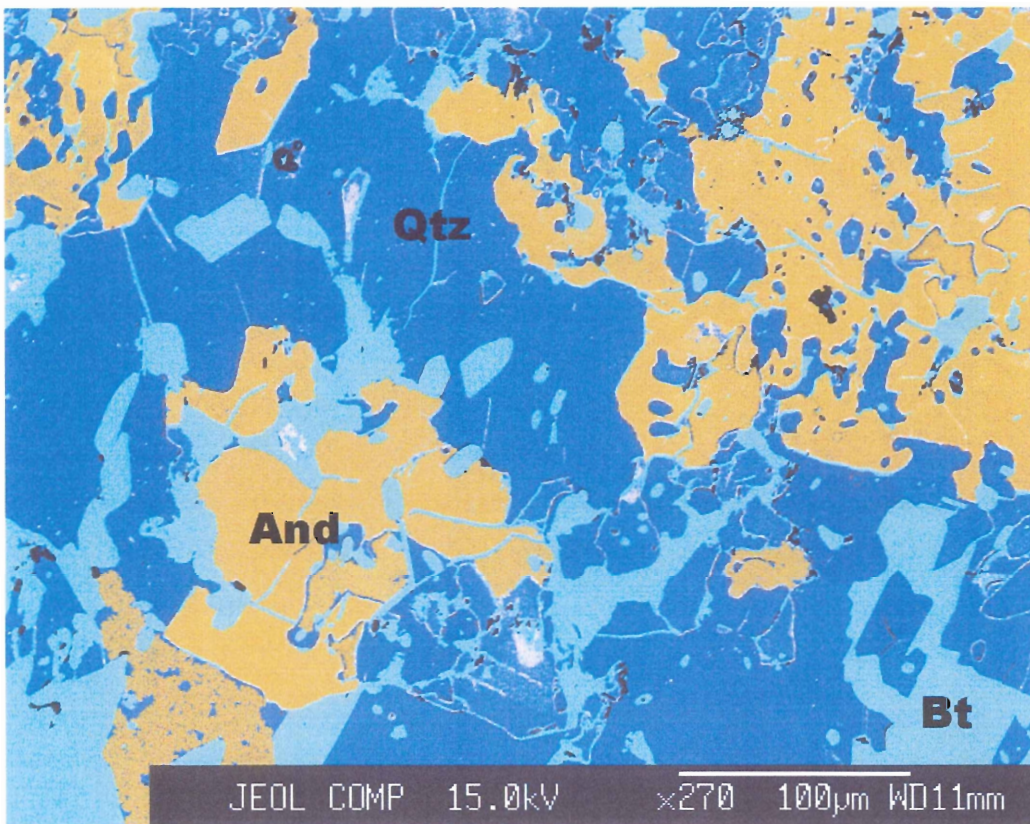


Fig 4.16: Spongy andalusite/quartz in high grade Bluestone member, sample WL05-12.

4.4 Powder X-ray diffraction results

Hicks (1996) used XRD analysis (2 μm fraction) in Halifax Formation rocks from the Mahone Bay area to study sheet silicate distribution. Her data showed that paragonite is present in the Cunard Member in chlorite zone samples. Microprobe analysis of micas in my study area showed high Na contents. XRD analysis was therefore performed to determine whether paragonite is also present in the study area.

Samples were prepared by crushing and sieving to a 125 μm fraction. XRD results did not reveal paragonite in any of the samples. One possible reason is the fine interleaving of muscovite and paragonite (< 50 μm scale). Livi et al. (1997) documented the problems with detecting paragonite in finely interlayered micas, as XRD cannot easily distinguish fine layers from a homogeneous structure on a μm scale. Further progress requires sample preparation techniques not available for this study.

Chapter 5

P-T conditions and metamorphic reactions

5.1 Introduction

For a given bulk composition, mineral stability, and therefore mineral assemblages and reactions, are determined by pressure and temperature. Determination of pressure and temperatures experienced by a rock of given composition allows a better understanding of the reactions and possible mineral assemblages at the time of contact metamorphism.

Reactions and associated isograds within the contact aureole depend on the bulk composition variations discussed in chapters 3 and 4, which include an increased Na content (expressed as paragonite), and higher Al_2O_3 content in Cunard Member rocks, as well as less C and higher SiO_2 content in Bluestone rocks. In some cases (e.g. biotite-in isograd), similar micro-scale chemistry (chlorite/muscovite stacks present in both units) allows the same reaction to occur in both the Bluestone and the Cunard Members at the same position in the aureole. In other cases, differences in bulk chemistry, notably high Al_2O_3 content, collectively result in a different sequence of mineral assemblages and isograds between the two units.

The reactions of interest to this study area are:

- (1) Biotite-in (both units)
- (2) Andalusite B-in (Bluestone)
- (3) Andalusite C-in (Cunard)

Other reactions, including those involving cordierite, are not considered here.

5.2 Reactions and P-T grid

5.2.1 Biotite-in

The biotite-in isograd is laterally continuous between the Bluestone and Cunard Members and is associated with similar textures. A reasonable interpretation is that the reaction responsible for the appearance of biotite is the same in both units.

Table 5.2.1: Mineral assemblages below and above biotite-in isograd

Minerals below biotite-in isograd:	Minerals above biotite-in isograd:
muscovite	muscovite
chlorite	biotite
cordierite	cordierite
quartz	quartz
albite	albite
(andalusite in Cunard Member)	(andalusite in Cunard Member)
(paragonite in Cunard Member)	(minor chlorite persists in both units)
oxides	oxides
sulphides	sulphides

Based on the above mineral assemblages, a likely reaction is:



The position of this reaction has been calculated using the computer program PTXSS (5.1, Fig 5.5). This reaction occurs at around 500°C at a pressure of 3 kb within the andalusite stability field, which is consistent with previously determined temperature estimates for these rocks (Mahoney 1996). The plotted positions are for the Mg -end member phases of the Fe↔Mg solid solutions (biotite, chlorite, and cordierite) due to uncertainties in thermodynamic parameters for Fe end members. Plots generated using the appropriate calculated activities show little to no variation in plot location, likely due to the near equal Fe/Mg ratios of the three minerals.

5.2.2 Andalusite C– in

Andalusite appears in the Cunard Member below the biotite isograd, leading to the unusual isograd sequence:



The appearance of andalusite below the biotite-in isograd is not included within any of the normal contact metamorphic facies series listed by Pattison et al (1991), suggesting that a relatively unusual reaction, possibly linked to the highly aluminous bulk composition, is responsible for the early appearance of andalusite.

Table 5.2.2: Mineral assemblages below and above Andalusite C-in isograd (Cunard Member only)

Minerals below Andalusite C-in isograd:	Minerals above Andalusite C-in isograd:
muscovite	muscovite
paragonite	andalusite
chlorite	chlorite
cordierite	cordierite
quartz	quartz
albite	albite
oxides (rutile)	oxides (rutile)
sulphides (pyrrhotite and pyrite)	sulphides (pyrrhotite and pyrite)

Constraints on the nature of this reaction are:

- It must involve minerals present below the andalusite C-in isograd.
- It must occur at lower temperature than the biotite-forming reaction (Reaction 5.1).
- It cannot produce biotite by the same reaction
- It must include a phase not present in Bluestone rocks.

Taken together, these constraints suggest paragonite to be the key reactant involved. Using the above mineral assemblages and constraints, a likely reaction is:

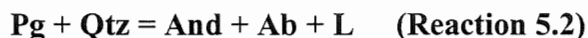
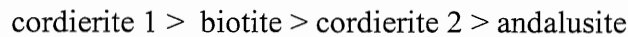


Figure 5.5 shows the position of Reaction 5.2, calculated using PTXSS for end-member paragonite. This reaction occurs at around 450°C in the andalusite stability field. Reaction 2 is a likely candidate for the reaction necessary to produce the andalusite C-in isograd. This reaction cannot occur in the paragonite-free Bluestone member, creating a laterally discontinuous andalusite-in isograd, which stops at the lithological contact with Bluestone member.

5.2.3 Andalusite B-in

Andalusite within the Bluestone member appears in a “normal” contact metamorphic isograd sequence of:



The appearance of biotite below andalusite is typical of contact metamorphism (Pattison et al 1991), with the progression up grade of biotite > cordierite > andalusite being the prevalent sequence in low-pressure meta-pelitic, contact metamorphic series.

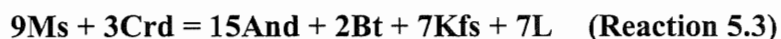
Table 5.2.3: Mineral assemblages below and above Andalusite B-in isograd

Minerals below Andalusite B-in:	Minerals above Andalusite B-in:
biotite	andalusite
muscovite	biotite
cordierite	muscovite
quartz	cordierite
oxides	quartz
sulphides	K-feldspar
plagioclase (An ₀₋₂₀)	plagioclase (An ₀₋₂₀)
K-feldspar (minor in sample PCR-10)	oxides
	sulphides

Determination of the andalusite-producing reaction was accomplished by visual inspection of thin sections (Fig 5.1, Fig 5.2), microprobe analyses of associated minerals (Fig 5.3, Fig 5.4), and calculations using PTXSS (Reaction 5.3, Fig 5.5). Below the andalusite B-in isograd, abundant ovoid cordierite is rimmed by muscovite and minor biotite. Above the isograd, biotite with minor muscovite rims ovoid xenoblastic andalusite. Further analysis by microprobe

and inspection of false color BSE images (Fig 5.3, Fig 5.4) suggests that the assemblage cordierite + muscovite is being replaced by biotite + andalusite.

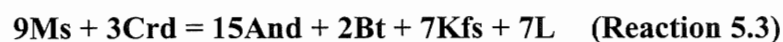
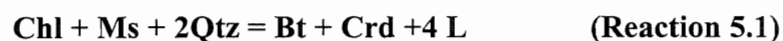
This textural information, coupled with the above mineral assemblages, suggests that the reaction responsible for the andalusite B-in isograd is:



Pattison et al (1991) have documented this reaction and its position, calculated using PTXSS (Berman 1988, 1991) for Mg end members, is plotted in Fig 5.5 (Reaction 5.3). At a pressure of 3 kb this reaction occurs at around 600°C.

5.2.5 Summary of isograds and reactions

Three reactions and their relative positions in P-T space are necessary to determine the relationship between the contrasting andalusite isograds in the Bluestone member and Cunard Member respectively. The two reactions must bracket the position of the biotite-in isograd, with andalusite-C at lower temperature and andalusite-B at a higher temperature.



The above reactions are possible given the bulk chemistry of the samples in the study areas. The two andalusite isograds formed by the above reactions are approximately 70°C apart for a pressure of 3 kb (5.1, 5.3 Fig 5.5). Reaction 5.1 allows for the biotite-in isograd to lie between the two andalusite-in isograds (closer to the andalusite C-in) in P-T space (Fig 5.5) at 560°C for a pressure of 3 kb.

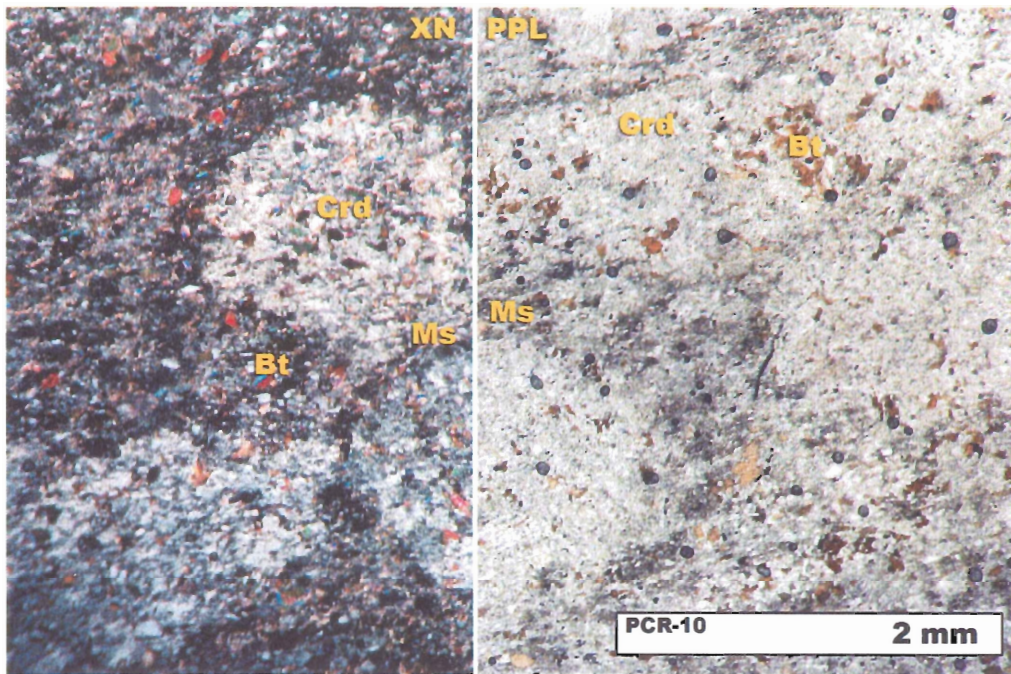


Fig 5.1: Muscovite with minor biotite rims around cordierite in sample PCR-10, below andalusite B-in isograd. XN on left, PPL on right.

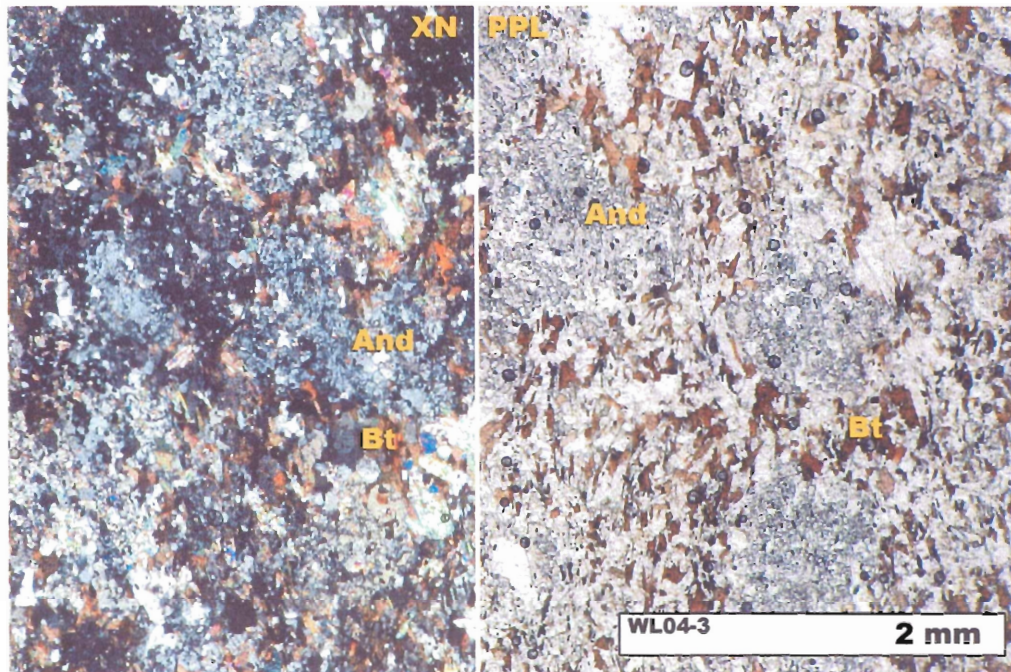


Fig 5.2: Biotite rims around andalusite in high-grade sample WL04-3, above andalusite B-in isograd. XN on left, PPL on right.

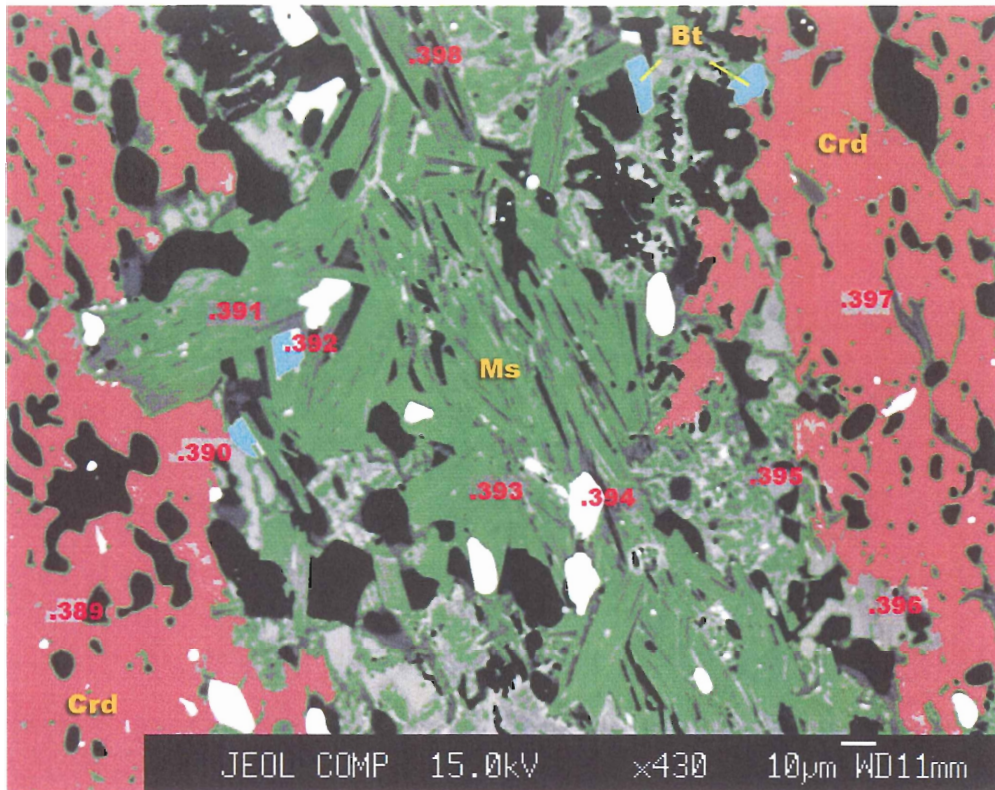


Fig 5.3: Sample WL05-15. False color BSE image showing muscovite (green) between cordierite (rose) below andalusite B-in isograd.

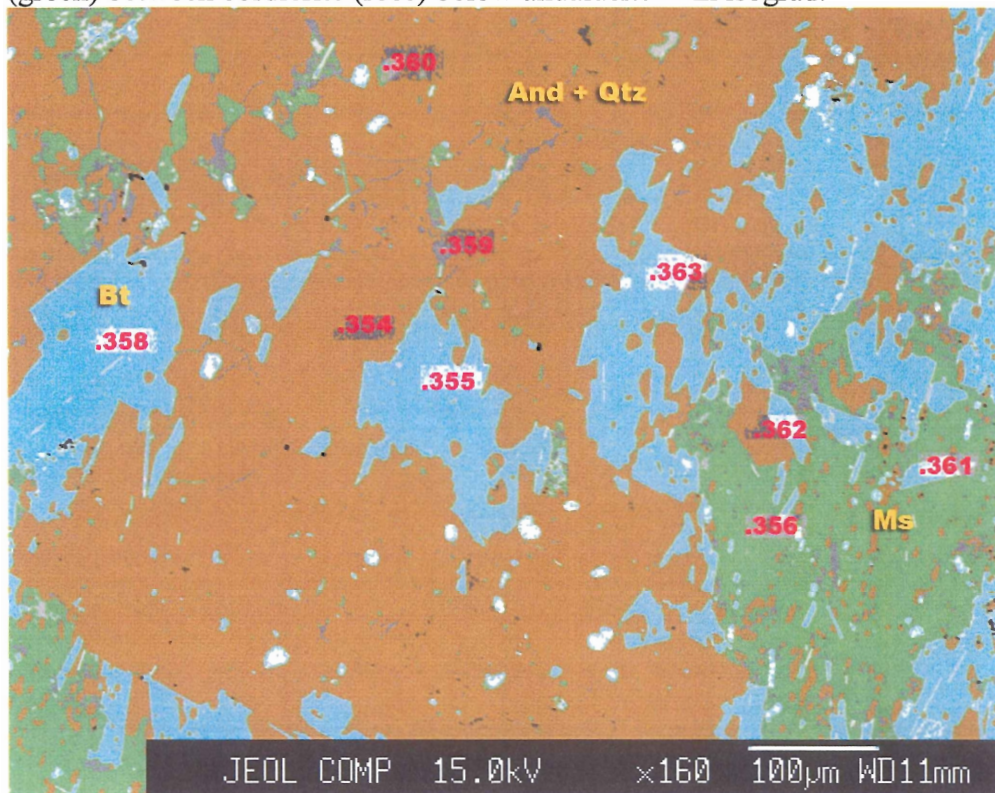


Fig 5.4: Sample WL05-12 False color BSE image showing biotite (blue) with minor muscovite (green) surrounding andalusite/quartz (brown)

5.2.4 P-T Grid

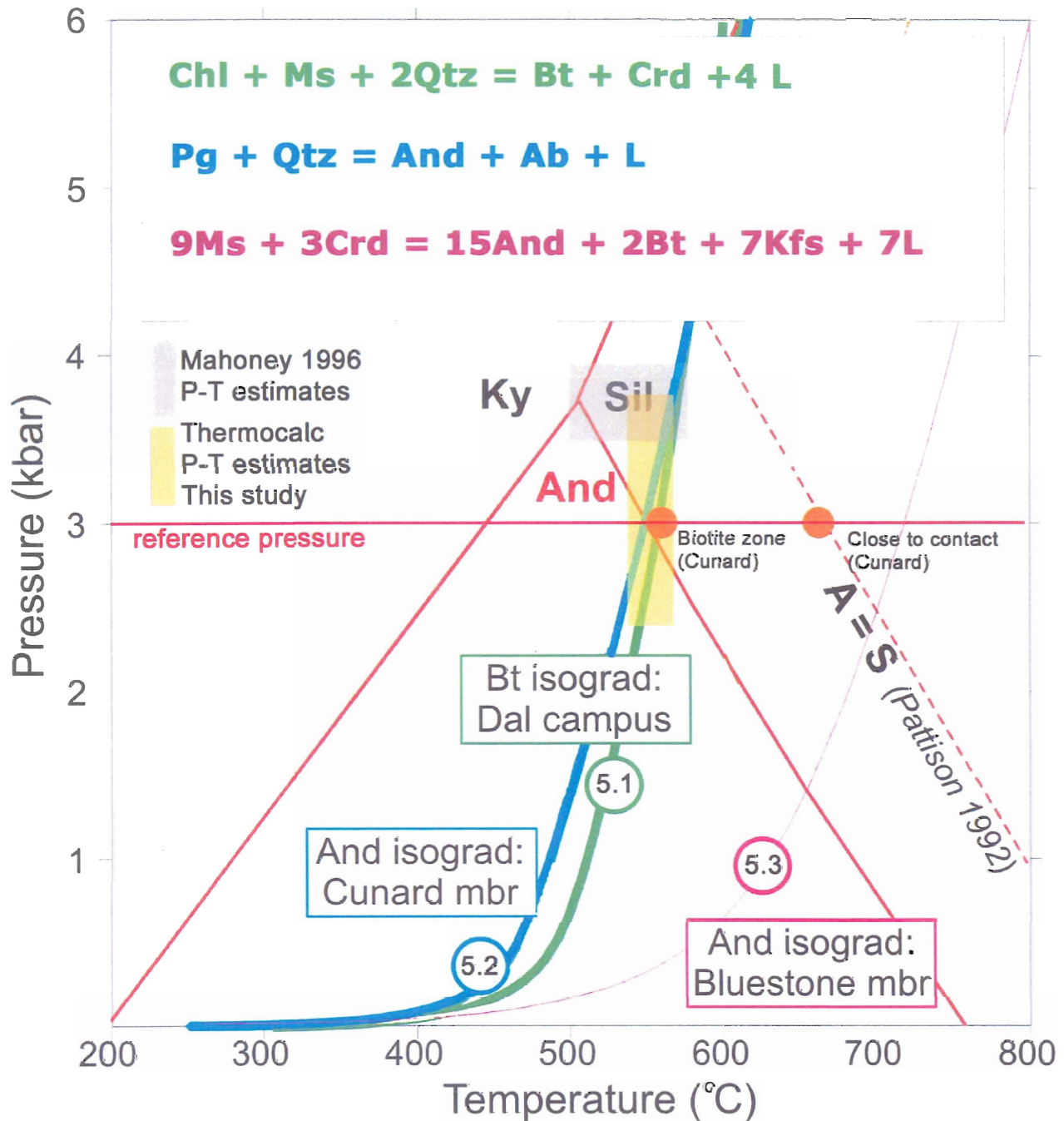


Fig 5.5: P-T grid of likely reactions and their distribution in P-T space. Calculated using PTXSS (Berman 1988,1991) using ideal solutions and Mg end members (biotite, chlorite, and cordierite). A=S is modified Al₂SiO₅ triple point and corresponding higher temperature location of the andalusite/sillimanite reaction as proposed by Pattison (1992). P-T estimates at 3 kb from sample location LSCN (biotite zone), T=551°C ± 6°C and AR05-S (close to contact), T=645°C ± 16°C calculated by ThermoCalc.

5.3 P-T conditions

5.3.1 Constraints from P-T grid

The P-T conditions in the Halifax Formation contact aureole are constrained to lie within the andalusite stability field, as andalusite is the dominant Al_2SiO_5 polymorph present throughout the rocks (only rare sillimanite at the contact). The position of the andalusite/kyanite/sillimanite triple point lies at $T = 500^\circ\text{C}$ and a maximum pressure of 3.7 kb (Holdaway 1971). Pattison (1992), however, argued that the Al_2SiO_5 triple point is actually higher and should be located ca 5 kb and 575°C based on observations of natural assemblages which could not form at temperatures and/or pressures of the standard Al_2SiO_5 triple point.

5.3.2 P-T estimates using ThermoCalc

ThermoCalc (Powell and Holland 1998) is a multi-equilibrium calculation software package that uses an internally consistent thermodynamic dataset. By manipulating the thermodynamic dataset, using known bulk compositions and mineral assemblages, ThermoCalc is able to produce numerous outputs involving mineral reactions including P-T estimates and pseudosections (petrogenetic grid for a specific bulk composition).

Using microprobe data from the Cunard Member, biotite zone sample LSCN, with an assumed equilibrium assemblage of muscovite, biotite, cordierite, chlorite and albite, estimates of: $T = 561^\circ\text{C} \pm 64^\circ\text{C}$ and $P = 3.3 \text{ kb} \pm 2.2 \text{ kb}$ were obtained using ThermoCalc in average P-T mode. Using the average temperature function of ThermoCalc, a temperature of $551^\circ\text{C} \pm 6^\circ\text{C}$ was estimated for a pressure of 3 kb. This point has been plotted on Fig 5.5. Differences in the ThermoCalc results are the result of the different types of calculations involved. Average P-T mode calculates both pressure and temperature, with pressure calculations being less precise, leading to large errors in both estimates. Average T mode calculates likely temperatures for a specified pressure, giving a more precise temperature calculation but requiring a known or

— assumed P. This value is within reported range for T and P of Halifax Formation rocks in the contact aureole at the northeast edge of the South Mountain Batholith (Mahoney 1996).

Additional microprobe data from sample AR05-5, a high-grade Cunard Member sample near the contact, was used with the assemblage muscovite, biotite, cordierite, plagioclase, in average T mode to estimate a temperature of $645^{\circ}\text{C} \pm 16^{\circ}\text{C}$ at a pressure of 3 kb. Figure 5.5 shows the position of this estimate on the petrogenetic grid and its relation to the reactions discussed earlier.

Chapter 6 Discussion and Conclusions

6.1 Discussion

Previous work on the contact aureole of the SMB failed to recognize the distinctive isograd sequence reported here for the Cunard Member. Other studies (e.g. Betts-Robinson 1998, Bhatnagar 1998) were concerned with features in the immediate vicinity of the contact and did not extend to the outer part of the aureole where the unusual isograd sequence occurs. Mahoney (1996), who studied the contact aureole throughout Nova Scotia, only sampled four points in the Halifax area, all at varying grades, two in the Cunard Member and two in the Bluestone member. She reported an isograd sequence of cordierite > biotite > andalusite based on a low-grade sample from Point Pleasant Park (Bluestone member) where andalusite is absent and a high-grade sample from Purcell's Cove Road (Bluestone member).

This more detailed study has led to the determination that the Halifax area is underlain by not one, but two distinct lithologies with different isograd sequences. Lithological differences from the outcrop level to the geochemical level are observable and reproducible; which supports the proposal that Halifax Formation on the Halifax Peninsula has two lithological units. The Cunard Member is a siltstone-poor, high-Al, paragonite-present (in most samples), graphite-rich black slate in which andalusite forms at lower temperature than biotite. The Bluestone member is a siltstone-rich, paragonite-absent, blue-grey slate in which the andalusite-in isograd occurs above the biotite-in isograd.

Two separate lithologies with different bulk-rock and mineral compositions account for the different andalusite-in isograds within those units. Where the mineral assemblage allows for the same reaction (biotite-in) across both units, the corresponding isograd is continuous. Where differences in bulk chemistry allow a specific reaction to occur in one unit and not in the other,

discontinuous isograds (andalusite C vs. andalusite B) end at unit boundaries. In particular, the Al-rich bulk composition of the Cunard Member and the resulting presence of paragonite at low-grade have led to the appearance of andalusite at a relatively low temperature and a corresponding discontinuity in the andalusite-in isograd, which is truncated by the Bluestone member to the southeast and the Goldenville Formation to the northwest.

In Meguma Group rocks of the Mahone Bay area, Hicks (1996) found paragonite only in the Cunard Member. To find the early andalusite elsewhere in Nova Scotia, a likely location would be anywhere the South Mountain Batholith is in direct contact with Cunard Member rocks. As shown by a regional metamorphic study (Mahoney 1996), small sample numbers can miss locally significant metamorphic anomalies like the early appearance of andalusite in the Halifax area.

A preliminary reconnaissance study of isograd distribution in the Hammond's Plains area (Lucasville Road – Glen Arbour), west of Halifax, indicates the appearance of andalusite before biotite in Cunard Member rocks of that area as well. Large chiastolite crystals 0.5 mm across and >2 cm are identifiable in outcrop ~2.5 km from the contact.

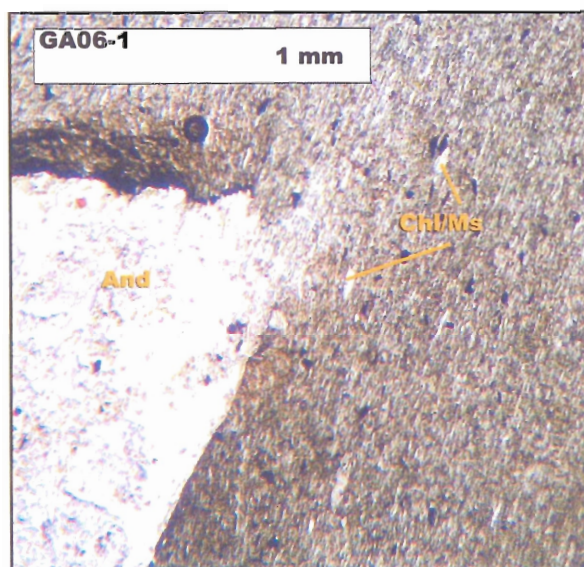


Fig 5.6: Andalusite apparently without biotite from sample GA06-1 (Cunard Member) ~2.5 km from contact in Glen Arbour. This indicates that andalusite appears before biotite in other parts of the Cunard Member. More work is needed.

6.2 Conclusions

The presence of two distinct andalusite isograds within the Halifax Formation in the study area can be explained in terms of the lithological and chemical variations between the Bluestone and Cunard Members. A series of likely reactions has been determined which accounts for the observed sequence of isograds. In particular, this study has demonstrated that:

1. The Halifax Formation on the Halifax Peninsula and surroundings consists of two distinct lithological units. The graphitic black slate of the Cunard Member underlies Halifax from the vicinity of Oakland Road northwest to Bedford Basin, where it overlies the Goldenville Formation. The silty, blue-grey Bluestone member overlies the Cunard Member from Oakland Road southeast into Point Pleasant Park, and outcrops in the Williams Lake - Purcell's Cove area across the North West Arm. The two units are distinguishable at all scales, from the outcrop level (color, siltstone content, and mineralogy), to the chemical differences in mineral compositions (e.g. Na content in Cunard Member white micas).
2. The elevated Na content within Cunard Member white mica probably reflects the presence of paragonite, possibly interlayered with muscovite at the micron scale. Breakdown of paragonite formed andalusite according to the reaction:



3. The Bluestone member, which lacks paragonite, formed andalusite at a higher temperature via the reaction:



4. In both units, chlorite/muscovite intergrowths inherited from low-grade regional metamorphism broke down to produce biotite via the reaction:



5. Using ThermoCalc, P-T conditions of $550^{\circ}\text{C} \pm 6^{\circ}\text{C}$ at $3.3 \text{ kb} \pm 2.2 \text{ kb}$ were calculated for sample LSCN, Cunard Member, biotite zone. These P-T estimates, and inferred reaction sequence, are compatible with the higher P-T Al_2SiO_5 triple point inferred by Pattison (1992).

6.3 Suggestions for further work

1. The presence of paragonite in Cunard Member rocks needs to be demonstrated directly, possibly using X-ray diffraction analysis on very fine-grained samples ($< 5 \mu\text{m}$).
2. A more detailed analysis of P-T conditions under which the mineral assemblages formed is required. Utilizing Raman spectrometry (Beysac et al 2002) on graphite in Cunard Member rocks could determine temperature variation throughout the aureole.
3. A study of sulphide and oxide distribution and their variations through the aureole and their effect (if any) on silicate assemblages is required.
4. Filling of the major gaps (Transect 3) in the isograd map would allow for better control on the location of the isograds in Halifax.
5. To understand the difference between idioblastic chiastolite versus xenoblastic, spongy andalusite will require further understanding on the role (if any) of graphite in andalusite formation.
6. A more detailed analysis of the effect of bulk composition on reactions in the aureole would require use of ThermoCalc to generate pseudosections based on bulk chemistry of the rocks in this study.

References

- Abbott, R.N. 1989. Internal structures in part of the South Mountain batholith, Nova Scotia, Canada, *Geological Society of America Bulletin* 101: 1493-1506
- Ami, H.M. 1900. Synopsis of the geology of Canada. Royal Society of Canada, *Proceedings and Transactions*, 6 (n.ser.):187-226
- Bhatnagar, P. 1998. Structural geology and deformation of the Meguma Group at the northeastern contact of the South Mountain Batholith, Halifax area. unpublished B.Sc. thesis, Dalhousie University, Halifax, N.S.
- Berman, R.G. 1988. Internally-consistent thermodynamic data for stoichiometric minerals in the system $\text{Na}_2\text{O}-\text{K}_2\text{O}-\text{CaO}-\text{MgO}-\text{FeO}-\text{Fe}_2\text{O}_3-\text{Al}_2\text{O}_3-\text{SiO}_2-\text{TiO}_2-\text{H}_2\text{O}-\text{CO}_2$. *Journal of Petrology* 29, 445-522.
- Berman, R.G. 1991 Thermobarometry using multiequilibrium calculations: a new technique with petrologic applications. *Canadian Mineralogist* 29, 833-55.
- Betts-Robertson, B.L. 1998. Silicate and sulphide mineral assemblages and metamorphic fabrics from pelites in the contact aureole of the South Mountain Batholith, Halifax area, Nova Scotia. B.Sc. Honours, Dalhousie University.
- Beysac, O., Goffe, B., Chopin, C., Rouzaud, J.N. 2002. Raman spectra of carbonaceous material in metasediments; a new geothermometer, *J. Metamorph. Geol.* 20 859-871.
- Carruzzo, S., Kontak, D.J., Reynolds, P.H., Clarke, D.B., Dunning, G. R., Selby, D., and Creaser, R.A. 2003. U/Pb, Re/Os, and Ar/Ar dating of the South Mountain Batholith and its mineral deposits. *Geochimica et Cosmochimica Acta*, Volume 67, Supplement 1, p.A54, Goldschmidt Conference 2003
- Clarke, D.B., and Halliday, A.N. 1980. Strontium isotope geology of the South Mountain Batholith, Nova Scotia. *Geochimica et Cosmochimica Acta*, 44: 1045-1058.
- Clarke, D.B., and Muecke, G.K. 1985. Review of the petrochemistry and origin of the South Mountain batholith and associated plutons, Nova Scotia, Canada. in: High heat production granites, hydrothermal circulation and ore genesis, IMM, pp. 41-54.
- Clarke, D.B., Halliday, A.N., Hamilton, P.J. 1988. Neodymium and strontium isotopic Constraints on the origin of the peraluminous granitoids of the South Mountain Batholith, Nova Scotia. *Chemical Geology*, 73: 15-24.
- Clarke, D.B., MacDonald, M.A., and Erdmann, S. 2004. Chemical variation in $\text{Al}_2\text{O}_3-\text{CaO}-\text{Na}_2\text{O}-\text{K}_2\text{O}$ space: controls on the peraluminosity of the South Mountain Batholith *Canadian Journal of Earth Sciences*, 41: 785-798.
- Deer, W. A., Howie, R. A., and Zussman, J. 1992 *An Introduction to Rock-Forming Minerals*. Longman, London.

- Fairbault, E.R. 1887. Report on geological surveys and explorations in the counties of Guysborough, Antigonish, Pictou, Colchester and Halifax, Nova Scotia. Geological Survey of Canada, Annual report for 1886, 2, Pt. P: 129-163
- Fairbault, E.R. 1914. Geology of the Port Mouton Area, Queens County, Nova Scotia Geological Survey of Canada, Summary Report 1913, Sessional Paper 26: pg 251-258
- Graves, M.C., 1976. The formation of gold-bearing quartz veins in Nova Scotia; unpublished M.Sc. Thesis, Dalhousie University, 166 pp.
- Graves, M.C., and Zentilli, M. 1982. A review of the geology of gold in Nova Scotia. In *Geology of Canadian gold deposits*. Canadian Institute of Mining and Metallurgy Special Vol. 24, pp. 233–242.
- Hicks, R.J. 1996. Low-grade metamorphism in the Meguma Group, southern Nova Scotia. unpublished M.Sc. thesis, Dalhousie University, Halifax, N.S.. 352 pp.
- Horne, R. J. and Culshaw, N. 2001: Flexural-slip folding in the Meguma Group, Nova Scotia Canada; *Journal of Structural Geology*, v. 23, p. 1631-1652.
- Horne, R. J. 1998 An evaluation of flexural-slip folding in the Meguma Group, Halifax and Ovens areas, southern Nova Scotia. unpublished M.Sc. thesis, Dalhousie University. 246 pp.
- Jackson, C.T. and Alger, F. 1828-29. Mineralogy and geology of a part of Nova Scotia. *American Journal of Science*, Vol. 14: pg 305-330; Vol. 15: pg 132-160,201-217
- Kerrick, D.M. 1990. The Al₂SiO₅ Polymorphs. *Reviews in Mineralogy*, Vol. 22, Mineralogical Society of America, Washington, D.C..
- Kerrick, D.M. 1993. Contact Metamorphism, *Reviews in Mineralogy*, Volume 26. Mineralogical Society of America, Washington, D.C..
- Lambert, R. St.J., Chamberlain, V.E., and Muecke, G.K. 1984. Rb–Sr age and geochemistry of the Halifax Formation, Meguma Group, N.S. Geological Association of Canada – Mineralogical Association of Canada, Program with Abstracts, 9: 81
- Lipovsky, P.S., Colpron, M., Stronghill, G. and Pigage, L. 2003. GeoFIELD v.2.2 – Data management and map production for the field geologist. Yukon Geological Survey Open File 2003-8(D).
- MacDonald, M. A. 2001. Geology of the South Mountain Batholith, Southwestern Nova Scotia. Nova Scotia Department of Natural Resources, Open File Report ME 2001-2.
- MacDonald, M.A., and Horne, R.J. 1988. Petrology of the zoned, peraluminous Halifax pluton, south-central Nova Scotia. *Maritime Sediments and Atlantic Geology*, 24: 33–46.

- MacDonald, M.A., Horne, R.J., Corey, M.C., and Ham, L.J. 1992. An overview of recent bedrock mapping and follow-up petrographic studies of the South Mountain Batholith, southwestern Nova Scotia, Canada. *Maritime Sediments and Atlantic Geology*, 28, 7–28.
- Mahoney, K.L. 1996. The contact metamorphic aureole of the South Mountain Batholith, Nova Scotia. unpublished M.Sc. thesis, Acadia, University, Wolfville, N.S., 156 p.
- O'Brien, B. H. 1986. Preliminary report on the geology of the Mahone Bay area, Nova Scotia Current Research, Part A, Geological Survey of Canada, Paper 86-1A, p. 439-444.
- O'Brien, B. H. 1988. A study of the Meguma Terrane in Lunenburg County, Nova Scotia Geological Survey of Canada, Open File 1823.
- Pattison, D.R.M., Tracy, R.J. 1991. Phase Equilibria and Thermobarometry of metapelites Chapter 4: Contact metamorphism, *Reviews in mineralogy* Volume 26, pp 105-182
- Pattison, D.R.M. 2002. Instability of Al_2SiO_5 'triple point' assemblages in muscovite +biotite +quartz-bearing metapelites, with implications. *American Mineralogist* 86, 1414-1422.
- Powell, R., Holland, J. T. B., and Worley, B. 1998, Calculated phase diagrams involving solid solutions via non-linear equations, with examples using THERMOCALC: *Journal of Metamorphic Geology*, 16, 577–588.
- Rogers, H. D. and White, C. E. 1984: Geology of the igneous-metamorphic complex of Shelburne and eastern Yarmouth counties, Nova Scotia; in Current Research, Part A, Geological Survey of Canada, Paper 84-1A, p. 463-465.
- Rogers, H. D. and Barr, S. M. 1988: Petrography of the Shelburne and Barrington Passage plutons, southern Nova Scotia; *Maritime Sediments and Atlantic Geology*, 24, 21-31.
- Schenk, P.E. 1970. Regional variation of the flysch-like Meguma Group (lower Paleozoic) of Nova Scotia, compared to recent sedimentation off the Scotian shelf. In *Flysch sedimentology in North America*. Edited by J. Lajoie. Geological Association of Canada, Special Paper 7, pp. 127–153.
- Schenk, P.E. 1971. Southeastern Atlantic Canada, northwestern Africa, and continental drift. *Canadian Journal of Earth Sciences*, 8: 1218–1251.
- Schenk, P.E. 1983. The Meguma terrane of Nova Scotia – an aid in trans-Atlantic correlation. In *Regional trends in the geology of the Appalachian–Caledonian–Hercynian–Mauritanide Orogen*. Edited by P.E. Schenk. Reidel, Dordrecht, The Netherlands, pp. 121–130.
- Schenk, P.E. 1991. Events and sea-level changes on Gondwana's margin: the Meguma Zone (Cambrian to Devonian) of Nova Scotia, Canada. *Geological Society of America Bulletin* 103: 512-521

- Schenk, P.E. 1995. Meguma Zone. In *Geology of the Appalachian– Caledonian Orogen in Canada and Greenland*. Edited by H. Williams. Geological Survey of Canada, *Geology of Canada*, No. 6, Chapt. 3, pp. 261–277.
- Schenk, P.E. 1997. Sequence stratigraphy and provenance on Gondwana's margin: The Meguma Zone (Cambrian to Devonian) of Nova Scotia, Canada. *Geological Society of America Bulletin* 109: 395-409
- Smith, P. K. 1985. Mylonitization and fluidized brecciation in southern Nova Scotia; in *Mines and Minerals Branch, Report of Activities, 1984*, eds. K. A. Mills and J. L. Bates; Nova Scotia Department of Mines and Energy, Report 85-1, 119-133.
- Stea, R.R., Mott, R.J., 1998. Deglaciation of Nova Scotia: stratigraphy and chronology of lake sediment cores and buried organic sections. *Geographie Physique et Quaternaire* 52, 3–21.
- Stevenson, I.M. 1959. Shubenacadie and Kennetcook map-areas, Colchester, Hants and Halifax Counties, Nova Scotia. Geological Survey of Canada, *Memoir* 302: 88p
- Stow, D.A.V., Alam, M. and Piper, D.J.W. 1984. Sedimentology of the Halifax Formation, Nova Scotia; Lower Paleozoic fine-grained turbidites. *Geological Society of London Special Publication*, 15, 127-144.
- Tinkham, D.K., Zuluaga, C.A., Stowell, H.H. 2003. Metapelite phase equilibria modeling in MnNCKFMASH: The effect of variable Al_2O_3 and $MgO/(MgO + FeO)$ on mineral stability. *American Mineralogist*, 88; 1174
- Tobey, N. 2006. A Geological Description of Point Pleasant Park. unpublished B.Sc. Thesis, Dalhousie University, 99 pp.
- van der Pluijm, B.A. and Kaars-Sijpesteijn, C.H., 1984. Chlorite-mica aggregates: morphology, orientation, development and bearing on cleavage formation. *Journal of Structural Geology*, 6, 399-407
- Winter, J.D. 2001. *An Introduction to Igneous and Metamorphic petrology*. Prentice-Hall, Inc., Englewood Cliffs, N.J.
- Williams, H. 1979. The Appalachian Orogen in Canada. *Canadian Journal of Earth Sciences*, 16: 792-807
- Woodman, J.E. 1904a. Nomenclature of the gold-bearing metamorphic series of Nova Scotia. *American Geology*, 33:363-370
- Woodman, J.E. 1904b. The sediments of the Meguma series of Nova Scotia. *American Geology*, 34:13-34

Appendix I: Microprobe data

For sample locations, refer to Appendix III, Fig C.2, Table C.1. Neil Tobey (Tobey 2006) supplied PPP samples

Table A.1: Muscovite: Cunard Member

Sample Point #	SGR03	SGR03	SGR03	SGR03	SGR03	SGR03	SGR03	SGR03	SGR03	SGR03	SGR03	SGR03
8	9	10	11	13	15	17	23	39	42	44	45	
SiO ₂	48.22	47.69	46.23	46.02	46.57	46.07	46.42	46.43	48.22	45.88	51.62	49.41
TiO ₂	0.25	0.52	0.10	0.05	0.10	0.12	0.04	0.10	0.05	0.14	0.10	0.07
Al ₂ O ₃	29.25	31.40	36.23	35.35	36.23	35.97	36.25	36.32	38.44	37.84	31.86	38.64
Cr ₂ O ₃	0.04	0.00	0.02	0.00	0.00	0.00	0.00	0.00	0.07	0.02	0.00	0.04
FeO	3.77	2.42	0.41	1.08	0.60	0.66	0.38	0.44	0.41	0.45	0.98	0.45
MnO	0.00	0.00	0.00	0.00	0.00	0.00	0.00	0.00	0.00	0.01	0.01	0.00
MgO	1.78	1.21	0.22	0.53	0.26	0.23	0.22	0.24	0.17	0.22	0.79	0.31
CaO	0.00	0.00	0.05	0.00	0.01	0.00	0.00	0.01	0.22	0.07	0.03	0.00
Na ₂ O	0.71	0.94	1.59	1.27	1.57	1.30	1.51	1.58	3.50	2.32	1.13	0.96
K ₂ O	8.12	8.67	7.88	7.91	7.38	7.75	7.97	7.63	4.59	7.21	6.49	7.11
Total	92.14	92.86	92.73	92.22	92.71	92.10	92.78	92.75	95.67	94.15	93.00	96.99
Cations corrected to 11 Oxygens												
Si	3.31	3.24	3.10	3.11	3.12	3.11	3.11	3.11	3.09	3.03	3.40	3.13
Ti	0.01	0.03	0.01	0.00	0.01	0.01	0.00	0.01	0.00	0.01	0.00	0.00
Al	2.37	2.51	2.86	2.82	2.86	2.86	2.86	2.87	2.90	2.95	2.47	2.89
Cr	0.00	0.00	0.00	0.00	0.00	0.00	0.00	0.00	0.00	0.00	0.00	0.00
Fe	0.22	0.14	0.02	0.06	0.03	0.04	0.02	0.02	0.02	0.02	0.05	0.02
Mn	0.00	0.00	0.00	0.00	0.00	0.00	0.00	0.00	0.00	0.00	0.00	0.00
Mg	0.18	0.12	0.02	0.05	0.03	0.02	0.02	0.02	0.02	0.02	0.08	0.03
Ca	0.00	0.00	0.00	0.00	0.00	0.00	0.00	0.00	0.02	0.00	0.00	0.00
Na	0.09	0.12	0.21	0.17	0.20	0.17	0.20	0.21	0.43	0.30	0.14	0.12
K	0.71	0.75	0.67	0.68	0.63	0.67	0.68	0.65	0.38	0.61	0.55	0.57
Cation Total	6.90	6.91	6.90	6.90	6.87	6.87	6.89	6.88	6.86	6.94	6.70	6.77
Mol% pa	11.73	14.20	23.38	19.69	24.44	20.37	22.33	24.01	52.67	32.69	20.83	17.14
Distance (km)	2.08	2.08	2.08	2.08	2.08	2.08	2.08	2.08	2.08	2.08	2.08	2.08

Mol% Pa = Na/(Na+K+Ca)x100%; Distance = distance from approximate nearest surface expression of the contact.

Sample Point #	SGR03 46	SGR03 47	SGR03 48	SGR03 49	iwk03 50	iwk03 51	iwk03 52	iwk03 53	iwk03 54	iwk03 56	iwk03 57	iwk03 58
SiO2	46.35	46.65	46.38	46.32	42.62	46.69	45.94	46.03	46.20	46.15	46.10	45.71
TiO2	0.22	0.03	0.04	0.13	0.01	0.12	0.04	0.09	0.05	0.17	0.08	0.17
Al2O3	37.26	37.53	37.25	37.67	35.13	37.87	37.40	38.14	37.10	38.34	37.91	37.75
Cr2O3	0.01	0.04	0.02	0.05	0.00	0.02	0.01	0.03	0.02	0.04	0.02	0.03
FeO	0.51	0.42	0.44	0.51	0.31	0.54	0.35	0.41	0.46	0.40	0.41	0.42
MnO	0.00	0.01	0.00	0.01	0.00	0.00	0.00	0.00	0.00	0.00	0.02	0.00
MgO	0.29	0.26	0.30	0.21	0.18	0.17	0.21	0.15	0.26	0.17	0.21	0.16
CaO	0.02	0.00	0.00	0.00	0.00	0.00	0.00	0.01	0.00	0.00	0.00	0.01
Na2O	1.36	1.50	1.49	1.50	2.40	1.82	1.87	1.82	1.79	2.16	1.58	2.12
K2O	8.49	8.58	8.50	8.59	7.90	7.83	7.79	8.03	8.03	7.67	8.47	7.80
Total	94.51	95.03	94.42	94.99	88.56	95.06	93.60	94.71	93.91	95.10	94.79	94.17
Cations corrected to 11 Oxygens 11												
Si	3.06	3.06	3.07	3.05	3.02	3.06	3.05	3.03	3.07	3.02	3.04	3.03
Ti	0.01	0.00	0.00	0.01	0.00	0.01	0.00	0.00	0.00	0.01	0.00	0.01
Al	2.90	2.91	2.90	2.92	2.93	2.92	2.93	2.96	2.90	2.96	2.94	2.95
Cr	0.00	0.00	0.00	0.00	0.00	0.00	0.00	0.00	0.00	0.00	0.00	0.00
Fe	0.03	0.02	0.02	0.03	0.02	0.03	0.02	0.02	0.03	0.02	0.02	0.02
Mn	0.00	0.00	0.00	0.00	0.00	0.00	0.00	0.00	0.00	0.00	0.00	0.00
Mg	0.03	0.03	0.03	0.02	0.02	0.02	0.02	0.02	0.03	0.02	0.02	0.02
Ca	0.00	0.00	0.00	0.00	0.00	0.00	0.00	0.00	0.00	0.00	0.00	0.00
Na	0.17	0.19	0.19	0.19	0.33	0.23	0.24	0.23	0.23	0.27	0.20	0.27
K	0.72	0.72	0.72	0.72	0.71	0.65	0.66	0.67	0.68	0.64	0.71	0.66
Cation Total	6.92	6.93	6.93	6.94	7.04	6.92	6.93	6.94	6.93	6.95	6.94	6.96
Mol% pa	19.51	21.01	20.97	20.99	31.61	26.09	26.83	25.61	25.36	29.93	22.14	29.16
Distance (km)	2.08	2.08	2.08	2.08	1.96	1.96	1.96	1.96	1.96	1.96	1.96	1.96

Mol% Pa = $\text{Na}/(\text{Na}+\text{K}+\text{Ca})\times 100\%$; Distance = distance from approximate nearest surface expression of the contact.

Sample Point #	iwk03	RTR04	RTR04	RTR04	LSCN	LSCN	LSCN	LSCN	LSCN	LSCN	SGR03	SGR03
59	73	75	77	87	101	102	103	104	108	114	115	
SiO2	45.52	50.66	45.73	44.14	46.69	46.71	42.41	48.31	46.65	45.72	51.05	44.98
TiO2	0.06	0.15	0.16	0.61	0.16	0.34	0.62	0.46	0.10	0.04	0.30	0.50
Al2O3	40.42	32.89	36.30	28.81	37.80	37.47	31.25	33.13	37.99	36.61	29.33	35.14
Cr2O3	0.00	0.00	0.00	0.00	0.00	0.06	0.06	0.00	0.02	0.01	0.03	0.06
FeO	0.26	1.43	0.85	8.42	0.69	0.83	6.53	2.18	0.54	1.77	1.73	1.39
MnO	0.00	0.00	0.00	0.06	0.00	0.00	0.02	0.00	0.00	0.00	0.00	0.00
MgO	0.08	0.85	0.36	2.85	0.32	0.41	2.88	1.73	0.30	0.95	3.10	0.83
CaO	0.94	0.00	0.00	0.00	0.00	0.00	0.00	0.00	0.00	0.00	0.00	0.00
Na2O	4.70	0.74	0.80	0.54	1.33	1.04	0.93	0.86	1.37	1.10	0.57	1.09
K2O	3.25	9.07	8.92	9.06	8.95	8.24	7.91	8.77	8.76	8.54	8.77	9.04
Total	95.22	95.80	93.13	94.48	95.94	95.10	92.61	95.43	95.72	94.74	94.86	93.04
Cations corrected to 11 Oxygens												
Si	2.94	3.30	3.07	3.08	3.05	3.06	2.98	3.19	3.05	3.04	3.37	3.05
Ti	0.00	0.01	0.01	0.03	0.01	0.02	0.03	0.02	0.00	0.00	0.01	0.03
Al	3.07	2.53	2.88	2.37	2.91	2.90	2.59	2.58	2.92	2.87	2.28	2.81
Cr	0.00	0.00	0.00	0.00	0.00	0.00	0.00	0.00	0.00	0.00	0.00	0.00
Fe	0.01	0.08	0.05	0.49	0.04	0.05	0.38	0.12	0.03	0.10	0.10	0.08
Mn	0.00	0.00	0.00	0.00	0.00	0.00	0.00	0.00	0.00	0.00	0.00	0.00
Mg	0.01	0.08	0.04	0.30	0.03	0.04	0.30	0.17	0.03	0.09	0.30	0.08
Ca	0.06	0.00	0.00	0.00	0.00	0.00	0.00	0.00	0.00	0.00	0.00	0.00
Na	0.59	0.09	0.10	0.07	0.17	0.13	0.13	0.11	0.17	0.14	0.07	0.14
K	0.27	0.75	0.77	0.81	0.74	0.69	0.71	0.74	0.73	0.72	0.74	0.78
Cation Total	6.95	6.85	6.91	7.15	6.95	6.88	7.12	6.93	6.94	6.96	6.88	6.98
Mol% pa	63.88	11.02	12.01	8.38	18.43	16.20	15.15	12.97	19.15	16.39	8.96	15.46
Distance (km)	1.96	0.92	0.92	0.92	1.19	1.19	1.19	1.19	1.19	1.19	2.08	2.08

Mol% Pa = Na/(Na+K+Ca)x100%; Distance = distance from approximate nearest surface expression of the contact.

Sample Point #	SGR03	SGR03	SGR03	SGR03	SGR03	SGR03	SGR03	MSBa3	MSBa	MSBa	MSBa	DP2
117	119	120	123	124	127	129	132	136	138	140	141	
SiO2	46.33	46.47	46.34	57.45	48.36	47.55	49.28	47.28	47.12	47.34	41.04	45.15
TiO2	0.11	0.25	0.04	0.09	0.06	0.21	0.12	0.21	0.22	0.38	0.20	0.18
Al2O3	36.33	36.02	37.81	30.86	38.84	34.66	34.83	38.27	38.61	37.18	33.07	36.30
Cr2O3	0.04	0.04	0.04	0.03	0.11	0.01	0.02	0.24	0.21	0.22	0.26	0.27
FeO	0.69	1.60	0.52	0.43	0.37	1.39	0.43	0.63	0.65	0.59	5.83	3.08
MnO	0.00	0.00	0.00	0.00	0.00	0.00	0.00	0.08	0.09	0.07	0.20	0.10
MgO	0.48	0.58	0.28	0.24	0.24	1.10	0.25	0.29	0.18	0.29	2.75	1.73
CaO	0.00	0.00	0.00	0.00	0.01	0.00	0.06	0.08	0.22	0.15	0.14	0.13
Na2O	1.26	1.40	1.41	1.08	1.20	1.05	2.05	1.58	2.76	1.41	1.53	0.17
K2O	8.73	8.31	8.58	6.78	8.17	9.13	6.97	8.51	6.46	8.15	5.22	6.80
Total	93.95	94.66	95.03	96.96	97.35	95.10	94.02	97.17	96.52	95.78	90.23	93.91
Cations corrected to 11 Oxygens												
Si	3.09	3.08	3.05	3.60	3.08	3.14	3.24	3.04	3.03	3.08	2.91	3.01
Ti	0.01	0.01	0.00	0.00	0.00	0.01	0.01	0.01	0.01	0.02	0.01	0.01
Al	2.85	2.81	2.93	2.28	2.92	2.70	2.70	2.90	2.93	2.85	2.76	2.85
Cr	0.00	0.00	0.00	0.00	0.01	0.00	0.00	0.01	0.01	0.01	0.01	0.01
Fe	0.04	0.09	0.03	0.02	0.02	0.08	0.02	0.03	0.04	0.03	0.35	0.17
Mn	0.00	0.00	0.00	0.00	0.00	0.00	0.00	0.00	0.01	0.00	0.01	0.01
Mg	0.05	0.06	0.03	0.02	0.02	0.11	0.02	0.03	0.02	0.03	0.29	0.17
Ca	0.00	0.00	0.00	0.00	0.00	0.00	0.00	0.01	0.02	0.01	0.01	0.01
Na	0.16	0.18	0.18	0.13	0.15	0.13	0.26	0.20	0.34	0.18	0.21	0.02
K	0.74	0.70	0.72	0.54	0.66	0.77	0.58	0.70	0.53	0.68	0.47	0.58
Cation Total	6.94	6.94	6.94	6.60	6.86	6.95	6.83	6.94	6.93	6.89	7.04	6.85
Mol% pa	18.00	20.42	20.05	19.58	18.29	14.84	30.74	21.86	38.69	20.58	30.32	3.78
Distance (km)	2.08	2.08	2.08	2.08	2.08	2.08	2.08	2.01	2.01	2.01	2.01	0.41

Mol% Pa = Na/(Na+K+Ca)x100%; Distance = distance from approximate nearest surface expression of the contact.

Sample Point #	DP2	Bsub	MBD	MBD	MBD	MBD	MBD	MBD	MBD	MBD	MBD	MBD
	147	149	179	182	184	187	188	189	193	194	195	196
SiO ₂	47.23	47.27	46.18	49.50	44.88	46.97	46.72	52.57	45.34	47.43	46.34	44.46
TiO ₂	0.30	0.15	0.20	0.10	0.10	0.02	0.26	0.15	0.07	0.84	0.06	0.42
Al ₂ O ₃	35.40	34.32	37.97	34.99	37.45	37.44	38.42	34.93	37.96	33.82	38.22	36.51
Cr ₂ O ₃	0.20	0.22	0.00	0.00	0.00	0.00	0.00	0.00	0.00	0.00	0.01	0.00
FeO	1.18	7.01	0.77	0.78	0.74	0.50	0.73	0.66	0.39	1.47	0.46	2.41
MnO	0.09	0.34	0.00	0.00	0.00	0.00	0.00	0.00	0.00	0.00	0.00	0.00
MgO	1.09	4.62	0.33	0.29	0.29	0.29	0.26	0.31	0.25	1.50	0.27	1.56
CaO	0.08	0.11	0.00	0.00	0.00	0.00	0.00	0.00	0.00	0.00	0.00	0.00
Na ₂ O	0.43	0.83	1.46	1.49	1.50	1.61	1.10	1.40	1.66	0.96	1.65	1.24
K ₂ O	9.86	3.01	7.98	7.38	8.17	8.27	6.96	7.19	8.10	8.84	8.23	7.51
Total	95.85	97.87	94.90	94.53	93.14	95.11	94.45	97.20	93.77	94.85	95.23	94.10
Cations corrected to 11 Oxygens												
Si	3.11	3.03	3.03	3.24	3.01	3.08	3.05	3.32	3.02	3.14	3.03	2.97
Ti	0.01	0.01	0.01	0.01	0.00	0.00	0.01	0.01	0.00	0.04	0.00	0.02
Al	2.75	2.59	2.94	2.70	2.96	2.89	2.96	2.60	2.98	2.64	2.95	2.88
Cr	0.01	0.01	0.00	0.00	0.00	0.00	0.00	0.00	0.00	0.00	0.00	0.00
Fe	0.06	0.38	0.04	0.04	0.04	0.03	0.04	0.04	0.02	0.08	0.03	0.14
Mn	0.00	0.02	0.00	0.00	0.00	0.00	0.00	0.00	0.00	0.00	0.00	0.00
Mg	0.11	0.44	0.03	0.03	0.03	0.03	0.03	0.03	0.03	0.15	0.03	0.16
Ca	0.01	0.01	0.00	0.00	0.00	0.00	0.00	0.00	0.00	0.00	0.00	0.00
Na	0.06	0.10	0.19	0.19	0.20	0.20	0.14	0.17	0.21	0.12	0.21	0.16
K	0.83	0.25	0.67	0.62	0.70	0.69	0.58	0.58	0.69	0.75	0.69	0.64
Cation Total	6.94	6.84	6.91	6.81	6.95	6.92	6.81	6.75	6.94	6.93	6.94	6.97
Mol% pa	6.20	28.92	21.85	23.50	21.87	22.82	19.27	22.84	23.69	14.16	23.41	20.16
Distance (km)	0.41	1.29	1.31	1.31	1.31	1.31	1.31	1.31	1.31	1.31	1.31	1.31

Mol% Pa = Na/(Na+K+Ca)x100%; Distance = distance from approximate nearest surface expression of the contact.

Sample Point #	rtr04-1	rtr04-1	rtr04-1	rtr04-1	AR04-1	AR04-1	AR04-1	AR04-1	AR04-1	AR05-3	AR05-3	AR05-5
SiO ₂	47.03	46.18	48.24	46.92	45.48	45.98	46.72	45.10	45.44	51.30	46.05	51.02
TiO ₂	0.14	0.22	0.54	0.27	0.49	0.27	0.63	0.61	0.50	0.05	0.66	0.00
Al ₂ O ₃	37.15	36.33	31.79	35.95	37.12	37.13	35.94	36.43	36.47	31.41	36.33	32.37
Cr ₂ O ₃	0.00	0.02	0.05	0.01	0.00	0.00	0.01	0.02	0.05	0.01	0.00	0.00
FeO	0.87	1.27	3.14	1.74	0.86	1.00	1.15	1.02	1.05	0.48	1.11	0.78
MnO	0.00	0.00	0.03	0.00	0.00	0.00	0.00	0.00	0.00	0.00	0.00	0.00
MgO	0.40	0.63	1.86	0.84	0.45	0.55	0.73	0.61	0.59	0.33	0.63	0.56
CaO	0.00	0.00	0.00	0.00	0.00	0.00	0.00	0.00	0.00	0.00	0.00	0.00
Na ₂ O	0.94	0.82	0.50	0.85	0.51	0.52	0.53	0.52	0.54	0.37	0.48	0.48
K ₂ O	9.34	9.15	8.59	9.14	9.41	9.39	9.63	9.67	9.45	8.81	9.76	8.96
Total	95.87	94.62	94.74	95.71	94.33	94.85	95.34	93.98	94.10	92.75	95.03	94.16
Cations corrected to 11 Oxygens												
Si	3.08	3.07	3.22	3.09	3.03	3.04	3.08	3.03	3.04	3.42	3.05	3.36
Ti	0.01	0.01	0.03	0.01	0.02	0.01	0.03	0.03	0.03	0.00	0.03	0.00
Al	2.86	2.84	2.50	2.79	2.91	2.90	2.80	2.88	2.87	2.47	2.84	2.51
Cr	0.00	0.00	0.00	0.00	0.00	0.00	0.00	0.00	0.00	0.00	0.00	0.00
Fe	0.05	0.07	0.17	0.10	0.05	0.06	0.06	0.06	0.06	0.03	0.06	0.04
Mn	0.00	0.00	0.00	0.00	0.00	0.00	0.00	0.00	0.00	0.00	0.00	0.00
Mg	0.04	0.06	0.18	0.08	0.04	0.05	0.07	0.06	0.06	0.03	0.06	0.06
Ca	0.00	0.00	0.00	0.00	0.00	0.00	0.00	0.00	0.00	0.00	0.00	0.00
Na	0.12	0.11	0.06	0.11	0.07	0.07	0.07	0.07	0.07	0.05	0.06	0.06
K	0.78	0.78	0.73	0.77	0.80	0.79	0.81	0.83	0.81	0.75	0.83	0.75
Cation Total	6.93	6.94	6.90	6.94	6.92	6.92	6.92	6.95	6.94	6.74	6.94	6.79
Mol% pa	13.22	11.99	8.15	12.42	7.62	7.80	7.76	7.50	8.03	5.94	7.05	7.43
Distance (km)	0.92	0.92	0.92	0.92	0.46	0.46	0.46	0.46	0.46	0.19	0.19	0.09

Mol% Pa = Na/(Na+K+Ca)x100%; Distance = distance from approximate nearest surface expression of the contact.

Sample	AR05-5	AR05-5	AR05-5	AR05-5	rr05-3
Point #	330	335	337	342	350
SiO ₂	45.75	45.99	45.90	46.35	47.59
TiO ₂	0.00	0.00	0.07	0.00	0.20
Al ₂ O ₃	37.18	36.61	35.84	36.54	34.40
Cr ₂ O ₃	0.00	0.00	0.00	0.00	0.00
FeO	0.80	1.32	1.86	0.83	0.51
MnO	0.00	0.00	0.00	0.00	0.01
MgO	0.56	0.95	1.27	0.69	0.31
CaO	0.00	0.00	0.00	0.00	0.01
Na ₂ O	0.53	0.44	0.39	0.52	1.56
K ₂ O	10.40	9.07	8.83	10.25	8.03
Total	95.23	94.38	94.15	95.18	92.62
Cations corrected to 11 Oxygens					
Si	3.03	3.06	3.07	3.07	3.20
Ti	0.00	0.00	0.00	0.00	0.01
Al	2.91	2.87	2.82	2.85	2.72
Cr	0.00	0.00	0.00	0.00	0.00
Fe	0.04	0.07	0.10	0.05	0.03
Mn	0.00	0.00	0.00	0.00	0.00
Mg	0.06	0.09	0.13	0.07	0.03
Ca	0.00	0.00	0.00	0.00	0.00
Na	0.07	0.06	0.05	0.07	0.20
K	0.88	0.77	0.75	0.87	0.69
Cation Total	6.99	6.92	6.92	6.97	6.88
Mol% pa	7.19	6.91	6.17	7.08	22.72
Distance (km)	0.09	0.09	0.09	0.09	1.71

Mol% Pa = $\text{Na}/(\text{Na}+\text{K}+\text{Ca})\times 100\%$; Distance = distance from approximate nearest surface expression of the contact.

Table A.2: Muscovite: Bluestone member

Sample Point #	Ib04-1 205	Ib04-1 207	WI05-10 216	WI05-10 218	WI05-10 219	WI05-10 225	WI05-10 227	Pcr-10 228	Pcr-10 233	Pcr-10 235	Pcr-10 238	Pcr-10 239
SiO2	43.55	45.85	46.74	46.18	46.70	45.54	44.90	46.15	46.21	46.37	46.69	45.81
TiO2	0.04	0.13	0.82	0.35	0.36	0.35	0.01	0.24	0.78	0.92	0.75	0.54
Al2O3	35.09	37.87	36.82	37.19	37.00	36.92	32.27	37.17	36.94	37.03	37.07	36.36
Cr2O3	0.00	0.02	0.05	0.03	0.01	0.01	0.04	0.04	0.05	0.11	0.29	0.13
FeO	0.59	0.50	1.01	1.24	1.06	1.10	5.36	1.00	0.88	1.30	1.00	1.28
MnO	0.00	0.00	0.00	0.00	0.00	0.00	0.15	0.00	0.00	0.00	0.00	0.00
MgO	0.41	0.33	0.47	0.40	0.43	0.42	2.39	0.35	0.30	0.36	0.31	0.47
CaO	0.00	0.04	0.00	0.00	0.00	0.00	0.35	0.00	0.00	0.00	0.00	0.00
Na2O	1.00	1.43	0.55	0.60	0.55	0.59	0.09	0.50	0.52	0.57	0.38	0.41
K2O	8.13	8.95	9.54	9.87	9.57	9.78	4.84	9.54	9.51	9.61	8.82	8.87
Total	88.80	95.12	95.99	95.86	95.67	94.71	90.39	94.99	95.20	96.27	95.32	93.87
Cations corrected to 11 Oxygens												
Si	3.06	3.02	3.06	3.04	3.07	3.03	3.11	3.05	3.05	3.04	3.06	3.06
Ti	0.00	0.01	0.04	0.02	0.02	0.02	0.00	0.01	0.04	0.05	0.04	0.03
Al	2.91	2.94	2.84	2.88	2.86	2.90	2.64	2.90	2.87	2.86	2.87	2.86
Cr	0.00	0.00	0.00	0.00	0.00	0.00	0.00	0.00	0.00	0.01	0.02	0.01
Fe	0.03	0.03	0.06	0.07	0.06	0.06	0.31	0.06	0.05	0.07	0.06	0.07
Mn	0.00	0.00	0.00	0.00	0.00	0.00	0.01	0.00	0.00	0.00	0.00	0.00
Mg	0.04	0.03	0.05	0.04	0.04	0.04	0.25	0.04	0.03	0.04	0.03	0.05
Ca	0.00	0.00	0.00	0.00	0.00	0.00	0.03	0.00	0.00	0.00	0.00	0.00
Na	0.14	0.18	0.07	0.08	0.07	0.08	0.01	0.06	0.07	0.07	0.05	0.05
K	0.73	0.75	0.80	0.83	0.80	0.83	0.43	0.80	0.80	0.80	0.74	0.76
Cation Total	6.91	6.97	6.91	6.95	6.92	6.96	6.79	6.92	6.91	6.93	6.85	6.88
Mol% pa	15.65	19.48	8.01	8.51	7.95	8.48	2.59	7.47	7.73	8.29	6.15	6.66
Distance (km)	2.36	2.36	0.98	0.98	0.98	0.98	0.98	1.55	1.55	1.55	1.55	1.55

Mol% Pa = Na/(Na+K+Ca)x100%; Distance = distance from approximate nearest surface expression of the contact.

Sample Point #	Per-10	WI05-4	WI05-4	WI05-4	WI05-4	WI05-4	WI05-4	WI05-4	WI05-4	wI05-12	wI05-12	wI05-12	wI05-12
SiO2	46.40	46.31	45.94	45.48	44.21	45.27	45.30	46.45	46.55	46.53	50.80	46.41	
TiO2	0.48	0.17	0.12	0.33	0.00	0.01	0.44	0.12	0.03	0.07	0.03	0.51	
Al2O3	36.68	35.98	35.86	35.90	30.79	31.54	35.72	36.88	29.42	29.67	28.30	31.02	
Cr2O3	0.07	0.05	0.03	0.05	0.04	0.04	0.06	0.08	0.00	0.00	0.00	0.00	
FeO	0.97	1.48	1.04	1.08	6.69	6.78	1.19	1.23	8.55	8.47	3.74	3.38	
MnO	0.00	0.00	0.00	0.00	0.13	0.14	0.00	0.00	0.17	0.15	0.03	0.03	
MgO	0.41	0.62	0.44	0.40	2.85	2.91	0.43	0.40	3.32	3.01	1.14	0.89	
CaO	0.01	0.00	0.00	0.00	0.07	0.07	0.00	0.00	0.08	0.09	0.06	0.02	
Na2O	0.43	0.58	0.57	0.59	0.12	0.09	0.51	0.55	0.40	0.52	0.10	0.22	
K2O	9.51	10.53	10.48	10.47	6.83	5.01	10.01	10.11	4.61	4.40	3.11	8.47	
Total	94.96	95.73	94.47	94.30	91.74	91.85	93.65	95.82	93.12	92.91	87.30	90.95	
Cations corrected to 11 Oxygens													
Si	3.07	3.07	3.08	3.06	3.09	3.12	3.06	3.06	3.18	3.18	3.52	3.23	
Ti	0.02	0.01	0.01	0.02	0.00	0.00	0.02	0.01	0.00	0.00	0.00	0.03	
Al	2.86	2.81	2.83	2.84	2.54	2.56	2.84	2.86	2.37	2.39	2.31	2.54	
Cr	0.00	0.00	0.00	0.00	0.00	0.00	0.00	0.00	0.00	0.00	0.00	0.00	
Fe	0.05	0.08	0.06	0.06	0.39	0.39	0.07	0.07	0.49	0.49	0.22	0.20	
Mn	0.00	0.00	0.00	0.00	0.01	0.01	0.00	0.00	0.01	0.01	0.00	0.00	
Mg	0.04	0.06	0.04	0.04	0.30	0.30	0.04	0.04	0.34	0.31	0.12	0.09	
Ca	0.00	0.00	0.00	0.00	0.01	0.01	0.00	0.00	0.01	0.01	0.00	0.00	
Na	0.06	0.07	0.07	0.08	0.02	0.01	0.07	0.07	0.05	0.07	0.01	0.03	
K	0.80	0.89	0.90	0.90	0.61	0.44	0.86	0.85	0.40	0.39	0.28	0.75	
CatTotal	6.91	7.00	6.99	6.99	6.95	6.83	6.96	6.96	6.86	6.84	6.46	6.87	
Mol% pa	6.41	7.65	7.71	7.80	2.44	2.64	7.23	7.65	11.48	14.83	4.51	3.79	
Distance (Km)	1.55	0.38	0.38	0.38	0.38	0.38	0.38	0.38	0.94	0.94	0.94	0.94	

Mol% Pa = $\text{Na}/(\text{Na}+\text{K}+\text{Ca})\times 100\%$; Distance = distance from approximate nearest surface expression of the contact.

Sample Point #	w105-12	w105-12	w105-12	w105-15	w105-15	w105-15	w105-15	w105-15	w105-15	w105-15	w105-15	w105-15	w105-15
SiO2	48.07	47.93	46.74	48.57	46.45	46.96	46.99	45.70	47.03	45.90	50.30	47.44	
TiO2	0.20	0.06	0.07	0.07	0.53	0.88	0.55	0.52	0.37	0.03	0.35	0.34	
Al2O3	32.94	33.82	33.51	33.09	36.96	36.56	37.55	36.45	37.80	31.67	34.71	36.91	
Cr2O3	0.00	0.00	0.00	0.02	0.09	0.07	0.06	0.28	0.01	0.03	0.00	0.01	
FeO	1.46	0.68	0.49	4.48	1.40	1.47	1.12	1.06	0.88	7.78	0.77	1.24	
MnO	0.01	0.01	0.00	0.06	0.02	0.01	0.00	0.00	0.00	0.08	0.01	0.00	
MgO	0.46	0.27	0.16	1.45	0.36	0.38	0.29	0.27	0.28	2.90	0.26	0.44	
CaO	0.01	0.01	0.02	0.53	0.00	0.00	0.00	0.00	0.01	0.24	0.49	0.01	
Na2O	0.35	0.46	0.50	0.36	0.44	0.58	0.55	0.46	0.45	0.24	2.06	0.46	
K2O	8.77	9.35	7.63	5.95	9.37	9.67	9.28	9.01	9.66	2.87	7.48	9.89	
Total	92.29	92.59	89.12	94.57	95.64	96.59	96.39	93.75	96.49	91.74	96.41	96.73	
Cations corrected to 11 Oxygens													
Si	3.25	3.23	3.24	3.21	3.05	3.07	3.06	3.06	3.06	3.13	3.24	3.09	
Ti	0.01	0.00	0.00	0.00	0.03	0.04	0.03	0.03	0.02	0.00	0.02	0.02	
Al	2.63	2.69	2.73	2.58	2.86	2.81	2.88	2.87	2.90	2.55	2.63	2.83	
Cr	0.00	0.00	0.00	0.00	0.00	0.00	0.00	0.02	0.00	0.00	0.00	0.00	
Fe	0.08	0.04	0.03	0.25	0.08	0.08	0.06	0.06	0.05	0.44	0.04	0.07	
Mn	0.00	0.00	0.00	0.00	0.00	0.00	0.00	0.00	0.00	0.00	0.00	0.00	
Mg	0.05	0.03	0.02	0.14	0.04	0.04	0.03	0.03	0.03	0.30	0.02	0.04	
Ca	0.00	0.00	0.00	0.04	0.00	0.00	0.00	0.00	0.00	0.02	0.03	0.00	
Na	0.05	0.06	0.07	0.05	0.06	0.07	0.07	0.06	0.06	0.03	0.26	0.06	
K	0.76	0.80	0.67	0.50	0.79	0.81	0.77	0.77	0.80	0.25	0.61	0.82	
Cation Total	6.83	6.85	6.76	6.77	6.90	6.92	6.90	6.89	6.90	6.73	6.86	6.92	
Mol% pa	5.74	6.87	9.04	7.89	6.67	8.39	8.26	7.17	6.55	10.62	28.35	6.63	
Distance (km)	0.94	0.94	0.94	1.29	1.29	1.29	1.29	1.29	1.29	1.29	1.29	1.29	

Mol% Pa = $\text{Na}/(\text{Na}+\text{K}+\text{Ca})\times 100\%$; Distance = distance from approximate nearest surface expression of the contact.

Sample Point #	wl05-15 409	wl05-15 410	ppp19 11n	ppp19 13n	ppp19 14n	ppp19 15n	ppp19 16n	ppp19 18n	ppp19 20n	ppp3 21n	ppp3 22n	ppp3 24n
SiO2	48.30	47.69	45.77	48.84	47.32	48.04	47.76	47.19	47.00	49.41	47.12	49.45
TiO2	0.55	0.60	0.04	0.05	0.01	0.05	0.02	0.08	0.16	0.01	0.04	0.02
Al2O3	36.17	37.10	36.73	33.60	32.73	34.03	32.87	37.39	36.73	33.29	32.16	31.29
Cr2O3	0.00	0.08	0.00	0.00	0.00	0.00	0.00	0.00	0.00	0.00	0.00	0.00
FeO	1.13	0.88	0.83	6.21	6.05	5.67	6.26	0.71	1.10	9.29	8.85	10.98
MnO	0.00	0.00	0.00	0.11	0.09	0.09	0.11	0.00	0.00	0.28	0.22	0.34
MgO	0.35	0.35	0.37	2.42	2.38	2.15	2.41	0.31	0.47	3.64	3.17	4.40
CaO	0.00	0.00	0.00	0.07	0.08	0.07	0.07	0.00	0.00	0.05	0.06	0.01
Na2O	0.51	0.49	1.03	0.68	1.13	1.15	1.26	1.00	0.98	0.30	0.31	0.27
K2O	9.40	9.89	9.19	2.75	3.57	4.49	3.49	9.44	9.10	2.44	4.56	1.44
Total	96.41	97.09	93.98	94.76	93.37	95.72	94.25	96.12	95.53	98.73	96.48	98.20
Cations corrected to 11 Oxygens												
Si	3.14	3.09	3.06	3.19	3.16	3.14	3.16	3.08	3.09	3.14	3.11	3.17
Ti	0.03	0.03	0.00	0.00	0.00	0.00	0.00	0.00	0.00	0.00	0.00	0.00
Al	2.77	2.83	2.89	2.58	2.58	2.62	2.57	2.87	2.84	2.49	2.50	2.37
Cr	0.00	0.00	0.00	0.00	0.00	0.00	0.00	0.00	0.00	0.00	0.00	0.00
Fe	0.06	0.05	0.05	0.34	0.34	0.31	0.35	0.04	0.06	0.49	0.49	0.59
Mn	0.00	0.00	0.00	0.01	0.01	0.01	0.01	0.00	0.00	0.02	0.01	0.02
Mg	0.03	0.03	0.04	0.24	0.24	0.21	0.24	0.03	0.05	0.34	0.31	0.42
Ca	0.00	0.00	0.00	0.01	0.01	0.00	0.01	0.00	0.00	0.00	0.00	0.00
Na	0.06	0.06	0.13	0.09	0.15	0.15	0.16	0.13	0.12	0.04	0.04	0.03
K	0.78	0.82	0.78	0.23	0.30	0.37	0.29	0.79	0.76	0.20	0.38	0.12
Cation Total	6.87	6.91	6.95	6.67	6.78	6.81	6.78	6.93	6.92	6.73	6.85	6.72
Mol% pa	7.57	7.02	14.53	26.80	32.21	27.73	35.00	13.87	14.02	15.67	9.25	21.74
Distance (Km)	1.29	1.29	1.52	1.52	1.52	1.52	1.52	1.52	1.52	0.68	0.68	0.68

Mol% Pa = Na/(Na+K+Ca)x100%; Distance = distance from approximate nearest surface expression of the contact.

Sample Point #	ppp3 27n	ppp3 28n	ppp3 36n	ppp19 3n	ppp3 41n	ppp3 46n	ppp3 48n	ppp3 49n	ppp19 4n	ppp3 53n	ppp19 5n	ppp5b 61n
SiO2	50.07	47.41	47.17	46.26	48.18	45.53	46.90	46.67	44.49	47.12	49.15	47.48
TiO2	0.62	0.63	0.79	0.01	0.58	0.16	0.46	0.59	0.00	0.02	0.00	0.02
Al2O3	37.56	36.46	36.13	33.65	33.48	36.22	36.94	36.40	33.64	32.57	31.17	37.06
Cr2O3	0.00	0.00	0.00	0.00	0.00	0.00	0.00	0.00	0.00	0.00	0.00	0.00
FeO	1.18	1.12	0.93	5.60	1.35	0.92	0.79	0.93	6.63	11.40	6.09	0.89
MnO	0.04	0.03	0.01	0.06	0.00	0.00	0.00	0.00	0.09	0.22	0.06	0.00
MgO	0.38	0.35	0.28	2.29	0.77	0.39	0.30	0.29	2.64	4.17	2.37	0.29
CaO	0.00	0.00	0.01	0.06	0.01	0.00	0.00	0.00	0.06	0.02	0.04	0.00
Na2O	0.55	0.53	0.55	0.90	0.40	0.31	0.44	0.51	0.57	0.43	1.09	1.01
K2O	8.57	10.26	10.02	3.49	9.96	8.68	9.82	8.80	3.12	2.06	3.34	9.52
Total	99.44	97.10	95.97	92.31	94.84	92.22	95.65	94.19	91.23	98.02	93.30	96.28
Cations corrected to 11 Oxygens												
Si	3.14	3.08	3.10	3.12	3.20	3.08	3.08	3.09	3.05	3.06	3.27	3.09
Ti	0.00	0.00	0.00	0.00	0.00	0.00	0.00	0.00	0.00	0.00	0.00	0.00
Al	2.77	2.80	2.79	2.67	2.62	2.89	2.86	2.84	2.72	2.49	2.44	2.85
Cr	0.00	0.00	0.00	0.00	0.00	0.00	0.00	0.00	0.00	0.00	0.00	0.00
Fe	0.06	0.06	0.05	0.32	0.07	0.05	0.04	0.05	0.38	0.62	0.34	0.05
Mn	0.00	0.00	0.00	0.00	0.00	0.00	0.00	0.00	0.01	0.01	0.00	0.00
Mg	0.04	0.03	0.03	0.23	0.08	0.04	0.03	0.03	0.27	0.40	0.24	0.03
Ca	0.00	0.00	0.00	0.00	0.00	0.00	0.00	0.00	0.00	0.00	0.00	0.00
Na	0.07	0.07	0.07	0.12	0.05	0.04	0.06	0.07	0.08	0.05	0.14	0.13
K	0.69	0.85	0.84	0.30	0.84	0.75	0.82	0.74	0.27	0.17	0.28	0.79
Cation Total	6.76	6.89	6.88	6.76	6.87	6.85	6.89	6.83	6.77	6.81	6.72	6.94
Mol% pa	8.92	7.31	7.62	27.86	5.76	5.15	6.39	8.14	21.50	23.79	32.90	13.88
Distance (Km)	0.68	0.68	0.68	1.52	0.68	0.68	0.68	0.68	1.52	0.68	1.52	1.43

Mol% Pa = Na/(Na+K+Ca)x100%; Distance = distance from approximate nearest surface expression of the contact.

Sample	ppp5b	ppp5b	ppp5b
Point #	62n	65n	67n
SiO2	45.63	46.66	47.06
TiO2	0.17	0.20	0.04
Al2O3	32.71	36.68	35.12
Cr2O3	0.00	0.00	0.00
FeO	5.64	0.76	1.00
MnO	0.04	0.00	0.00
MgO	2.04	0.40	0.70
CaO	0.04	0.00	0.00
Na2O	0.39	0.87	0.66
K2O	5.44	9.34	8.87
Total	92.09	94.92	93.44
Cations corrected to 11 Oxygens			
Si	3.12	3.08	3.15
Ti	0.00	0.00	0.00
Al	2.63	2.86	2.77
Cr	0.00	0.00	0.00
Fe	0.32	0.04	0.06
Mn	0.00	0.00	0.00
Mg	0.21	0.04	0.07
Ca	0.00	0.00	0.00
Na	0.05	0.11	0.09
K	0.47	0.79	0.76
Cation Total	6.81	6.92	6.89
Mol% pa	9.77	12.48	10.18
Distance (Km)	1.43	1.43	1.43

Mol% Pa = $\text{Na}/(\text{Na}+\text{K}+\text{Ca})\times 100\%$; Distance = distance from approximate nearest surface expression of the contact.

Table A.3: Biotite: Cunard Member

Sample Point #	RTR04 67	RTR04 74	RTR04 76	LSCN 83	LSCN 84	LSCN 85	LSCN 86	LSCN 105	DP2 143	DP2 145	Bsub 160	Bsub 161
SiO2	37.32	31.40	31.44	35.49	40.17	36.03	34.85	33.77	36.51	37.12	35.48	35.92
TiO2	1.40	1.30	1.44	1.29	1.00	1.36	1.24	1.19	2.21	1.71	1.48	1.31
Al2O3	19.06	20.68	21.11	20.82	27.62	20.83	20.78	21.28	19.43	20.40	21.63	21.26
Cr2O3	0.09	0.06	0.08	0.05	0.09	0.10	0.11	0.12	0.36	0.27	0.33	0.27
FeO	22.58	25.12	25.81	19.74	11.69	19.37	19.84	21.04	18.71	17.75	21.60	20.80
MnO	0.23	0.27	0.27	0.05	0.02	0.06	0.05	0.08	0.15	0.15	0.20	0.22
MgO	6.09	7.02	6.93	9.45	5.13	9.66	9.65	10.12	9.68	9.75	8.27	8.46
CaO	0.02	0.06	0.01	0.02	0.00	0.01	0.00	0.03	0.10	0.10	0.09	0.11
Na2O	0.16	0.12	0.13	0.16	0.61	0.21	0.18	0.13	0.20	0.24	0.22	0.25
K2O	6.38	5.84	5.63	6.82	7.42	7.01	6.65	5.71	8.96	9.02	6.72	6.94
Total	93.33	91.88	92.84	93.90	93.74	94.64	93.35	93.47	96.32	96.49	96.03	95.53
Cations corrected to 11 Oxygens												
Si	2.87	2.52	2.50	2.69	2.88	2.71	2.66	2.59	2.73	2.74	2.66	2.69
Ti	0.08	0.08	0.09	0.07	0.05	0.08	0.07	0.07	0.12	0.09	0.08	0.07
Al	1.73	1.96	1.98	1.86	2.33	1.84	1.87	1.92	1.71	1.78	1.91	1.88
Cr	0.01	0.00	0.01	0.00	0.01	0.01	0.01	0.01	0.02	0.02	0.02	0.02
Fe	1.45	1.69	1.72	1.25	0.70	1.22	1.27	1.35	1.17	1.10	1.35	1.30
Mn	0.02	0.02	0.02	0.00	0.00	0.00	0.00	0.00	0.01	0.01	0.01	0.01
Mg	0.70	0.84	0.82	1.07	0.55	1.08	1.10	1.16	1.08	1.07	0.92	0.94
Ca	0.00	0.01	0.00	0.00	0.00	0.00	0.00	0.00	0.01	0.01	0.01	0.01
Na	0.02	0.02	0.02	0.02	0.08	0.03	0.03	0.02	0.03	0.03	0.03	0.04
K	0.63	0.60	0.57	0.66	0.68	0.67	0.65	0.56	0.85	0.85	0.64	0.66
Cation Total	7.50	7.73	7.72	7.64	7.28	7.64	7.66	7.67	7.73	7.70	7.64	7.64
Mol% Annite	67.54	66.74	67.63	53.96	56.12	52.97	53.55	53.85	52.03	50.51	59.43	58.00
Mol% Phlogopite	32.46	33.26	32.37	46.04	43.88	47.03	46.45	46.15	47.97	49.49	40.57	42.00

Mol% Annite = Fe/(Fe+Mg)x100%; Mol% Phlogopite = Mg/(Fe+Mg)x100%;

Sample Point #	Bsub	RTR04	AR04-1	AR04-1	AR04-1	AR04-1	AR04-1	AR04-1	AR04-1	AR04-1	AR05-3	AR05-3	AR05-3
SiO ₂	35.73	32.29	34.75	34.43	34.39	35.18	35.10	34.37	34.59	33.72	33.90	34.34	
TiO ₂	1.30	1.62	2.59	2.39	1.98	1.72	1.80	1.73	1.88	2.41	2.85	1.84	
Al ₂ O ₃	21.04	20.15	20.10	20.97	19.65	20.04	21.25	20.72	20.90	20.19	19.68	19.92	
Cr ₂ O ₃	0.28	0.07	0.10	0.15	0.08	0.10	0.11	0.07	0.05	0.39	0.50	0.08	
FeO	20.71	22.84	20.82	20.06	20.23	19.61	20.53	20.39	20.74	19.91	19.79	19.99	
MnO	0.20	0.25	0.05	0.04	0.09	0.08	0.09	0.09	0.07	0.12	0.08	0.10	
MgO	8.50	6.19	7.93	7.84	7.63	8.44	8.07	7.94	8.02	7.54	7.56	8.38	
CaO	0.09	0.09	0.00	0.00	0.01	0.02	0.01	0.00	0.00	0.00	0.00	0.07	
Na ₂ O	0.24	2.79	0.14	0.17	0.17	0.17	0.15	0.14	0.14	0.12	0.11	0.23	
K ₂ O	6.79	8.01	8.79	8.81	8.48	8.53	8.42	8.74	8.69	9.27	9.37	7.54	
Total	94.87	94.28	95.28	94.86	92.71	93.89	95.53	94.19	95.09	93.67	93.83	92.50	
Cations corrected to 11 Oxygens													
Si	2.70	2.55	2.65	2.63	2.69	2.70	2.66	2.65	2.64	2.63	2.64	2.68	
Ti	0.07	0.10	0.15	0.14	0.12	0.10	0.10	0.10	0.11	0.14	0.17	0.11	
Al	1.87	1.88	1.81	1.89	1.81	1.82	1.90	1.88	1.88	1.85	1.80	1.83	
Cr	0.02	0.00	0.01	0.01	0.00	0.01	0.01	0.00	0.00	0.02	0.03	0.01	
Fe	1.31	1.51	1.33	1.28	1.32	1.26	1.30	1.31	1.32	1.30	1.29	1.30	
Mn	0.01	0.02	0.00	0.00	0.01	0.01	0.01	0.01	0.00	0.01	0.01	0.01	
Mg	0.96	0.73	0.90	0.89	0.89	0.97	0.91	0.91	0.91	0.88	0.88	0.97	
Ca	0.01	0.01	0.00	0.00	0.00	0.00	0.00	0.00	0.00	0.00	0.00	0.01	
Na	0.04	0.43	0.02	0.03	0.03	0.02	0.02	0.02	0.02	0.02	0.02	0.04	
K	0.65	0.81	0.86	0.86	0.85	0.84	0.81	0.86	0.85	0.92	0.93	0.75	
Cation Total	7.63	8.03	7.73	7.72	7.72	7.72	7.71	7.75	7.74	7.76	7.75	7.69	
Mol% Annite	57.75	67.42	59.54	58.96	59.81	56.59	58.81	59.04	59.19	59.70	59.51	57.23	
Mol% Phlogopite	42.25	32.58	40.46	41.04	40.19	43.41	41.19	40.96	40.81	40.30	40.49	42.77	

Mol% Annite = $\text{Fe}/(\text{Fe}+\text{Mg})\times 100\%$; Mol% Phlogopite = $\text{Mg}/(\text{Fe}+\text{Mg})\times 100\%$;

Sample Point #	AR05-3	AR05-5	AR05-5	AR05-5	AR05-5	AR05-5	AR05-5
SiO ₂	34.77	34.71	34.66	34.22	34.47	34.90	35.61
TiO ₂	1.65	1.12	1.32	1.33	1.43	2.71	1.87
Al ₂ O ₃	20.38	21.08	20.34	20.54	20.63	19.51	20.40
Cr ₂ O ₃	0.00	0.00	0.00	0.00	0.00	0.00	0.00
FeO	18.53	18.48	18.61	18.44	18.97	19.07	18.36
MnO	0.01	0.01	0.02	0.02	0.00	0.02	0.01
MgO	9.15	9.45	9.40	9.47	9.47	8.92	9.62
CaO	0.00	0.00	0.00	0.00	0.00	0.00	0.00
Na ₂ O	0.15	0.12	0.13	0.14	0.14	0.11	0.09
K ₂ O	8.71	9.17	9.10	9.05	9.10	9.21	9.37
Total	93.35	94.13	93.58	93.22	94.22	94.44	95.34
Cations corrected to 11 Oxygens							
Si	2.68	2.65	2.67	2.65	2.64	2.67	2.69
Ti	0.10	0.06	0.08	0.08	0.08	0.16	0.11
Al	1.85	1.90	1.85	1.87	1.86	1.76	1.81
Cr	0.00	0.00	0.00	0.00	0.00	0.00	0.00
Fe	1.19	1.18	1.20	1.19	1.22	1.22	1.16
Mn	0.00	0.00	0.00	0.00	0.00	0.00	0.00
Mg	1.05	1.08	1.08	1.09	1.08	1.02	1.08
Ca	0.00	0.00	0.00	0.00	0.00	0.00	0.00
Na	0.02	0.02	0.02	0.02	0.02	0.02	0.01
K	0.85	0.89	0.89	0.89	0.89	0.90	0.90
Cation Total	7.74	7.79	7.79	7.80	7.80	7.75	7.76
Mol% Annite	53.16	52.31	52.61	52.19	52.92	54.54	51.69
Mol% Phlogopite	46.84	47.69	47.39	47.81	47.08	45.46	48.31

Mol% Annite = $\text{Fe}/(\text{Fe}+\text{Mg})\times 100\%$; Mol% Phlogopite = $\text{Mg}/(\text{Fe}+\text{Mg})\times 100\%$;

Table A.4: Biotite: Cunard Member

Sample Point #	wl05-10	wl05-10	pcr10	pcr10	pcr10	pcr10	wl05-4	wl05-4	wl05-4	wl05-4	wl05-4
	215	223	234	243	244	245	257	263	264	267	268
SiO2	34.09	34.16	33.20	33.66	30.29	30.60	33.9605	33.8259	33.3771	33.8233	34.2882
TiO2	2.72	2.74	2.80	1.04	1.22	1.27	2.2142	1.4795	2.296	1.8523	2.4863
Al2O3	20.85	20.74	20.54	21.89	18.03	18.37	20.1067	20.1819	20.0447	21.037	20.0273
Cr2O3	0.18	0.13	0.20	0.14	0.21	0.17	0.2036	0.1421	0.1891	0.2193	0.2441
FeO	24.03	23.82	25.18	25.46	23.08	23.45	23.2759	22.7641	23.2957	24.5246	24.3201
MnO	0.16	0.17	0.07	0.10	0.12	0.11	0.2669	0.2217	0.2215	0.2159	0.1949
MgO	6.55	6.39	5.07	6.02	4.95	4.96	6.2935	6.5165	6.1377	5.5708	5.7339
CaO	0.00	0.02	0.00	0.01	0.14	0.16	0.0258	0	0.0029	0.0024	0.0088
Na2O	0.10	0.09	0.06	0.07	0.10	0.10	0.1136	0.1336	0.088	0.0816	0.1386
K2O	8.66	8.74	8.22	7.55	6.25	6.30	9.067	9.2457	9.4517	9.2011	9.1208
Total	97.37	97.00	95.32	95.94	84.39	85.49	95.5278	94.5111	95.1045	96.5284	96.5631
	Cations corrected to 11 Oxygens										
Si	2.59	2.60	2.59	2.59	2.65	2.65	2.6301	2.6444	2.607	2.6048	2.6367
Ti	0.16	0.16	0.16	0.06	0.08	0.08	0.13	0.0869	0.1353	0.1078	0.1441
Al	1.86	1.86	1.89	1.99	1.86	1.87	1.8359	1.8601	1.8458	1.9096	1.815
Cr	0.01	0.01	0.01	0.01	0.01	0.01	0.01	0.0088	0.0121	0.0132	0.0143
Fe	1.52	1.52	1.64	1.64	1.69	1.70	1.507	1.4883	1.5224	1.5796	1.5642
Mn	0.01	0.01	0.00	0.01	0.01	0.01	0.0176	0.0143	0.0143	0.0143	0.0132
Mg	0.74	0.72	0.59	0.69	0.65	0.64	0.7271	0.759	0.715	0.6391	0.6578
Ca	0.00	0.00	0.00	0.00	0.01	0.01	0.0022	0	0	0	0.0011
Na	0.02	0.01	0.01	0.01	0.02	0.02	0.02	0.0198	0.0132	0.0121	0.0209
K	0.84	0.85	0.82	0.74	0.70	0.70	0.90	0.9218	0.9416	0.9042	0.8954
Cation Total	7.75	7.74	7.71	7.73	7.69	7.69	7.77	7.8034	7.8067	7.7847	7.7627
Mol% Annite	67.28	67.65	73.61	70.34	72.33	72.60	67.45	66.23	68.04	71.19	70.40
Mol% Phlogopite	32.72	32.35	26.39	29.66	27.67	27.40	32.55	33.77	31.96	28.81	29.60

Mol% Annite = $\text{Fe}/(\text{Fe}+\text{Mg})\times 100\%$; Mol% Phlogopite = $\text{Mg}/(\text{Fe}+\text{Mg})\times 100\%$;

Sample Point #	wl05-4 270	wl05-12 355	wl05-12 358	wl05-12 361	wl05-12 363	wl05-12 373	wl05-15 380	wl05-15 383	wl05-15 386	wl05-15 392	ppp19 17n
SiO2	33.9819	33.5359	33.5072	34.175	33.7943	32.7835	34.0888	34.2411	33.7859	34.1472	32.7741
TiO2	0.8158	2.7389	2.6931	2.4892	3.1743	2.2595	2.4291	2.5382	2.6919	3.1704	1.23
Al2O3	21.3765	18.4386	18.3714	19.3418	18.3628	18.605	20.8995	21.0722	20.5845	20.4875	20.9463
Cr2O3	0.1578	0.1082	0.0739	0.1225	0.0625	0.0627	0.348	0.2993	0.1623	0.1633	0.042
FeO	24.6627	24.4009	24.0686	23.6796	24.4566	25.1442	24.4183	25.0059	25.427	24.307	24.9841
MnO	0.2308	0.1325	0.1142	0.1158	0.1047	0.1086	0.1103	0.0961	0.1029	0.0763	0.188
MgO	6.3362	5.0801	4.9819	5.4114	5.2203	4.219	4.7569	4.6287	5.0499	5.0182	6.7744
CaO	0.0084	0.047	0.045	0.0609	0.0524	0.0499	0.021	0.0324	0.0205	0.0316	0
Na2O	0.0821	0.1317	0.1196	0.131	0.1132	0.0715	0.0979	0.0691	0.1004	0.0757	0.1016
K2O	9.3466	8.8621	8.9067	8.8427	8.9427	8.5613	8.839	8.7699	8.2426	8.9781	6.4645
Total	96.9988	93.476	92.8817	94.3699	94.2839	91.8653	96.0089	96.753	96.168	96.4554	93.5051
Cations corrected to 11 Oxygens											
Si	2.6048	2.6763	2.6873	2.6807	2.673	2.673	2.6301	2.6246	2.6092	2.6235	2.5773
Ti	0.0473	0.1639	0.1628	0.1463	0.1892	0.1386	0.1408	0.1463	0.1562	0.1837	0.0726
Al	1.9316	1.7347	1.7369	1.7886	1.7116	1.7875	1.9008	1.9041	1.8733	1.8546	1.9415
Cr	0.0099	0.0066	0.0044	0.0077	0.0044	0.0044	0.0209	0.0176	0.0099	0.0099	0.0022
Fe	1.5807	1.628	1.6148	1.5532	1.617	1.7149	1.5763	1.6027	1.6423	1.562	1.6434
Mn	0.0154	0.0088	0.0077	0.0077	0.0066	0.0077	0.0077	0.0066	0.0066	0.0055	0.0121
Mg	0.7238	0.6039	0.5962	0.6325	0.6149	0.5126	0.5467	0.5291	0.5808	0.5742	0.7942
Ca	0.0011	0.0044	0.0044	0.0055	0.0044	0.0044	0.0022	0.0022	0.0022	0.0022	0
Na	0.0121	0.0209	0.0187	0.0198	0.0176	0.011	0.0143	0.0099	0.0154	0.011	0.0154
K	0.9141	0.902	0.9119	0.8844	0.902	0.891	0.8701	0.858	0.8118	0.88	0.649
Cation Total	7.8408	7.7495	7.7451	7.7264	7.7407	7.7451	7.7099	7.7011	7.7077	7.7066	7.7077
Mol% Annite	68.59	72.94	73.03	71.06	72.45	76.99	74.25	75.18	73.87	73.12	67.42
Mol% Phlogopite	31.41	27.06	26.97	28.94	27.55	23.01	25.75	24.82	26.13	26.88	32.58

Mol% Annite = $\text{Fe}/(\text{Fe}+\text{Mg})\times 100\%$; Mol% Phlogopite = $\text{Mg}/(\text{Fe}+\text{Mg})\times 100\%$;

Sample Point #	ppp19 19n	ppp3 29n	ppp3 38n	ppp3 39n	ppp3 40n	ppp3 43n	ppp3 44n	ppp3 52n	ppp3 55n	ppp3 56n	ppp5b 58n
SiO2	33.6191	33.9543	33.0091	34.0706	33.2139	33.3581	33.5618	34.2991	33.5116	34.0687	34.1722
TiO2	1.0618	1.6477	2.2013	2.1587	2.2723	2.4473	2.4734	2.6164	2.0418	2.0584	1.0957
Al2O3	23.8316	21.0474	20.2909	20.4138	19.8991	20.6683	21.1005	21.2182	21.661	21.1071	20.8753
Cr2O3	0.0374	0.0929	0.1538	0.1303	0.1449	0.0583	0.0433	0.129	0.0879	0.129	0.0716
FeO	23.8568	24.8745	26.2675	25.1665	25.3645	23.6958	24.415	23.9384	24.1295	23.4915	23.6401
MnO	0.1756	0.1939	0.1525	0.0769	0.1027	0.1097	0.117	0.0996	0.1043	0.1102	0.137
MgO	6.5348	5.5478	5.1528	5.0994	5.4489	5.0832	5.1168	5.0819	5.2436	5.2387	6.863
CaO	0	0.0375	0.0422	0.0503	0.0645	0	0	0.0072	0.0201	0.0859	0
Na2O	0.2314	0.0483	0.0461	0.057	0.0382	0.049	0.0382	0.174	0.1654	0.1643	0.2594
K2O	6.1177	8.6628	6.8789	8.3836	7.633	8.6124	8.5108	8.7711	8.5981	8.5022	7.8812
Total	95.4663	96.1072	94.1952	95.6072	94.1821	94.0822	95.3769	96.335	95.5634	94.9561	94.9955
Cations corrected to 11 Oxygens											
Si	2.5509	2.6202	2.6004	2.6433	2.6169	2.6202	2.6037	2.6268	2.5916	2.64	2.64
Ti	0.0605	0.0957	0.1309	0.1254	0.1342	0.1441	0.1441	0.1507	0.1188	0.1199	0.0638
Al	2.1307	1.914	1.8843	1.8667	1.848	1.914	1.9294	1.9151	1.9745	1.9283	1.9008
Cr	0.0022	0.0055	0.0099	0.0077	0.0088	0.0033	0.0022	0.0077	0.0055	0.0077	0.0044
Fe	1.5136	1.6049	1.7303	1.6324	1.672	1.5565	1.584	1.5334	1.5609	1.5224	1.5279
Mn	0.011	0.0132	0.0099	0.0055	0.0066	0.0077	0.0077	0.0066	0.0066	0.0077	0.0088
Mg	0.7392	0.638	0.605	0.5896	0.6402	0.5951	0.5918	0.5797	0.605	0.605	0.7909
Ca	0	0.0033	0.0033	0.0044	0.0055	0	0	0.0011	0.0022	0.0066	0
Na	0.0341	0.0077	0.0066	0.0088	0.0055	0.0077	0.0055	0.0253	0.0253	0.0242	0.0385
K	0.5918	0.8525	0.6908	0.8294	0.7678	0.8635	0.8426	0.8569	0.8481	0.8404	0.7766
Cation Total	7.634	7.755	7.6714	7.7132	7.7055	7.7121	7.711	7.7033	7.7385	7.7022	7.7517
Mol% Annite	67.19	71.55	74.09	73.47	72.31	72.34	72.80	72.57	72.07	71.56	65.89
Mol% Phlogopite	32.81	28.45	25.91	26.53	27.69	27.66	27.20	27.43	27.93	28.44	34.11

Mol% Annite = $\text{Fe}/(\text{Fe}+\text{Mg})\times 100\%$; Mol% Phlogopite = $\text{Mg}/(\text{Fe}+\text{Mg})\times 100\%$;

Sample Point #	ppp5b 60n	ppp5b 66n	ppp5b 68n	ppp19 9n
SiO2	33.9657	33.8	33.8077	33.3874
TiO2	1.2968	1.3154	1.2046	1.2771
Al2O3	20.5569	20.8225	20.4017	21.2196
Cr2O3	0.0492	0.0372	0.0113	0.1785
FeO	23.377	23.0296	22.6564	23.6284
MnO	0.1065	0.1134	0.1129	0.213
MgO	6.8761	6.8277	7.1135	6.4254
CaO	0	0	0	0
Na2O	0.2169	0.1603	0.1577	0.1867
K2O	7.8859	7.9888	7.7638	7.8911
Total	94.331	94.095	93.2297	94.4073
Cations corrected to 11 Oxygens				
Si	2.6422	2.6323	2.651	2.6015
Ti	0.0759	0.077	0.0715	0.0748
Al	1.8843	1.9118	1.8854	1.9492
Cr	0.0033	0.0022	0.0011	0.011
Fe	1.5202	1.5004	1.4861	1.54
Mn	0.0066	0.0077	0.0077	0.0143
Mg	0.7975	0.7931	0.8316	0.7469
Ca	0	0	0	0
Na	0.033	0.0242	0.0242	0.0286
K	0.7821	0.7942	0.7766	0.7843
Cation Total	7.7451	7.7429	7.7352	7.7506
Mol% Annite	65.59	65.42	64.12	67.34
Mol% Phlogopite	34.41	34.58	35.88	32.66

Mol% Annite = $\text{Fe}/(\text{Fe}+\text{Mg})\times 100\%$; Mol% Phlogopite = $\text{Mg}/(\text{Fe}+\text{Mg})\times 100\%$;

Table A.5: Chlorite: Cunard Member

Sample Point #	sgr03 6	sgr03 7	sgr03 14	sgr03 19	sgr03 20	sgr03 21	sgr03 22	iwk03 27	iwk03 28	LSCN 91	LSCN 92	LSCN 96
SiO2	23.63	23.56	24.27	23.90	23.60	26.62	24.31	24.65	23.82	28.66	23.83	24.52
TiO2	0.02	0.03	0.09	0.04	0.02	0.09	0.07	0.03	0.04	0.08	0.05	0.09
Al2O3	24.32	23.49	23.62	23.95	23.99	23.19	23.94	21.96	23.40	23.03	23.91	24.74
Cr2O3	0.04	0.01	0.08	0.10	0.07	0.02	0.04	0.04	0.06	0.03	0.00	0.07
FeO	25.58	24.12	25.40	25.39	25.64	22.55	24.65	22.83	24.09	25.40	25.58	25.92
MnO	0.30	0.32	0.35	0.32	0.35	0.32	0.32	0.25	0.32	0.13	0.10	0.14
MgO	13.11	13.20	12.86	13.07	13.33	12.84	12.76	15.25	13.66	12.96	13.06	13.43
CaO	0.00	0.00	0.00	0.00	0.00	0.06	0.02	0.01	0.02	0.00	0.00	0.02
Na2O	0.01	0.00	0.04	0.00	0.00	0.19	0.06	0.14	0.16	0.00	0.00	0.02
K2O	0.02	0.02	0.04	0.04	0.01	0.36	0.26	0.06	0.10	0.00	0.01	0.02
Total	87.02	84.75	86.75	86.82	87.02	86.23	86.42	85.22	85.66	90.28	86.55	88.96
Cations corrected to 28 Oxygens												
Si	5.03	5.12	5.17	5.10	5.03	5.60	5.19	5.29	5.12	5.78	5.10	5.09
Ti	0.00	0.01	0.01	0.01	0.00	0.01	0.01	0.01	0.01	0.01	0.01	0.01
Al	6.10	6.02	5.94	6.02	6.03	5.75	6.02	5.56	5.93	5.47	6.03	6.05
Cr	0.01	0.00	0.01	0.02	0.01	0.00	0.01	0.01	0.01	0.01	0.00	0.01
Fe	4.55	4.38	4.53	4.53	4.57	3.97	4.40	4.10	4.33	4.28	4.58	4.50
Mn	0.05	0.06	0.06	0.06	0.06	0.06	0.06	0.04	0.06	0.02	0.02	0.03
Mg	4.16	4.28	4.09	4.15	4.23	4.02	4.06	4.88	4.38	3.89	4.16	4.16
Ca	0.00	0.00	0.00	0.00	0.00	0.01	0.00	0.00	0.01	0.00	0.00	0.01
Na	0.00	0.00	0.02	0.00	0.00	0.08	0.03	0.06	0.07	0.00	0.00	0.01
K	0.01	0.01	0.01	0.01	0.00	0.10	0.07	0.01	0.03	0.00	0.00	0.01
Cation total	19.91	19.87	19.85	19.89	19.95	19.59	19.84	19.96	19.94	19.47	19.89	19.87
X _{Fe}	0.52	0.51	0.53	0.52	0.52	0.50	0.52	0.46	0.50	0.52	0.52	0.52
X _{Mg}	0.48	0.49	0.47	0.48	0.48	0.50	0.48	0.54	0.50	0.48	0.48	0.48

Sample Point #	LSCN 97	LSCN 100	LSCN 110	LSCN 112	sgr03 113	sgr03 116	sgr03 118	sgr03 121	sgr03 128	MSBa 130	MSBa 131	MSBa 133
SiO ₂	23.93	29.81	30.24	28.47	24.25	34.84	24.23	23.97	23.99	24.87	24.50	25.13
TiO ₂	0.09	0.13	0.09	0.01	0.03	0.11	0.09	0.00	0.03	0.19	0.18	0.21
Al ₂ O ₃	24.17	27.25	27.22	26.86	24.46	30.49	24.25	25.04	25.15	25.27	25.59	24.61
Cr ₂ O ₃	0.07	0.20	0.12	0.03	0.09	0.05	0.12	0.09	0.08	0.27	0.32	0.29
FeO	25.86	18.84	20.32	22.90	25.39	12.04	24.85	24.70	24.76	24.61	24.59	24.13
MnO	0.11	0.09	0.07	0.13	0.35	0.18	0.34	0.33	0.36	0.54	0.55	0.54
MgO	13.22	9.23	5.48	9.93	13.16	6.15	13.44	13.35	13.01	13.12	13.64	13.88
CaO	0.00	0.00	0.05	0.11	0.00	0.00	0.00	0.00	0.00	0.10	0.08	0.10
Na ₂ O	0.01	0.44	0.74	0.04	0.00	0.76	0.01	0.00	0.00	0.06	0.06	0.06
K ₂ O	0.00	2.32	3.05	0.06	0.02	4.16	0.03	0.01	0.03	0.21	0.09	0.09
Total	87.45	88.31	87.39	88.53	87.75	88.79	87.35	87.50	87.42	89.24	89.59	89.04
Cations corrected to 28 Oxygens												
Si	5.07	5.98	6.19	5.75	5.10	6.65	5.11	5.04	5.05	5.12	5.03	5.17
Ti	0.01	0.02	0.01	0.00	0.01	0.02	0.01	0.00	0.01	0.03	0.03	0.03
Al	6.03	6.44	6.57	6.39	6.07	6.87	6.03	6.21	6.24	6.14	6.19	5.98
Cr	0.01	0.03	0.02	0.01	0.01	0.01	0.02	0.01	0.01	0.04	0.05	0.05
Fe	4.58	3.16	3.48	3.86	4.47	1.92	4.38	4.34	4.36	4.24	4.22	4.16
Mn	0.02	0.02	0.01	0.02	0.06	0.03	0.06	0.06	0.06	0.09	0.10	0.10
Mg	4.17	2.76	1.67	2.99	4.13	1.75	4.23	4.18	4.08	4.03	4.17	4.26
Ca	0.00	0.00	0.01	0.02	0.00	0.00	0.00	0.00	0.00	0.02	0.02	0.02
Na	0.00	0.17	0.29	0.02	0.00	0.28	0.00	0.00	0.00	0.03	0.02	0.03
K	0.00	0.59	0.80	0.01	0.00	1.01	0.01	0.00	0.01	0.05	0.02	0.03
Cation total	19.90	19.15	19.05	19.07	19.85	18.54	19.86	19.85	19.82	19.80	19.85	19.81
X _{Fe}	0.52	0.53	0.68	0.56	0.52	0.52	0.51	0.51	0.52	0.51	0.50	0.49
X _{Mg}	0.48	0.47	0.32	0.44	0.48	0.48	0.49	0.49	0.48	0.49	0.50	0.51

Sample Point #	MSBa	MSBa	Bsub	Bsub	Bsub	Bsub	Bsub	Bsub	Bsub	Bsub	MBD	MBD
	137	139	150	151	153	154	159	165	166	167	174	175
SiO2	24.57	24.58	24.76	25.06	31.36	24.32	23.98	24.05	24.13	24.10	23.31	23.52
TiO2	0.23	0.21	0.21	0.24	0.13	0.18	0.17	0.21	0.23	0.23	0.01	0.13
Al2O3	24.81	25.54	24.16	25.34	29.69	23.95	24.51	24.67	24.62	24.40	24.95	24.56
Cr2O3	0.30	0.30	0.26	0.26	0.25	0.26	0.27	0.31	0.28	0.28	0.05	0.08
FeO	24.59	24.19	27.91	26.70	21.89	27.92	27.49	28.09	28.07	28.09	24.94	24.63
MnO	0.53	0.57	0.30	0.27	0.25	0.28	0.27	0.31	0.28	0.28	0.17	0.15
MgO	13.07	12.56	12.54	11.48	6.18	12.36	12.27	11.73	12.03	11.98	14.40	14.43
CaO	0.10	0.10	0.10	0.11	0.69	0.10	0.10	0.11	0.13	0.11	0.00	0.01
Na2O	0.09	0.12	0.07	0.06	0.67	0.08	0.05	0.06	0.06	0.04	0.00	0.00
K2O	0.13	0.27	0.11	0.07	0.33	0.08	0.06	0.07	0.07	0.07	0.00	0.00
Total	88.42	88.44	90.41	89.59	91.44	89.50	89.16	89.61	89.90	89.58	87.84	87.52
Cations corrected to 28 Oxygens												
Si	5.12	5.10	5.12	5.18	6.05	5.09	5.03	5.03	5.03	5.04	4.90	4.95
Ti	0.04	0.03	0.03	0.04	0.02	0.03	0.03	0.03	0.04	0.04	0.00	0.02
Al	6.09	6.25	5.89	6.17	6.76	5.91	6.06	6.08	6.05	6.02	6.18	6.10
Cr	0.05	0.05	0.04	0.04	0.04	0.04	0.04	0.05	0.04	0.05	0.01	0.01
Fe	4.28	4.20	4.83	4.61	3.53	4.89	4.82	4.91	4.89	4.92	4.38	4.34
Mn	0.09	0.10	0.05	0.05	0.04	0.05	0.05	0.06	0.05	0.05	0.03	0.03
Mg	4.06	3.89	3.86	3.54	1.78	3.86	3.84	3.66	3.74	3.74	4.51	4.53
Ca	0.02	0.02	0.02	0.03	0.14	0.02	0.02	0.03	0.03	0.03	0.00	0.00
Na	0.04	0.05	0.03	0.02	0.25	0.03	0.02	0.02	0.03	0.02	0.00	0.00
K	0.03	0.07	0.03	0.02	0.08	0.02	0.02	0.02	0.02	0.02	0.00	0.00
Cation total	19.82	19.77	19.91	19.70	18.70	19.93	19.91	19.89	19.91	19.91	20.01	19.98
X _{Fe}	0.51	0.52	0.56	0.57	0.67	0.56	0.56	0.57	0.57	0.57	0.49	0.49
X _{Mg}	0.49	0.48	0.44	0.43	0.33	0.44	0.44	0.43	0.43	0.43	0.51	0.51

Sample Point #	MBD 178	MBD 180	MBD 181	iwk05 210	iwk05 212	AR05-5 338	rr05-3 351	rr05-5 353
SiO ₂	23.88	23.53	23.78	30.48	23.59	36.85	24.01	35.58
TiO ₂	0.06	0.10	0.09	0.07	0.09	0.00	0.07	0.19
Al ₂ O ₃	24.44	25.49	24.99	29.03	25.00	31.07	23.41	28.87
Cr ₂ O ₃	0.03	0.05	0.02	0.01	0.07	0.00	0.00	0.00
FeO	24.84	24.70	24.39	13.83	21.71	13.10	23.80	11.09
MnO	0.15	0.18	0.17	0.32	0.37	0.00	0.47	0.21
MgO	14.42	14.16	14.27	6.71	13.65	5.25	13.81	6.90
CaO	0.01	0.00	0.00	0.05	0.04	0.17	0.03	0.03
Na ₂ O	0.01	0.01	0.00	0.84	0.00	0.95	0.00	0.56
K ₂ O	0.00	0.02	0.00	2.03	0.01	2.77	0.09	2.93
Total	87.83	88.24	87.71	83.37	84.53	90.16	85.70	86.37
Cations corrected to 28 Oxygens								
Si	5.01	4.91	4.98	6.26	5.06	6.87	5.15	6.89
Ti	0.01	0.01	0.01	0.01	0.01	0.00	0.01	0.03
Al	6.04	6.27	6.17	7.02	6.33	6.82	5.92	6.59
Cr	0.01	0.01	0.00	0.00	0.01	0.00	0.00	0.00
Fe	4.36	4.31	4.27	2.37	3.89	2.04	4.27	1.79
Mn	0.03	0.03	0.03	0.06	0.07	0.00	0.09	0.03
Mg	4.51	4.40	4.45	2.05	4.37	1.46	4.42	1.99
Ca	0.00	0.00	0.00	0.01	0.01	0.03	0.01	0.01
Na	0.00	0.00	0.00	0.33	0.00	0.34	0.00	0.21
K	0.00	0.01	0.00	0.53	0.00	0.66	0.02	0.72
Cation total	19.96	19.95	19.92	18.65	19.75	18.22	19.89	18.26
X _{Fe}	0.49	0.49	0.49	0.54	0.47	0.58	0.49	0.47
X _{Mg}	0.51	0.51	0.51	0.46	0.53	0.42	0.51	0.53

Table A.6: Chlorite: Bluestone member

Sample	ppp19	ppp7	ib04-1	wl05-10
Point #	10n	72n	203	224
SiO₂	31.52	28.05	23.50	32.02
TiO₂	0.04	0.07	0.03	0.01
Al₂O₃	29.45	21.63	24.97	28.41
Cr₂O₃	0.00	0.00	0.04	0.05
FeO	20.61	19.64	22.72	16.79
MnO	0.28	1.88	0.33	0.27
MgO	5.77	16.51	13.92	9.40
CaO	0.12	0.15	0.00	0.15
Na₂O	0.27	0.01	0.23	0.03
K₂O	0.70	0.05	0.06	0.07
Total	88.77	87.99	85.81	87.19
Cations corrected to 28 Oxygens				
Si	6.21	5.72	5.00	6.27
Ti	0.00	0.00	0.01	0.00
Al	6.84	5.20	6.27	6.56
Cr	0.00	0.00	0.01	0.01
Fe	3.40	3.35	4.05	2.75
Mn	0.04	0.32	0.06	0.04
Mg	1.70	5.02	4.42	2.75
Ca	0.03	0.03	0.00	0.03
Na	0.10	0.00	0.10	0.01
K	0.17	0.01	0.02	0.02
Cation total	18.49	19.66	19.92	18.45
X_{Fe}	0.67	0.40	0.48	0.50
X_{Mg}	0.33	0.60	0.52	0.50

Table A.7: Plagioclase: Cunard Member

Sample Point #	sgr03 32	sgr03 33	sgr03 35	sgr03 36	sgr03 38	LSCN 89	LSCN 111	rtr04-1 200	AR04-1 291	AR05-3 298	AR05-5 314
SiO2	67.86	67.44	60.14	71.48	68.84	64.64	63.77	65.00	61.28	60.80	61.17
Al2O3	20.01	20.18	22.40	19.88	19.73	22.44	22.38	22.18	24.06	22.96	22.71
CaO	0.05	0.04	0.15	0.07	0.02	2.24	2.74	2.44	4.06	3.55	3.29
Na2O	11.98	10.98	8.70	10.82	11.68	10.17	10.08	10.45	9.21	9.79	9.64
K2O	0.03	0.08	1.44	0.06	0.21	0.27	0.04	0.03	0.07	0.09	0.01
Total	100.05	99.05	93.83	102.53	101.13	99.96	99.14	100.18	98.74	97.20	96.81
Cations corrected to 8 Oxygens											
Si	2.97	2.97	2.82	3.03	2.98	2.85	2.84	2.86	2.75	2.77	2.79
Al	1.03	1.05	1.24	0.99	1.01	1.16	1.17	1.15	1.27	1.23	1.22
Ca	0.00	0.00	0.01	0.00	0.00	0.11	0.13	0.12	0.20	0.17	0.16
Na	1.02	0.94	0.79	0.89	0.98	0.87	0.87	0.89	0.80	0.86	0.85
K	0.00	0.00	0.09	0.00	0.01	0.02	0.00	0.00	0.00	0.01	0.00
Cation Total	5.02	4.96	4.95	4.92	4.98	5.00	5.01	5.01	5.02	5.05	5.02
Mol%											
Anorthite	0.24	0.17	0.81	0.36	0.08	10.67	13.02	11.44	19.54	16.63	15.86
Mol% Albite	99.61	99.32	89.43	99.29	98.79	87.79	86.74	88.40	80.06	82.84	84.14

Mol% Anorthite = $\text{Ca}/(\text{Ca}+\text{Na}+\text{K}) \times 100\%$; Mol% Albite = $\text{Na}/(\text{Ca}+\text{Na}+\text{K}) \times 100\%$

Sample	AR05-5	AR05-5
Point #	326	329
SiO2	62.01	63.23
Al2O3	23.22	22.27
CaO	3.70	2.53
Na2O	9.67	10.06
K2O	0.00	0.00
Total	98.60	98.09
Cations corrected to 8 Oxygens		
Si	2.78	2.84
Al	1.23	1.18
Ca	0.18	0.12
Na	0.84	0.88
K	0.00	0.00
Cation Total	5.03	5.01
Mol% Anorthite	17.44	12.20
Mol% Albite	82.56	87.80

I. 93

Mol% Anorthite = $\text{Ca}/(\text{Ca}+\text{Na}+\text{K}) \times 100\%$; Mol% Albite = $\text{Na}/(\text{Ca}+\text{Na}+\text{K}) \times 100\%$

Table A.8: Plagioclase: Bluestone member

Sample	pcr10	pcr10	pcr10	wl05-04	wl05-04	wl05-12	ppp04-3	ppp04-3	ppp04-3	ppp04-3	ppp04-3
Point #	230	232	237	250	254	403	33n	34n	35n	45n	47n
SiO2	63.02	66.21	63.82	61.48	63.98	70.28	71.59	64.86	63.40	63.43	65.16
Al2O3	23.51	21.56	22.96	24.49	22.60	20.23	20.70	21.99	21.62	22.75	21.57
CaO	3.81	1.75	2.88	5.06	3.04	0.34	0.73	2.75	2.57	3.01	2.04
Na2O	9.57	10.90	10.21	8.91	10.03	10.55	10.08	10.31	10.40	9.70	10.43
K2O	0.08	0.04	0.06	0.14	0.17	0.15	0.34	0.13	0.15	0.10	0.08
Total	100.18	100.58	100.09	100.21	99.97	101.73	104.18	100.20	98.32	99.03	99.32
Cations corrected to 8 Oxygens											
Si	2.78	2.89	2.81	2.72	2.83	3.00	2.99	2.85	2.85	2.82	2.88
Al	1.22	1.11	1.19	1.28	1.18	1.02	1.02	1.14	1.14	1.19	1.12
Ca	0.18	0.08	0.14	0.24	0.14	0.02	0.03	0.13	0.12	0.14	0.10
Na	0.82	0.92	0.87	0.77	0.86	0.87	0.82	0.88	0.91	0.84	0.90
K	0.00	0.00	0.00	0.01	0.01	0.01	0.02	0.01	0.01	0.01	0.00
Cation Total	5.01	5.01	5.02	5.02	5.01	4.92	4.88	5.01	5.03	5.00	5.00
Mol% Anorthite	17.91	8.17	13.44	23.68	14.22	1.78	3.78	12.75	11.94	14.53	9.72
Mol% Albite	81.61	91.59	86.25	75.53	84.83	97.33	94.11	86.55	87.21	84.90	89.88

Mol% Anorthite = $\text{Ca}/(\text{Ca}+\text{Na}+\text{K}) \times 100\%$; Mol% Albite = $\text{Na}/(\text{Ca}+\text{Na}+\text{K}) \times 100\%$

Table A.9: K-Feldspar

Sample	AR04-1	AR05-3	AR05-5	AR05-5	wl05-10	wl05-10	pcr-10	pcr-10	wl05-4	wl05-4	wl05-4
Point #	294	300	328	339	217	226	229	236	252	253	255
SiO2	61.84	61.87	62.74	64.31	64.06	62.93	62.94	62.04	63.45	63.33	63.94
TiO2	0.04	0.00	0.00	0.00	0.01	0.03	0.02	0.08	0.06	0.04	0.05
Al2O3	19.23	18.92	19.13	19.56	19.16	19.33	19.61	18.88	18.99	18.94	18.93
Cr2O3	0.00	0.00	0.00	0.00	0.05	0.03	0.02	0.06	0.10	0.06	0.03
FeO	0.26	0.02	0.00	0.05	0.16	0.25	0.19	0.98	0.27	0.23	0.15
MnO	0.00	0.00	0.00	0.00	0.00	0.00	0.00	0.00	0.00	0.00	0.00
MgO	0.08	0.00	0.00	0.00	0.00	0.00	0.00	0.29	0.00	0.01	0.00
CaO	0.00	0.00	0.00	0.08	0.00	0.00	0.00	0.00	0.00	0.00	0.00
Na2O	1.67	1.45	1.45	2.52	1.97	1.53	1.52	0.86	1.19	1.45	1.94
K2O	13.61	14.44	14.37	12.92	13.13	13.74	13.62	14.26	14.87	14.27	13.99
Total	96.74	96.70	97.69	99.43	98.55	97.84	97.92	97.45	98.93	98.34	99.04
	Cations corrected to 8 Oxygens										
Si	2.94	2.95	2.95	2.96	2.97	2.95	2.95	2.94	2.96	2.96	2.97
Ti	0.00	0.00	0.00	0.00	0.00	0.00	0.00	0.00	0.00	0.00	0.00
Al	1.08	1.06	1.06	1.06	1.05	1.07	1.08	1.05	1.04	1.04	1.04
Cr	0.00	0.00	0.00	0.00	0.00	0.00	0.00	0.00	0.00	0.00	0.00
Fe	0.01	0.00	0.00	0.00	0.01	0.01	0.01	0.04	0.01	0.01	0.01
Mn	0.00	0.00	0.00	0.00	0.00	0.00	0.00	0.00	0.00	0.00	0.00
Mg	0.01	0.00	0.00	0.00	0.00	0.00	0.00	0.02	0.00	0.00	0.00
Ca	0.00	0.00	0.00	0.00	0.00	0.00	0.00	0.00	0.00	0.00	0.00
Na	0.15	0.13	0.13	0.22	0.18	0.14	0.14	0.08	0.11	0.13	0.17
K	0.82	0.88	0.86	0.76	0.78	0.82	0.81	0.86	0.88	0.85	0.83
Cation Total	5.01	5.03	5.01	5.00	4.98	4.99	4.99	5.00	5.01	5.00	5.01
Mol% Orthoclase	84.30	86.72	86.74	76.80	81.39	85.58	85.52	91.59	89.12	86.59	82.60
Mol% Anorthite	0.00	0.00	0.00	0.41	0.00	0.00	0.00	0.00	0.00	0.00	0.00
Mol% Albite	15.70	13.28	13.26	22.79	18.61	14.42	14.48	8.41	10.88	13.41	17.40

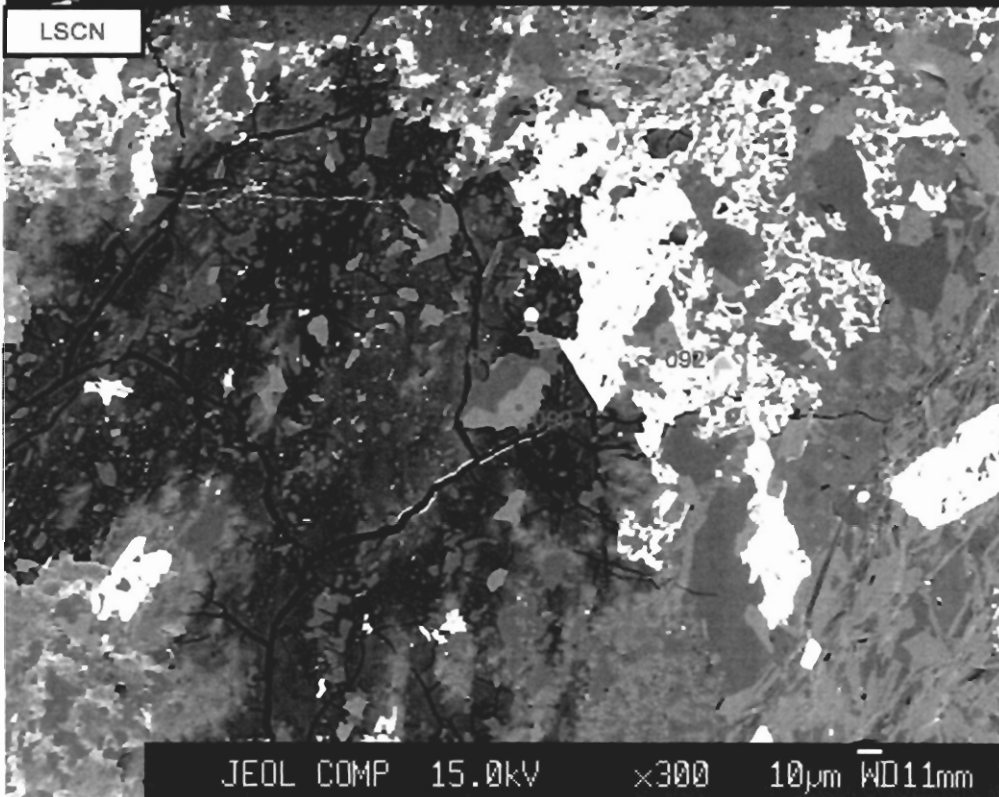
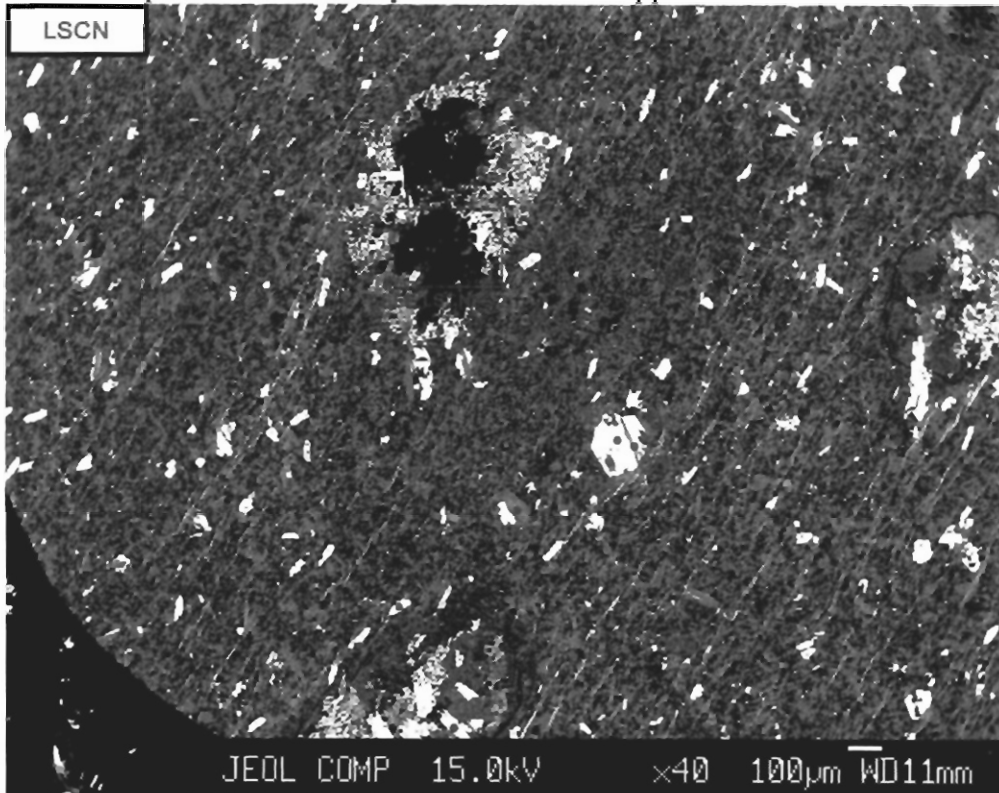
AR samples are Cunard, all others are Bluestone; All samples within 500m of contact.

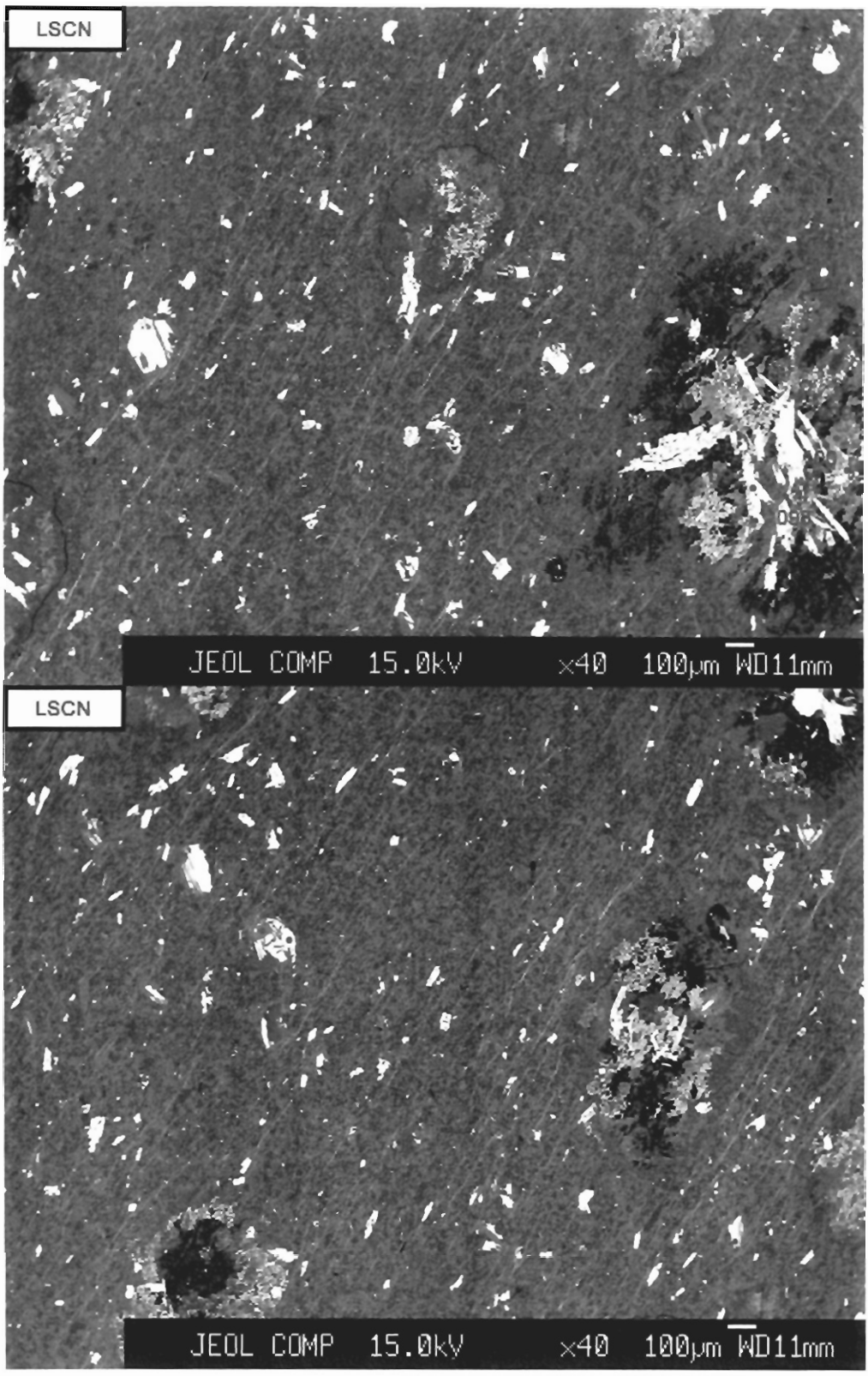
Sample Point #	wl05-4	wl05-4	wl05-4	wl05-12	wl05-12	wl05-15	wl05-15	wl05-12	wl05-12	wl05-12	wl05-15
SiO2	63.45	63.03	64.22	64.06	64.85	65.25	64.31	64.72	65.51	64.72	68.55
TiO2	0.03	0.00	0.01	0.11	0.09	0.10	0.07	0.06	0.01	0.05	0.04
Al2O3	19.02	18.74	19.28	16.88	16.80	19.32	19.61	19.16	18.93	18.97	19.23
Cr2O3	0.06	0.04	0.06	0.00	0.00	0.00	0.00	0.04	0.05	0.05	0.05
FeO	0.16	0.23	0.45	0.15	0.12	0.19	0.59	0.15	0.13	0.19	0.32
MnO	0.00	0.00	0.00	0.02	0.01	0.01	0.01	0.02	0.01	0.02	0.01
MgO	0.00	0.00	0.00	0.00	0.00	0.00	0.06	0.00	0.00	0.00	0.02
CaO	0.00	0.01	0.00	0.03	0.03	0.01	0.02	0.02	0.02	0.01	0.00
Na2O	1.18	1.90	2.16	1.41	1.51	1.82	1.73	1.55	1.52	1.18	1.38
K2O	14.78	14.16	13.72	14.26	13.98	13.56	13.34	13.81	13.91	14.77	12.99
Total	98.67	98.11	99.90	96.91	97.39	100.26	99.75	99.53	100.08	99.97	102.59
Cations corrected to 8 Oxygens											
Si	2.96	2.96	2.96	3.04	3.05	2.98	2.95	2.98	2.99	2.98	3.03
Ti	0.00	0.00	0.00	0.00	0.00	0.00	0.00	0.00	0.00	0.00	0.00
Al	1.05	1.04	1.05	0.94	0.93	1.04	1.06	1.04	1.02	1.03	1.00
Cr	0.00	0.00	0.00	0.00	0.00	0.00	0.00	0.00	0.00	0.00	0.00
Fe	0.01	0.01	0.02	0.01	0.00	0.01	0.02	0.01	0.00	0.01	0.01
Mn	0.00	0.00	0.00	0.00	0.00	0.00	0.00	0.00	0.00	0.00	0.00
Mg	0.00	0.00	0.00	0.00	0.00	0.00	0.00	0.00	0.00	0.00	0.00
Ca	0.00	0.00	0.00	0.00	0.00	0.00	0.00	0.00	0.00	0.00	0.00
Na	0.11	0.17	0.19	0.13	0.14	0.16	0.15	0.14	0.13	0.10	0.12
K	0.88	0.85	0.81	0.86	0.84	0.79	0.78	0.81	0.81	0.87	0.73
Cation Total	5.01	5.03	5.02	4.98	4.97	4.98	4.98	4.98	4.97	4.99	4.89
Mol% Orthoclase	89.14	83.07	80.69	86.80	85.77	83.07	83.50	85.34	85.71	89.14	86.16
Mol% Anorthite	0.00	0.00	0.00	0.16	0.16	0.00	0.09	0.08	0.08	0.08	0.00
Mol% Albite	10.86	16.93	19.31	13.04	14.06	16.93	16.41	14.57	14.20	10.77	13.84

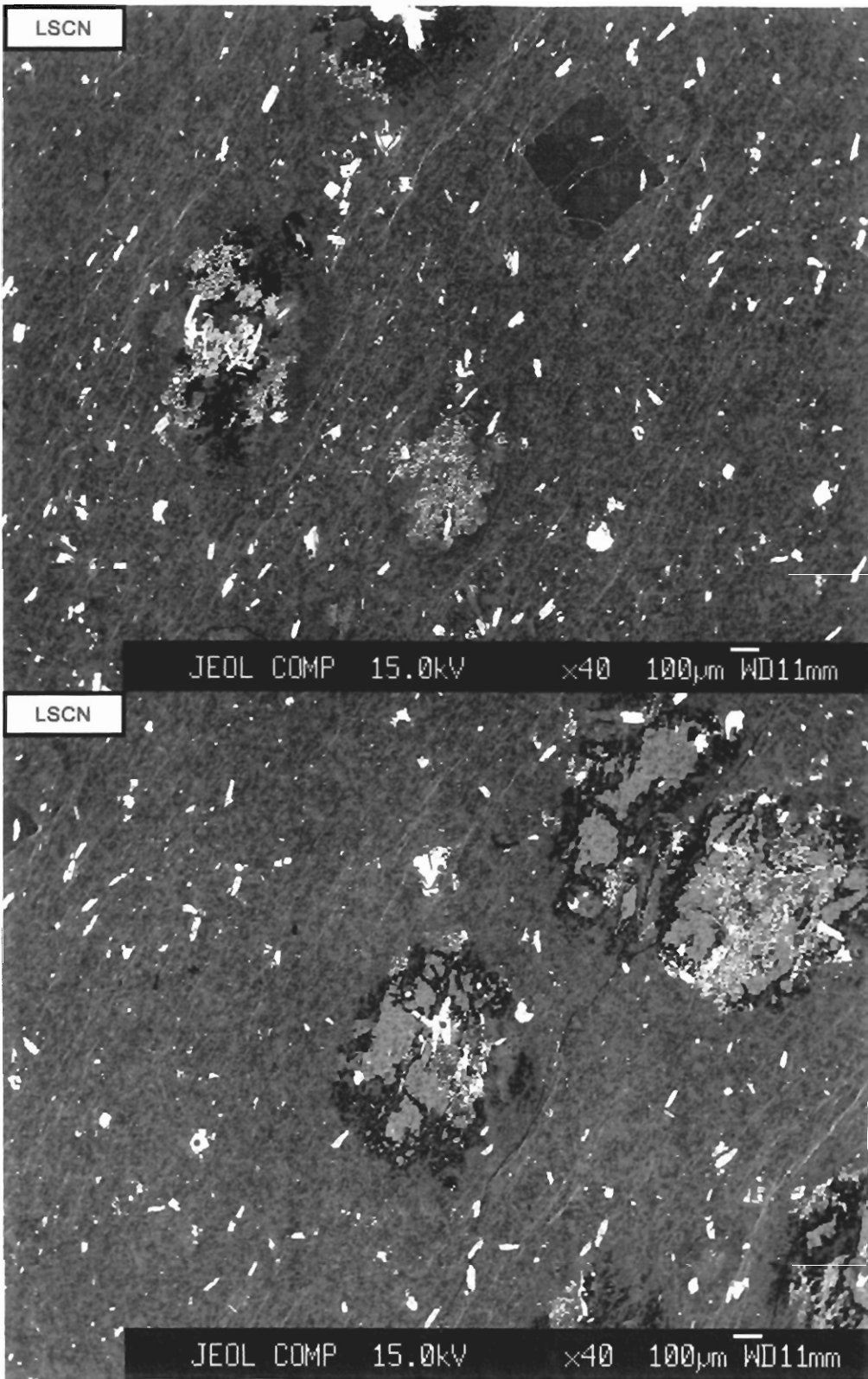
AR samples are Cunard, all others are Bluestone; All samples within 500m of contact.

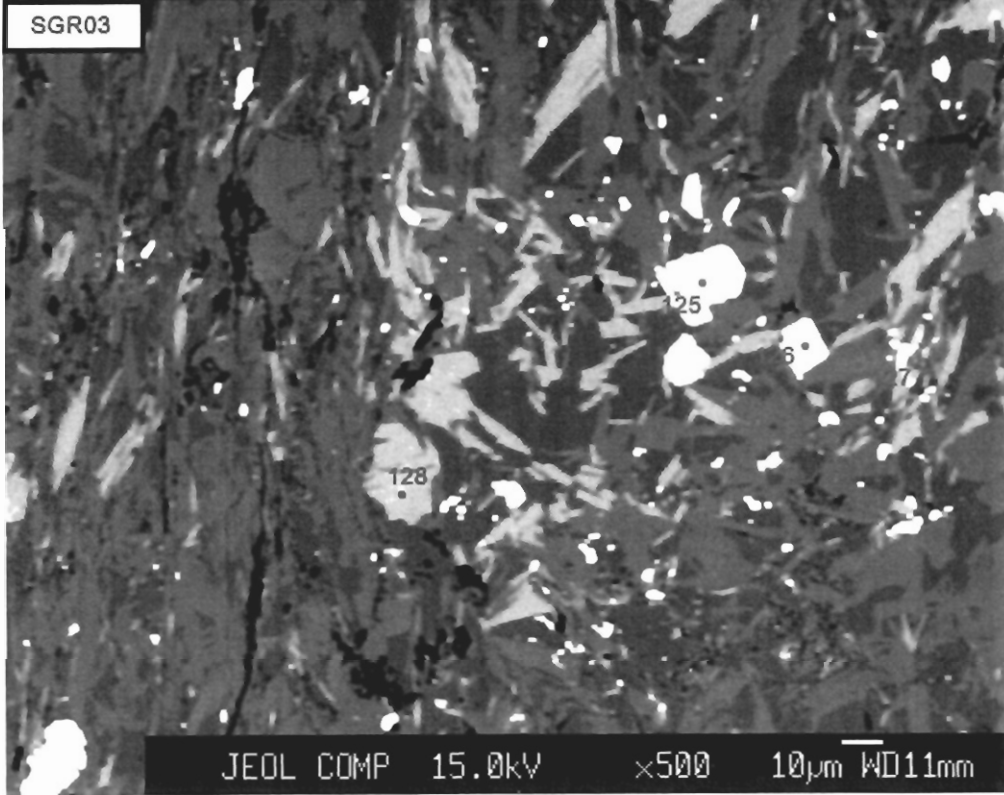
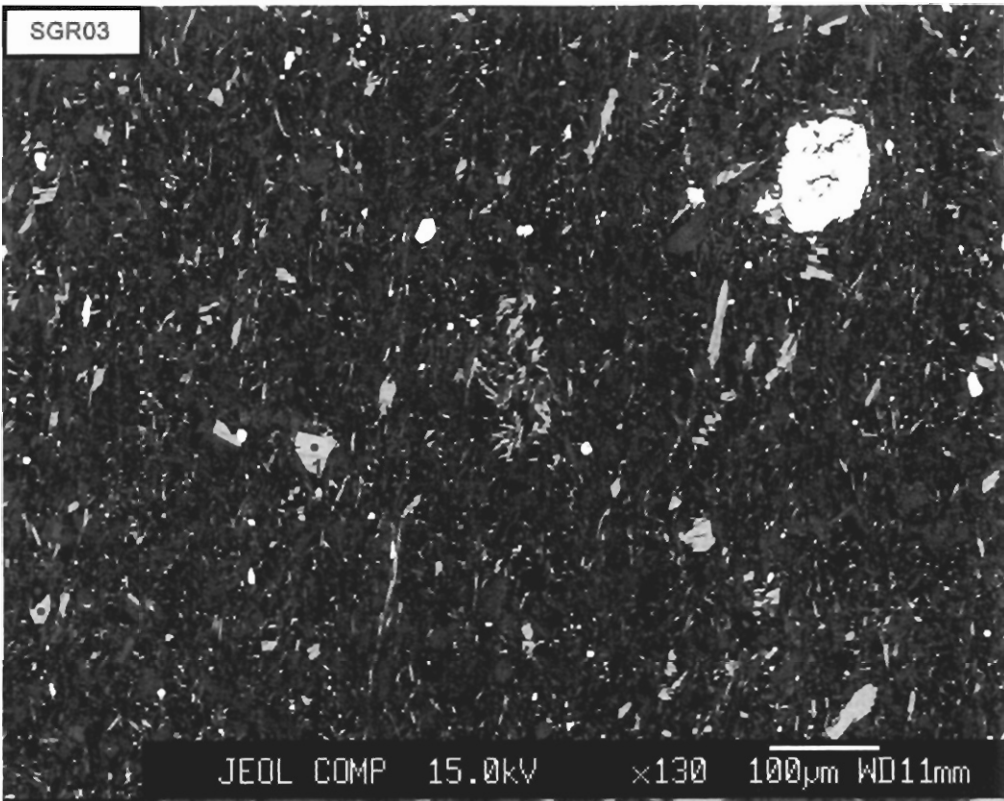
Appendix II: Microprobe BSE images

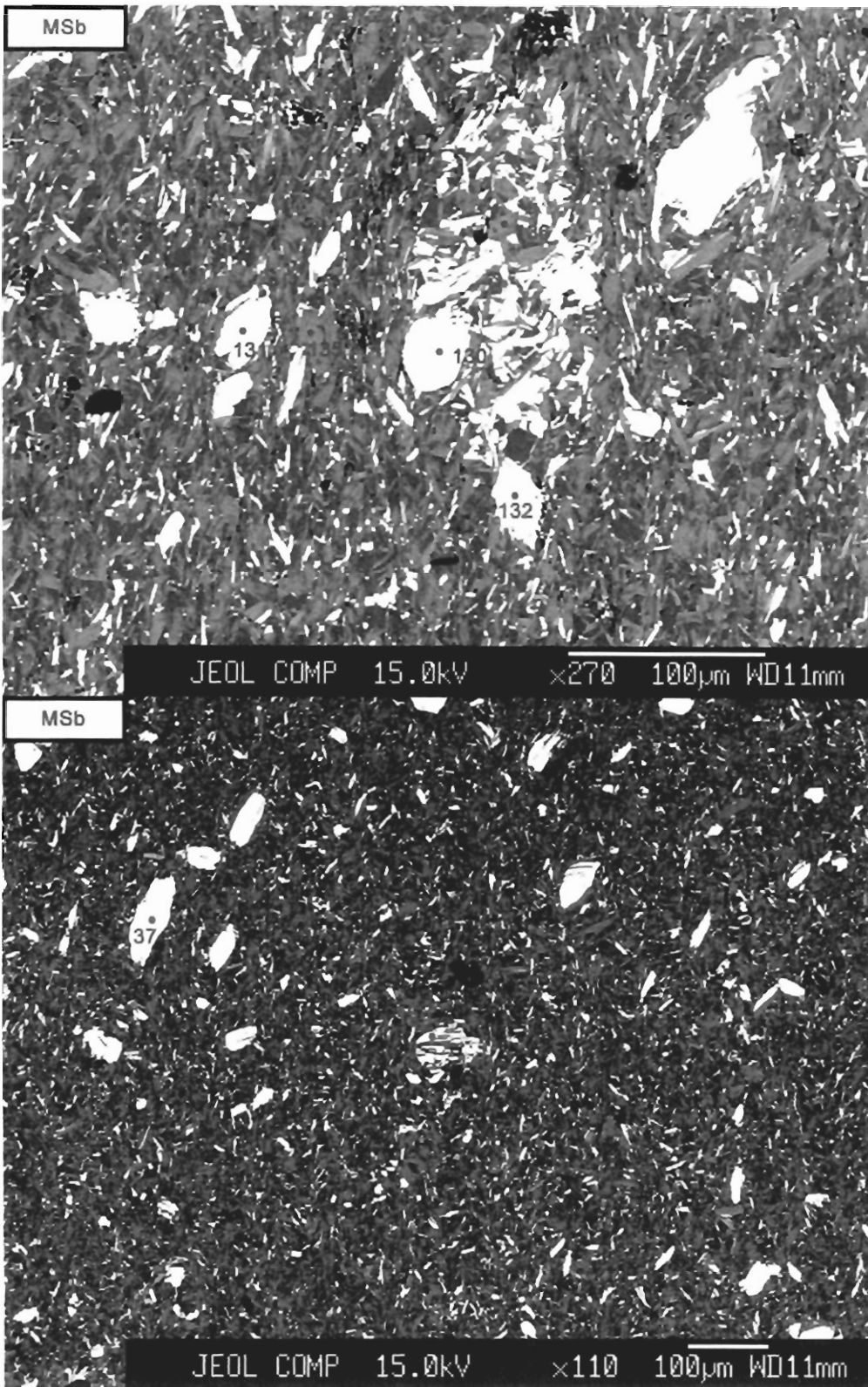
Sample number given in upper left/right corner, microprobe sample points labeled on pictures. Point analysis contained in Appendix I.

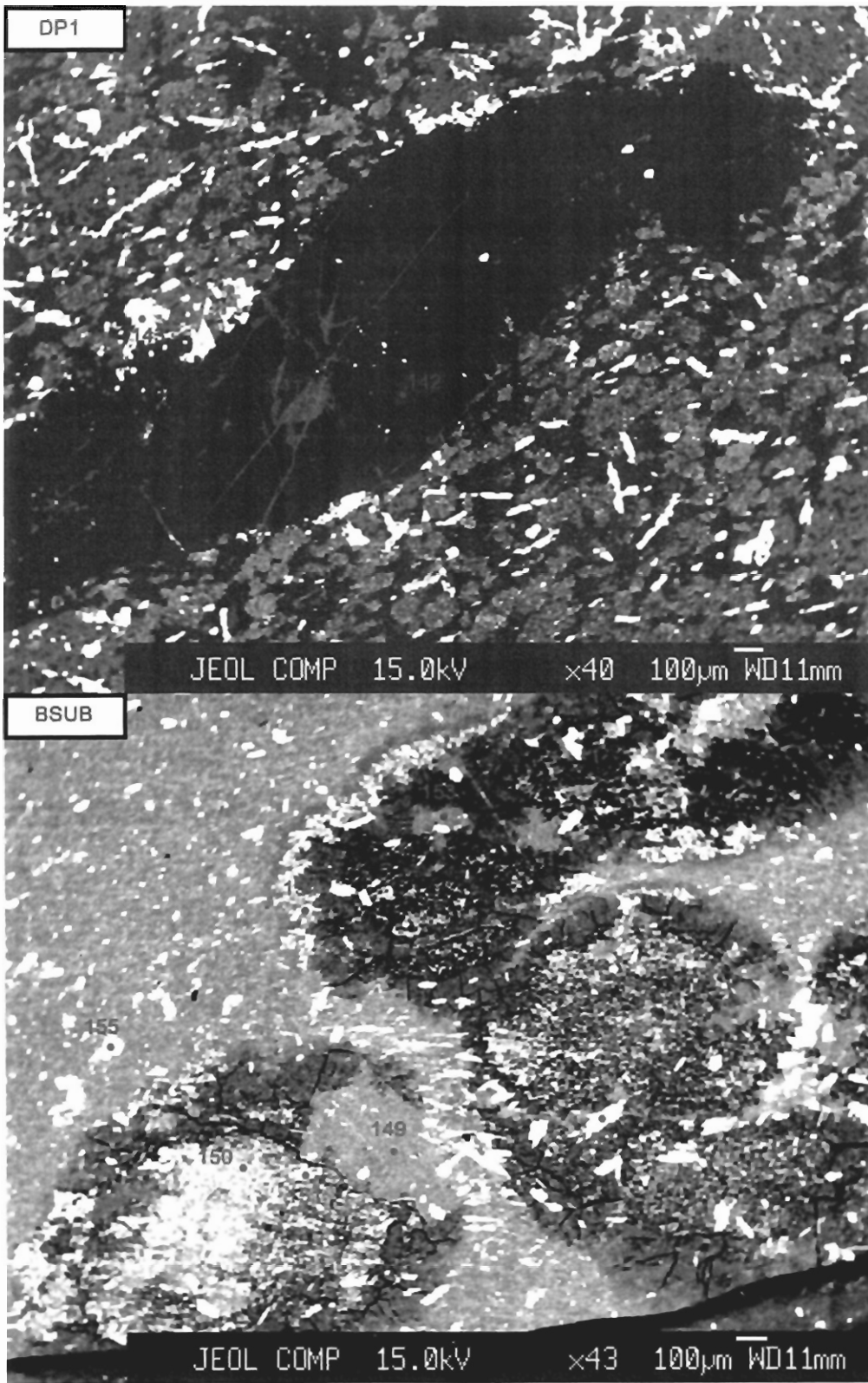


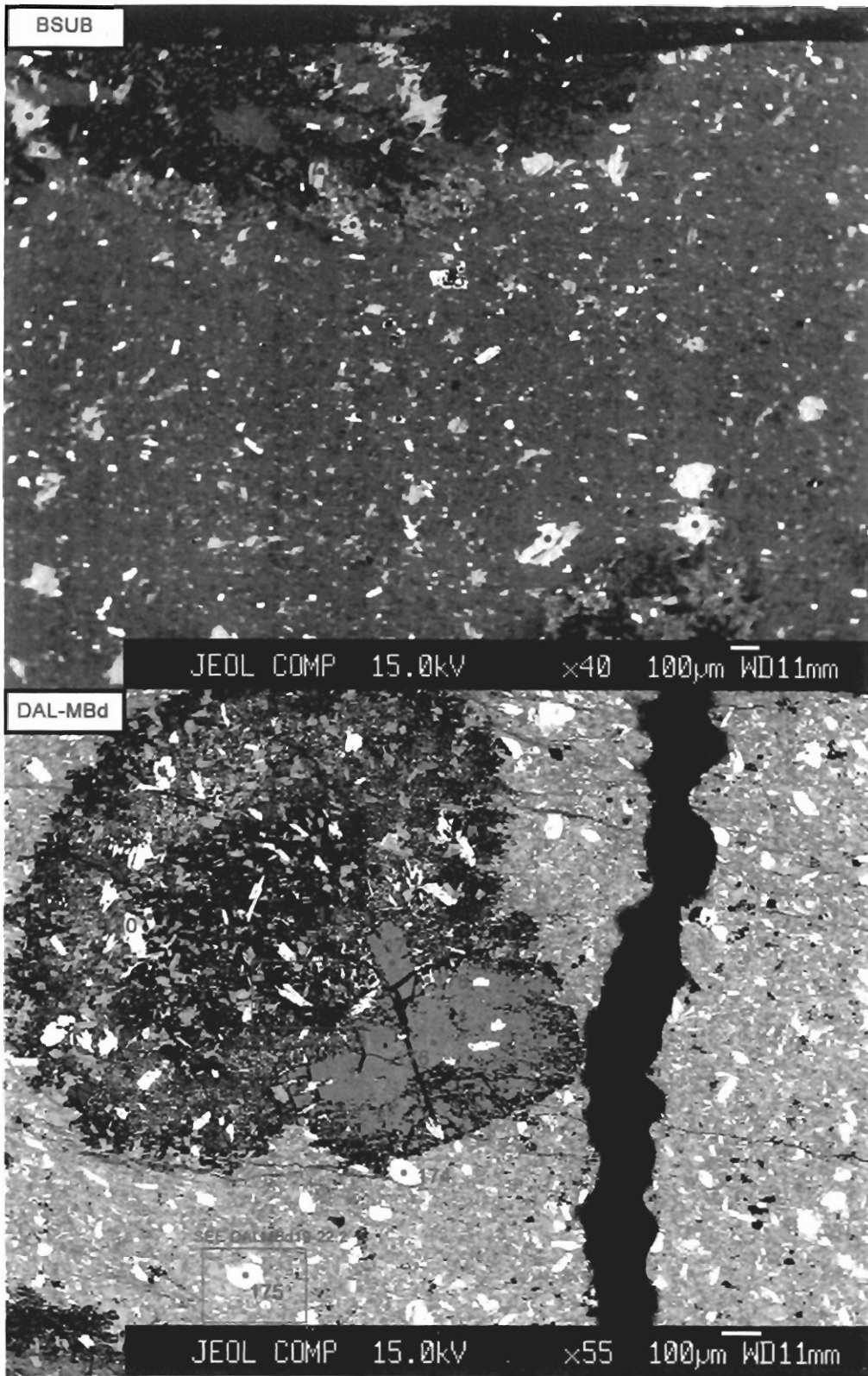


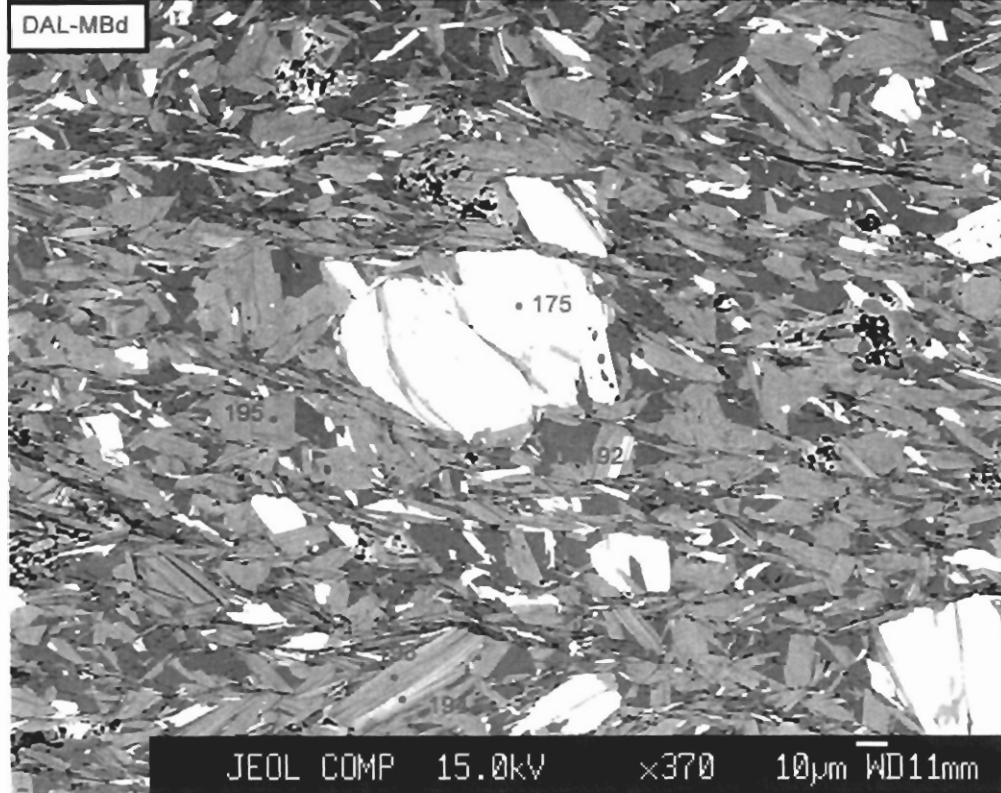
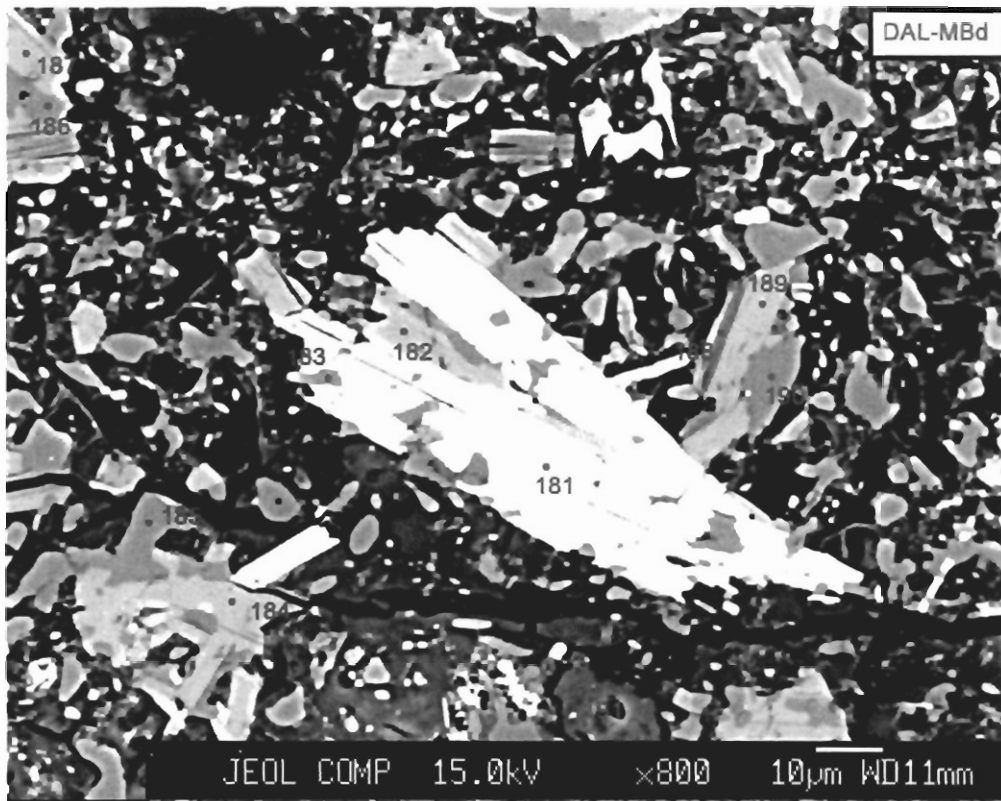


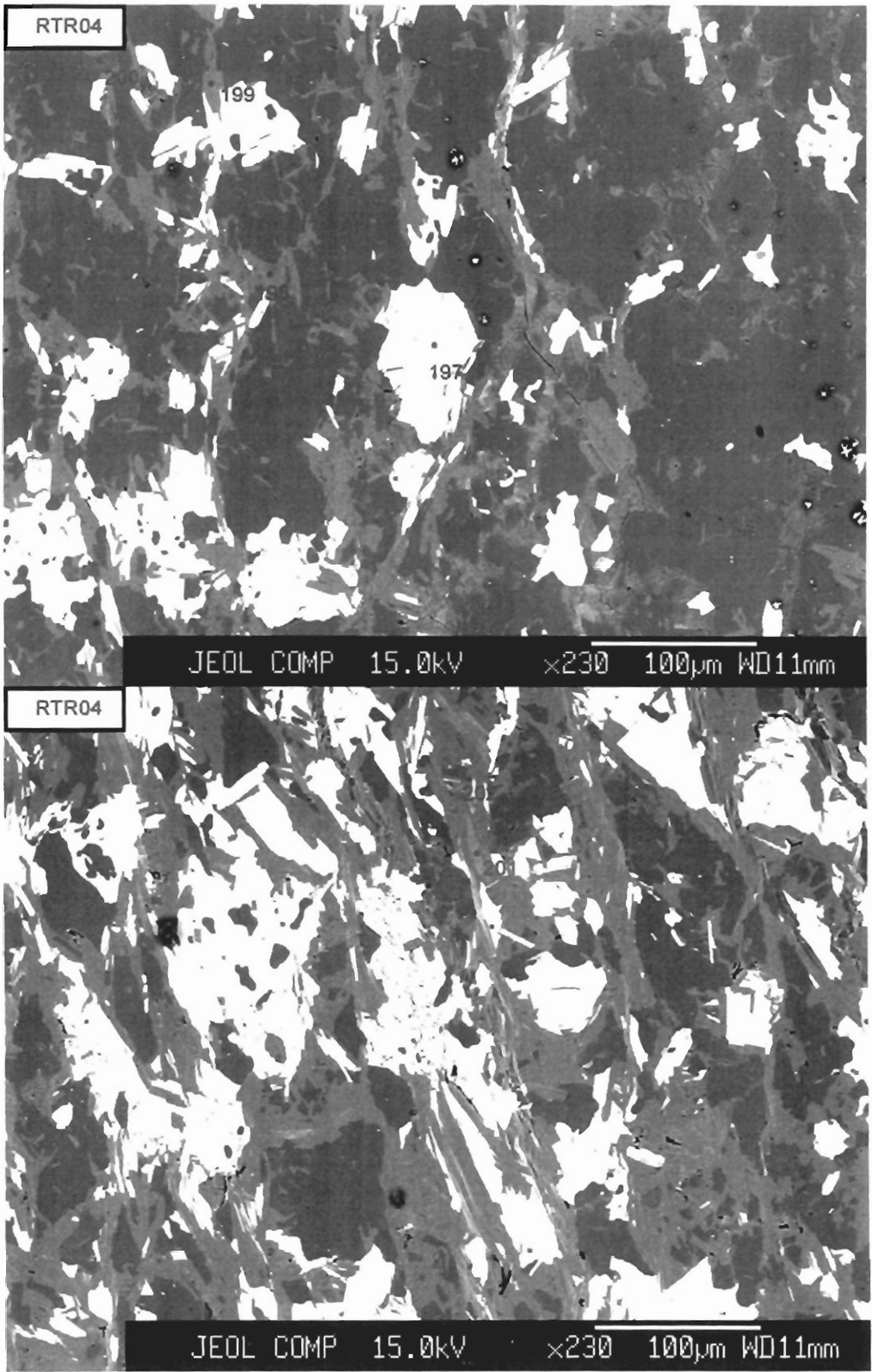


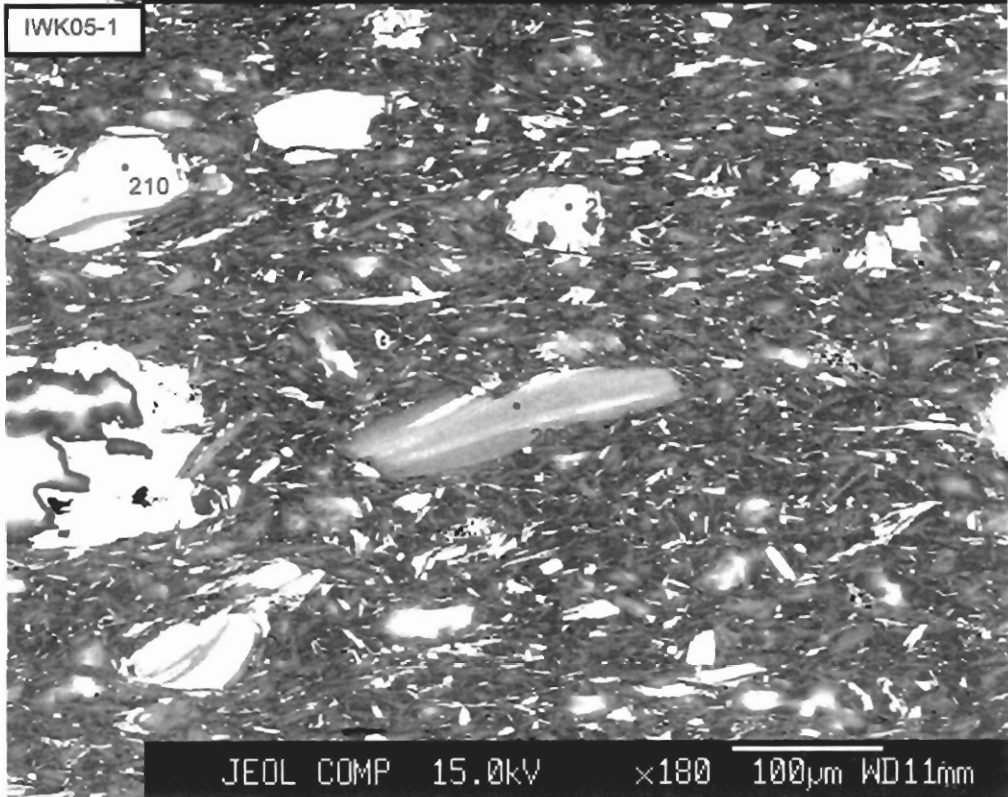
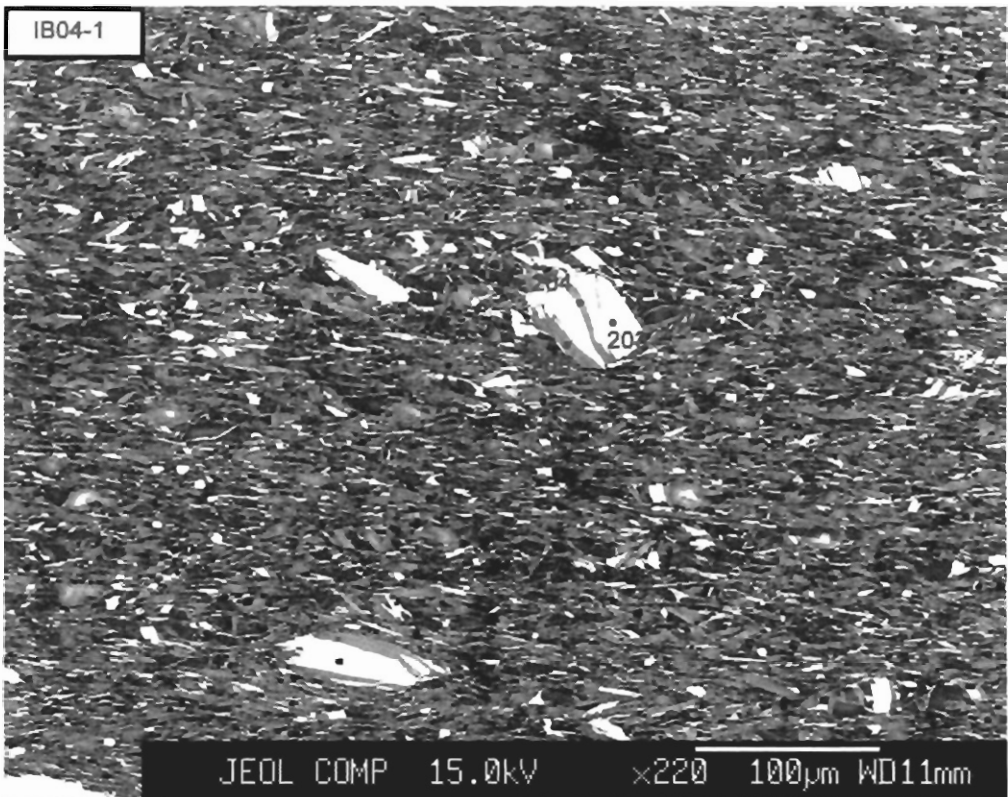


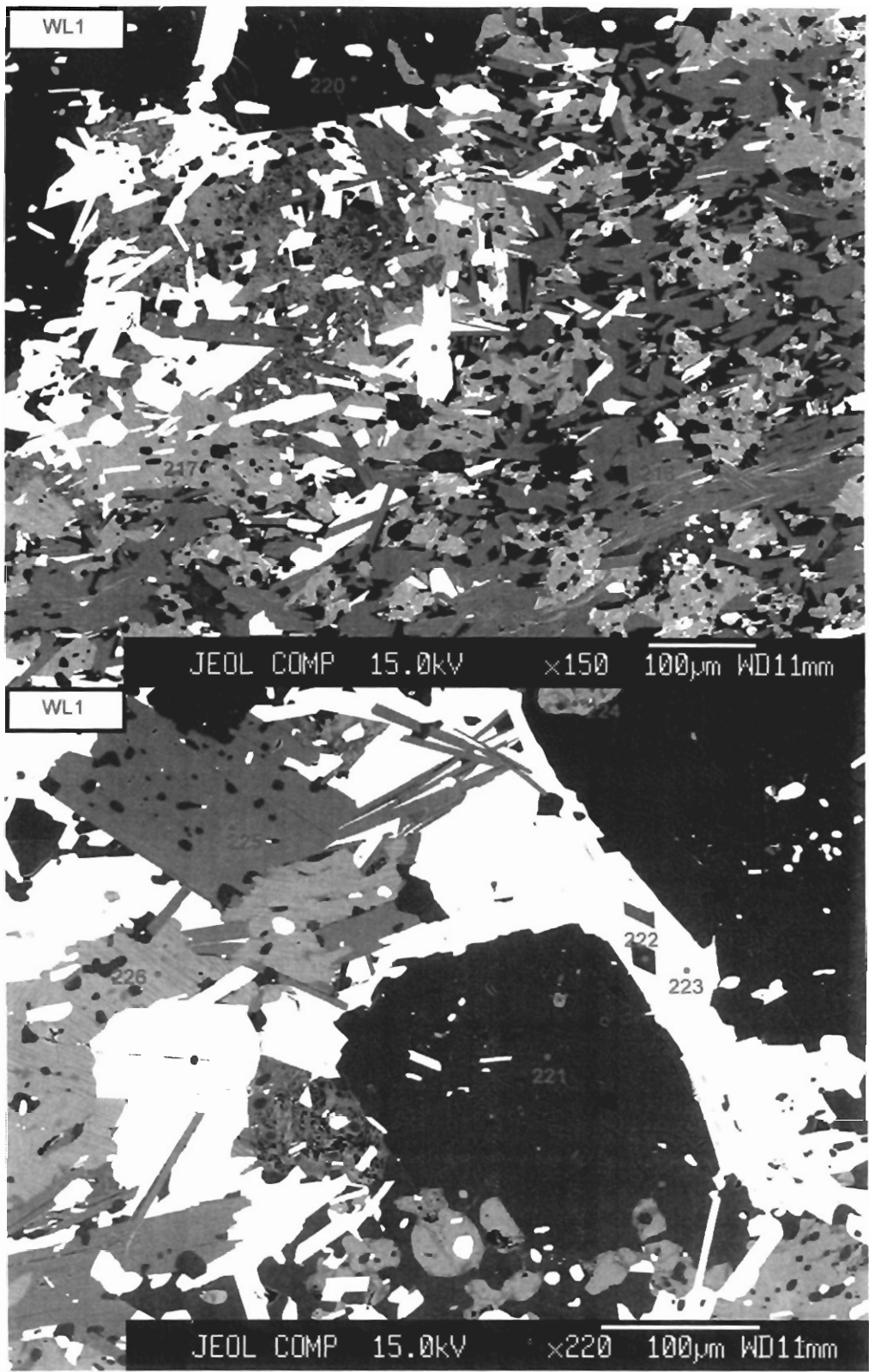


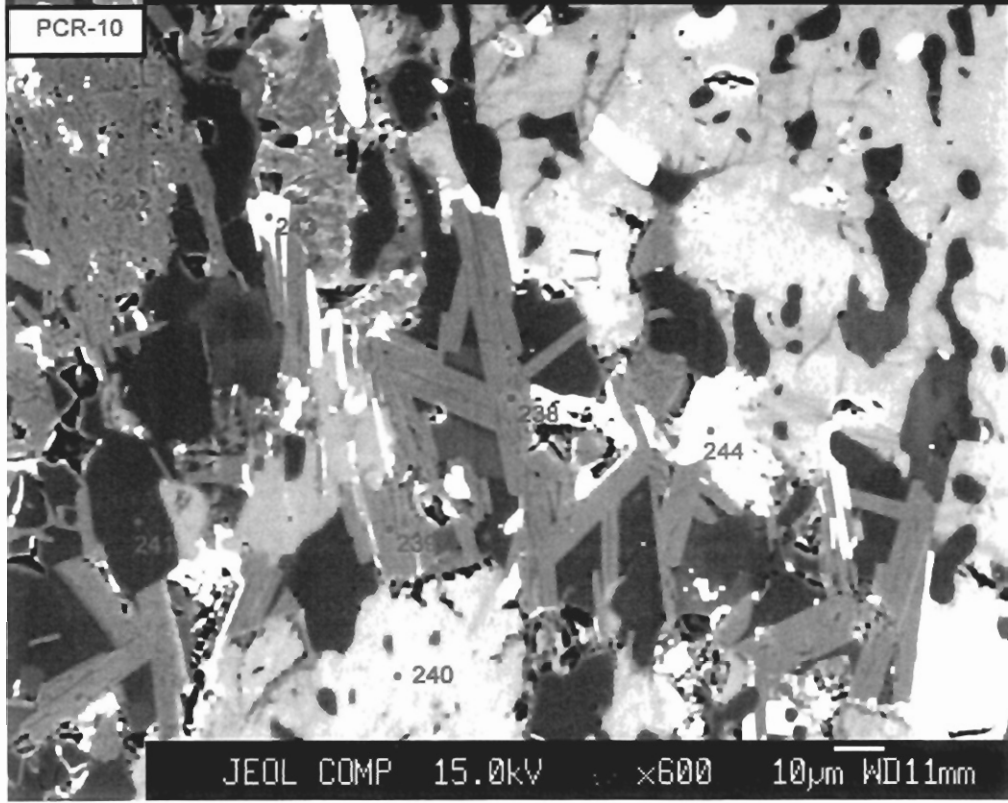
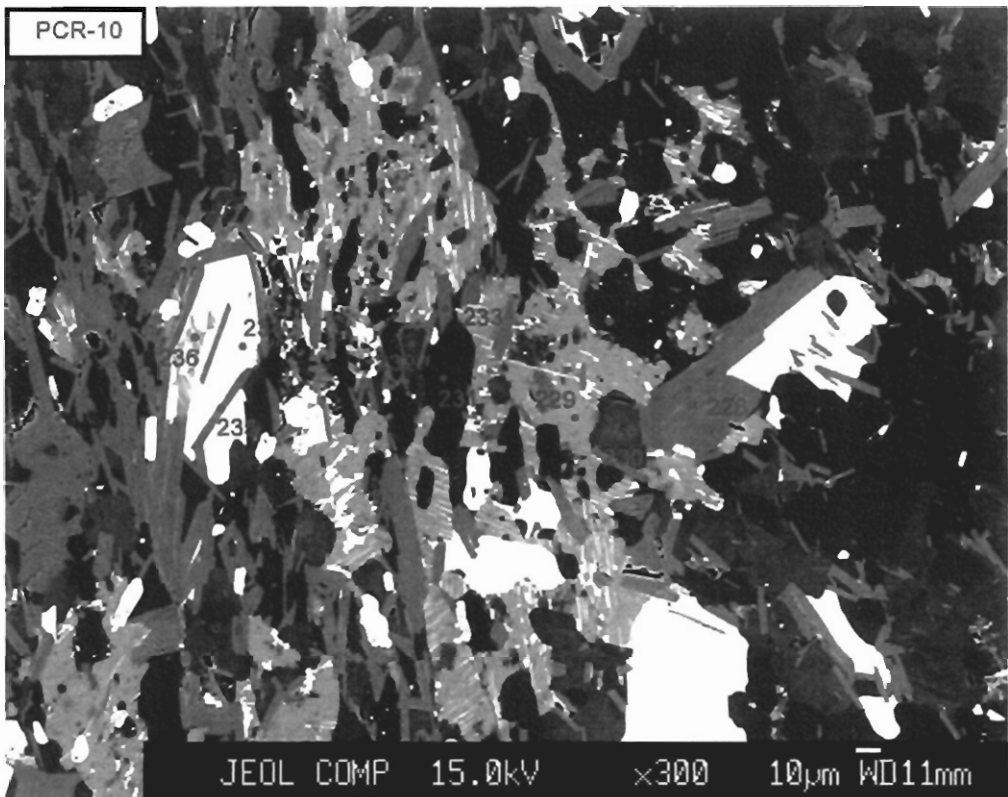


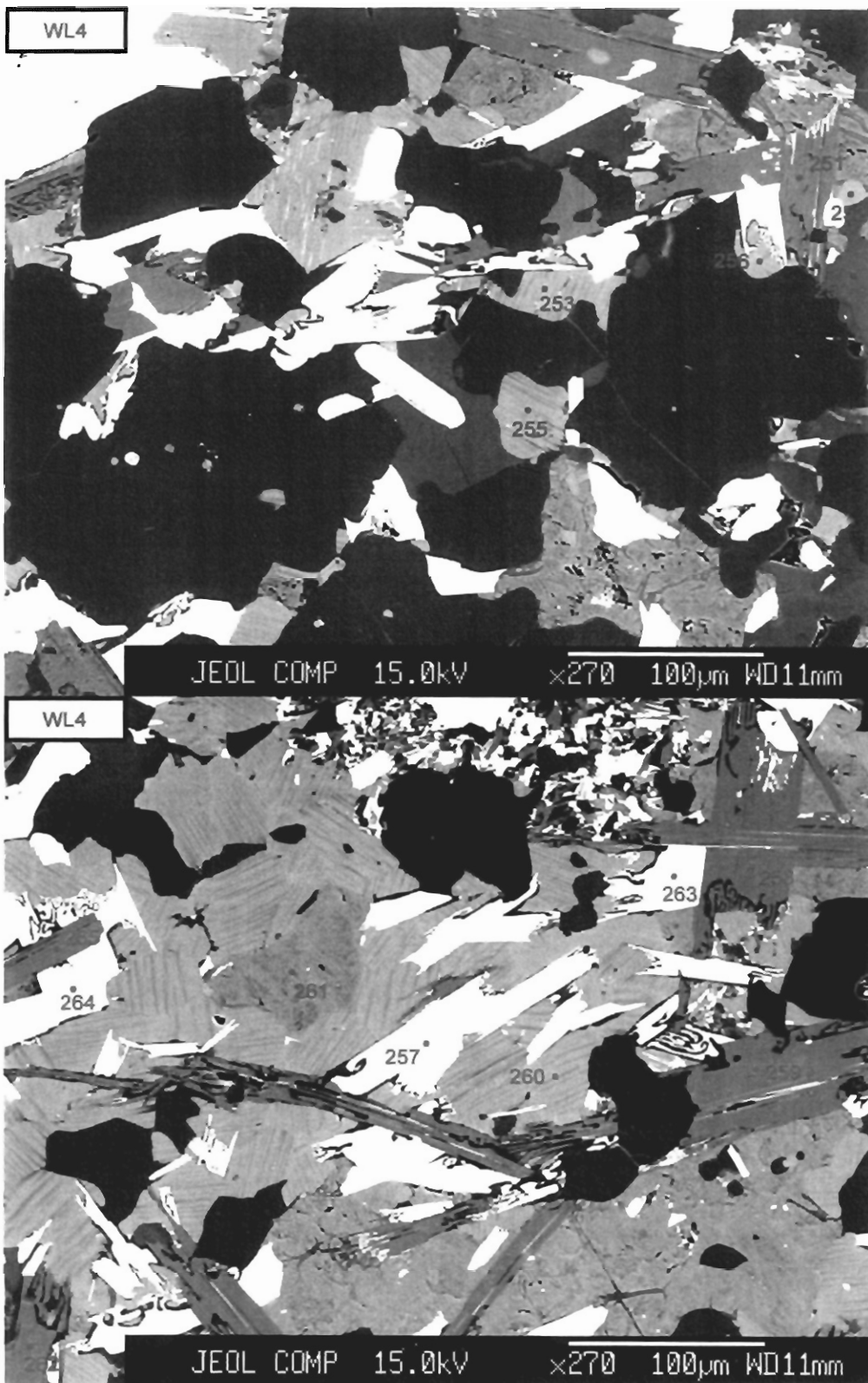


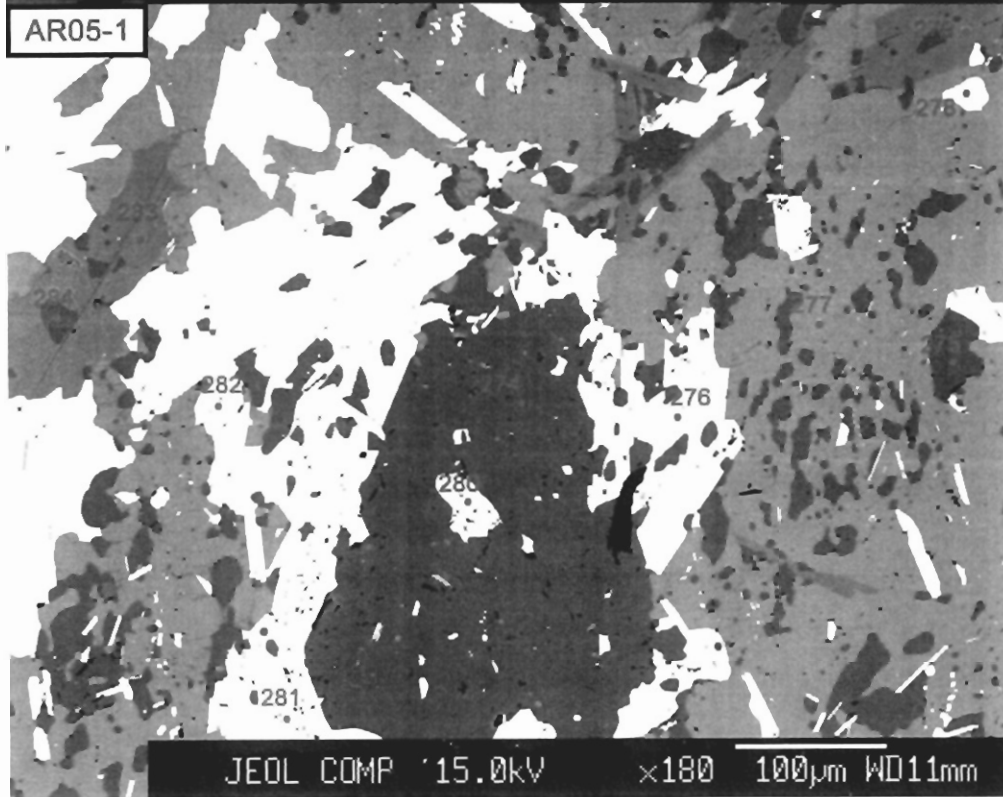
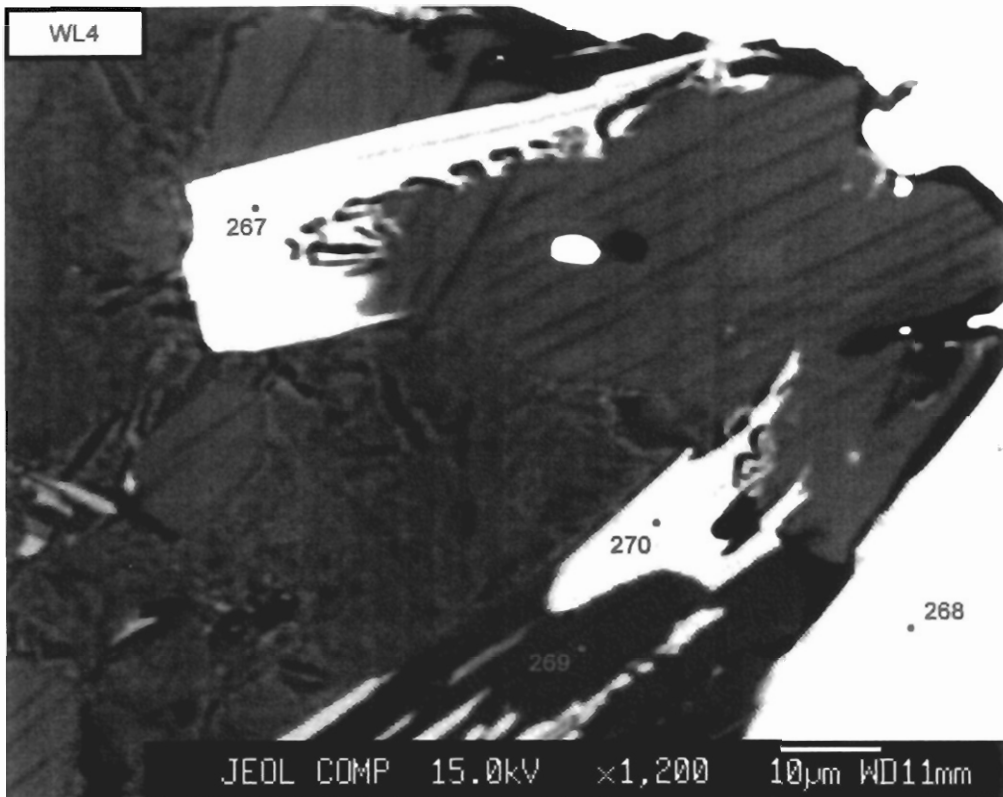


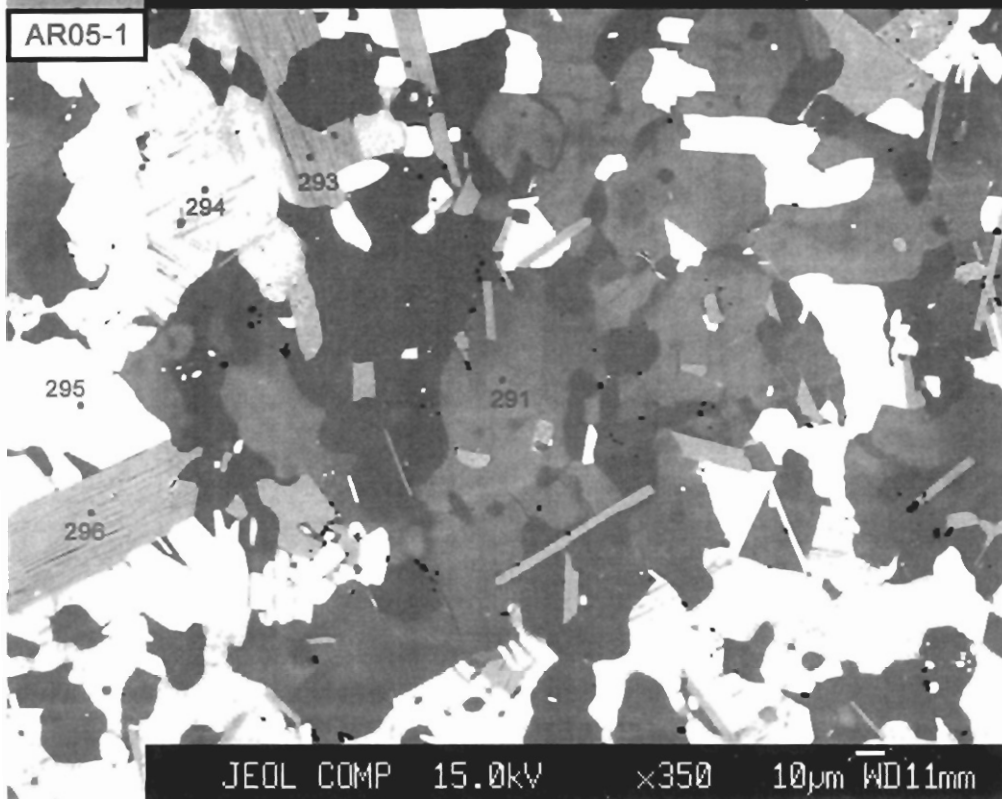
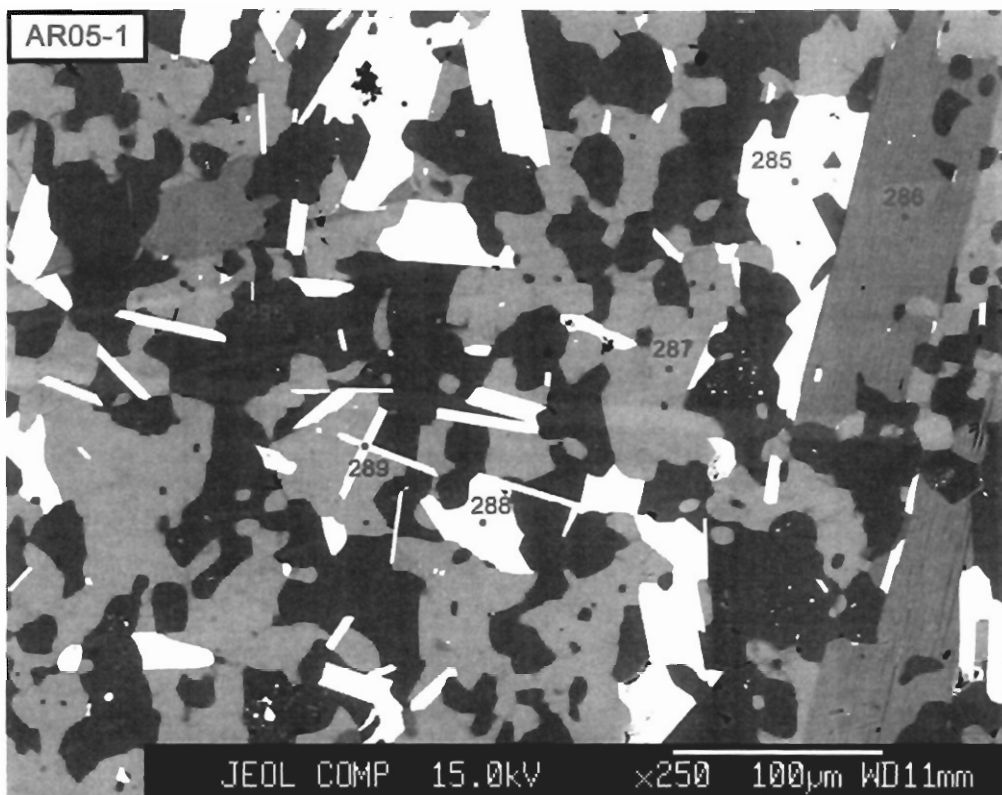


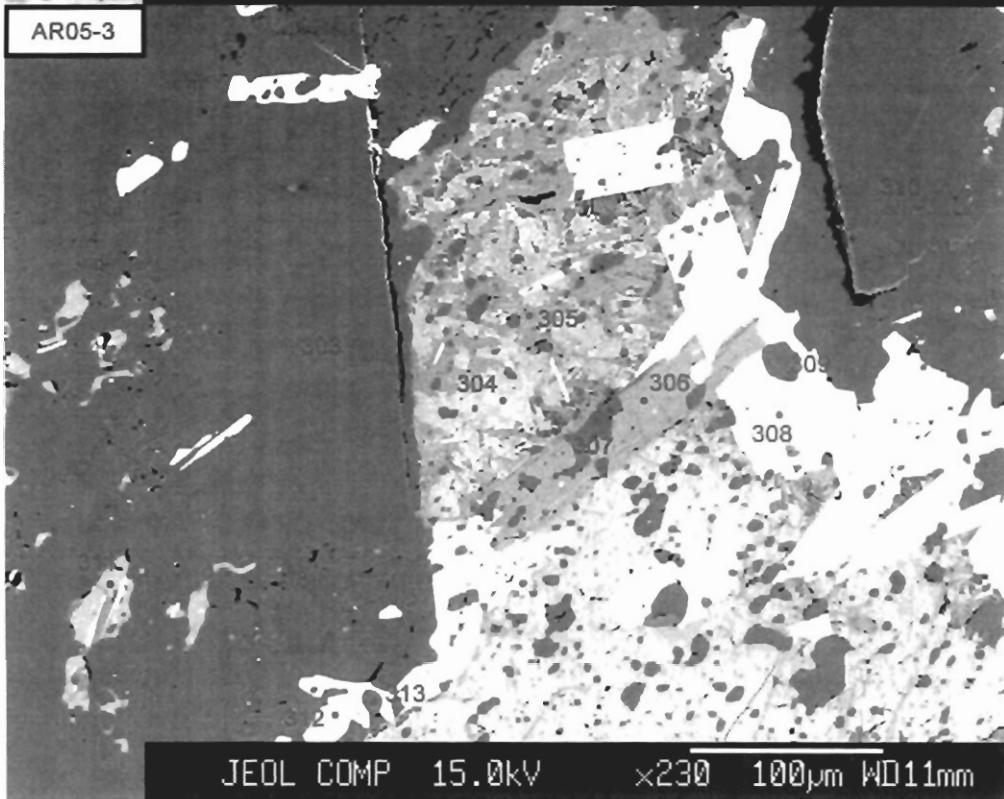
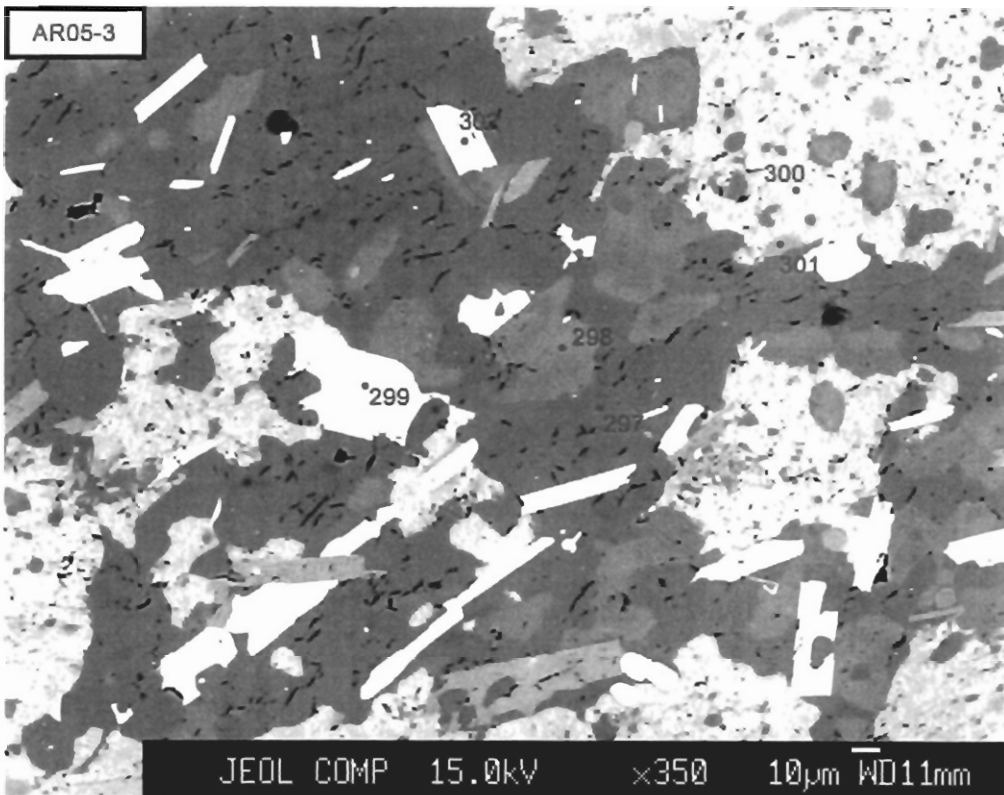


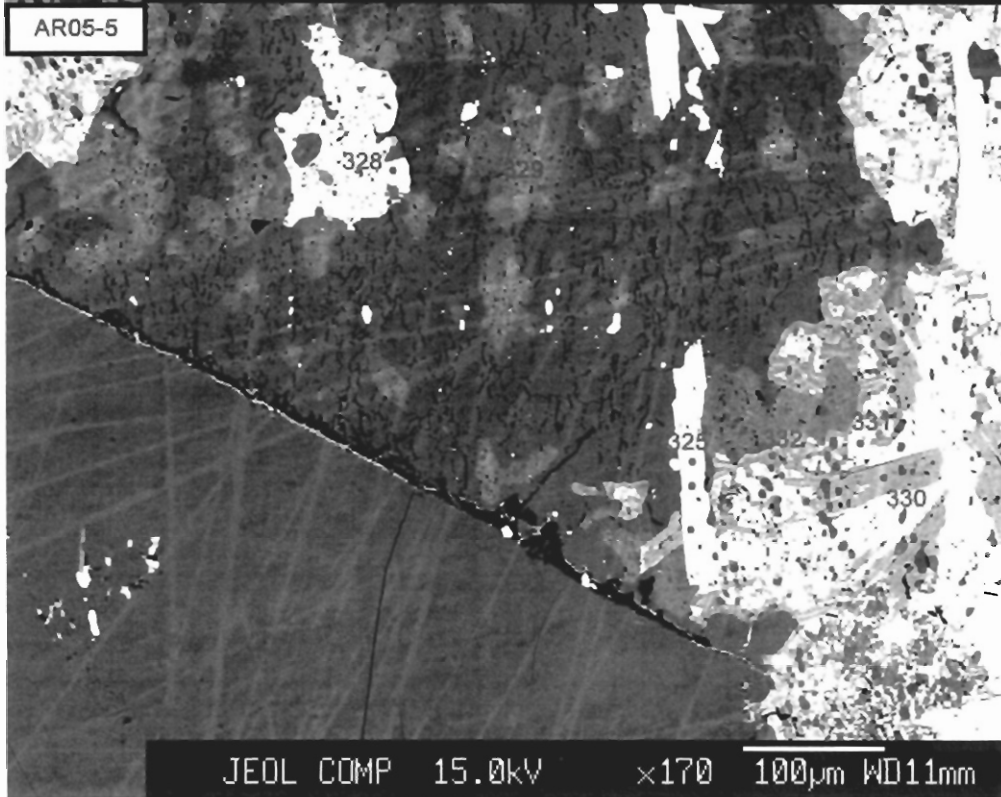
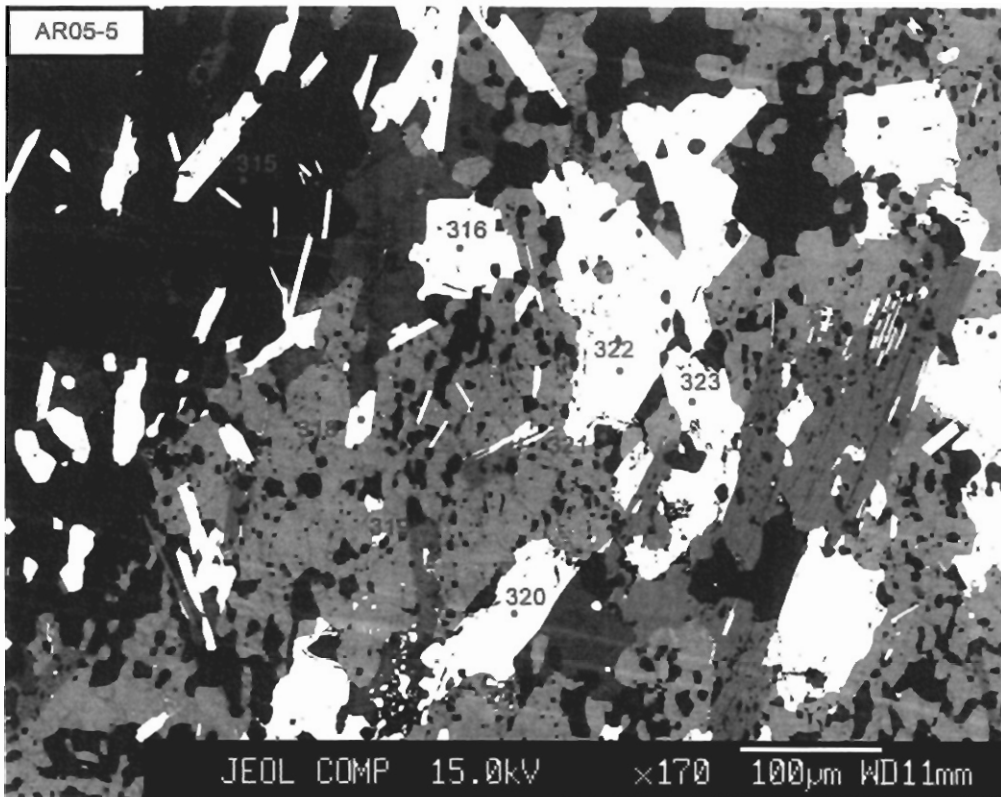


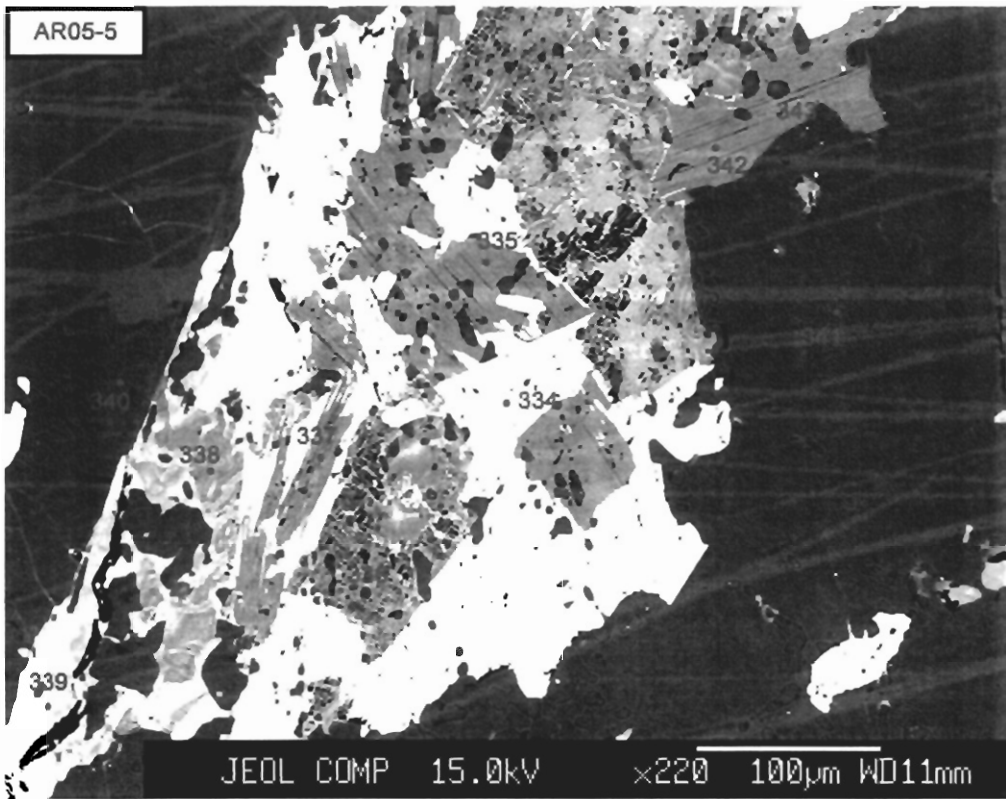












Appendix III: Maps

Sample	UTM Easting	UTM Northing	Unit
PPP04 - 3	454537	4940893	Bluestone
PPP04 - 5a, 5b	455233	4940950	Bluestone
PPP04 - 10	455334	4941158	Bluestone
PPP04 - 19	454704	4941863	Bluestone
WL05 - 15	452742	4941390	Bluestone
WL04 - 1	452123	4941196	Bluestone
PCR - 10	452736	4941391	Bluestone
IB04 - 1	454693	4942616	Bluestone
WL05 - 4	451722	4940882	Bluestone
WL05 -10	452235	4941072	Bluestone
WL05 - 12	452347	4941194	Bluestone
DAL - 99 - 1	452991	4942647	Cunard
LSCN	452927	4942769	Cunard
KILE - 04a, 04b	453169	4942877	Cunard
Mbd	453323	4942812	Cunard
HCM - 1, 2, 3	452536	4942529	Cunard
RTR04 - 1	453129	4942189	Cunard
IWK - 03	453650	4942883	Cunard
DAL03 - BSUB	453289	4942728	Cunard
SGR - 03	453667	4943268	Cunard
DP - 2	451891	4942500	Cunard
RR05-3	450493	4944682	Cunard
RR05-1	450595	4944112	Cunard
AR05 - 3	450180	4943071	Cunard
AR05 - 5, 6	449485	4943286	Cunard
AR04 - 1	450854	4943162	Cunard

Table C.1: UTM coordinates of sample locations (see Fig C.1) which have been analysed by microprobe for this study.

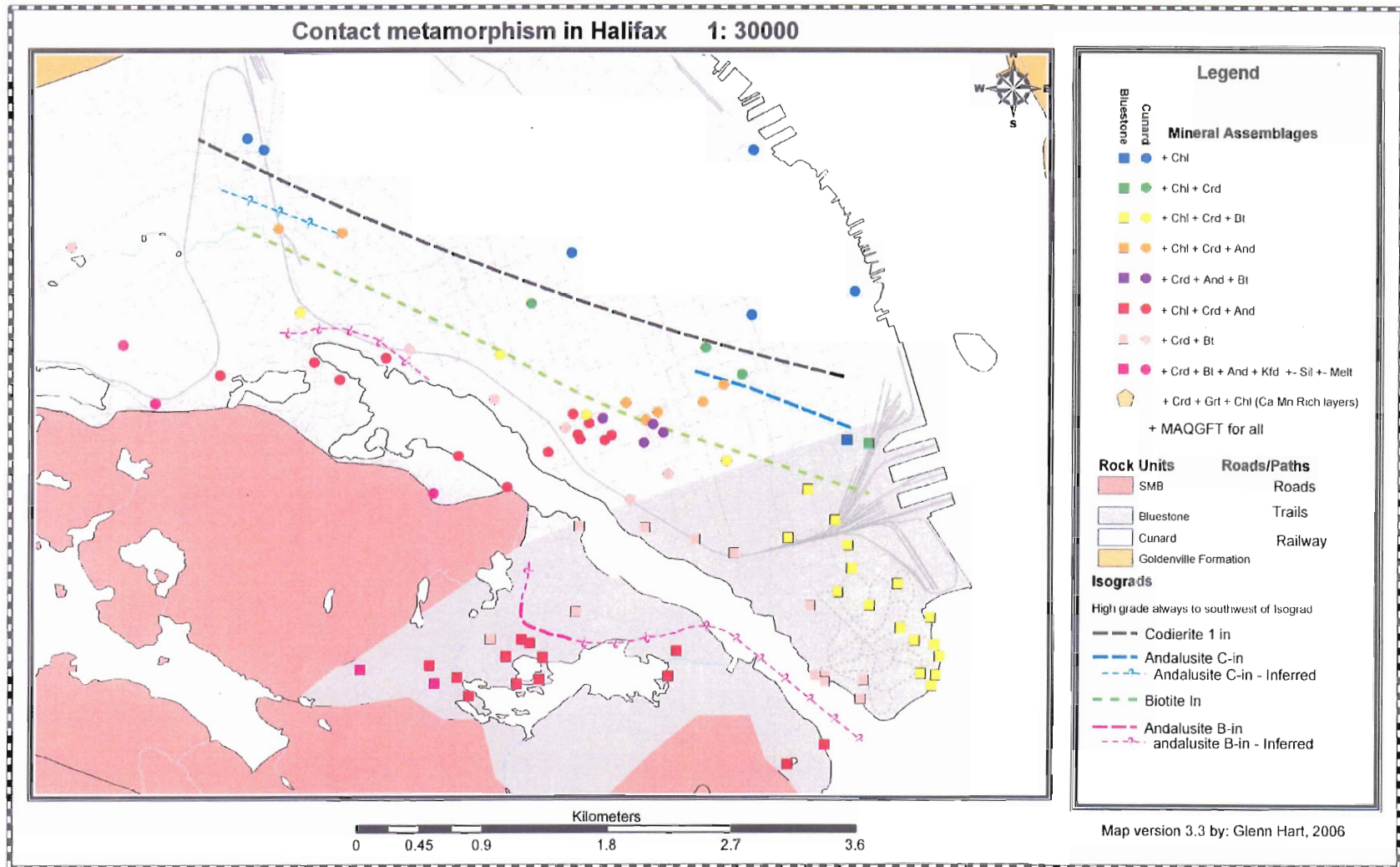


Fig C.1: Contact metamorphism map for study area. Showing mineral assemblage and isograd distribution in Halifax area.

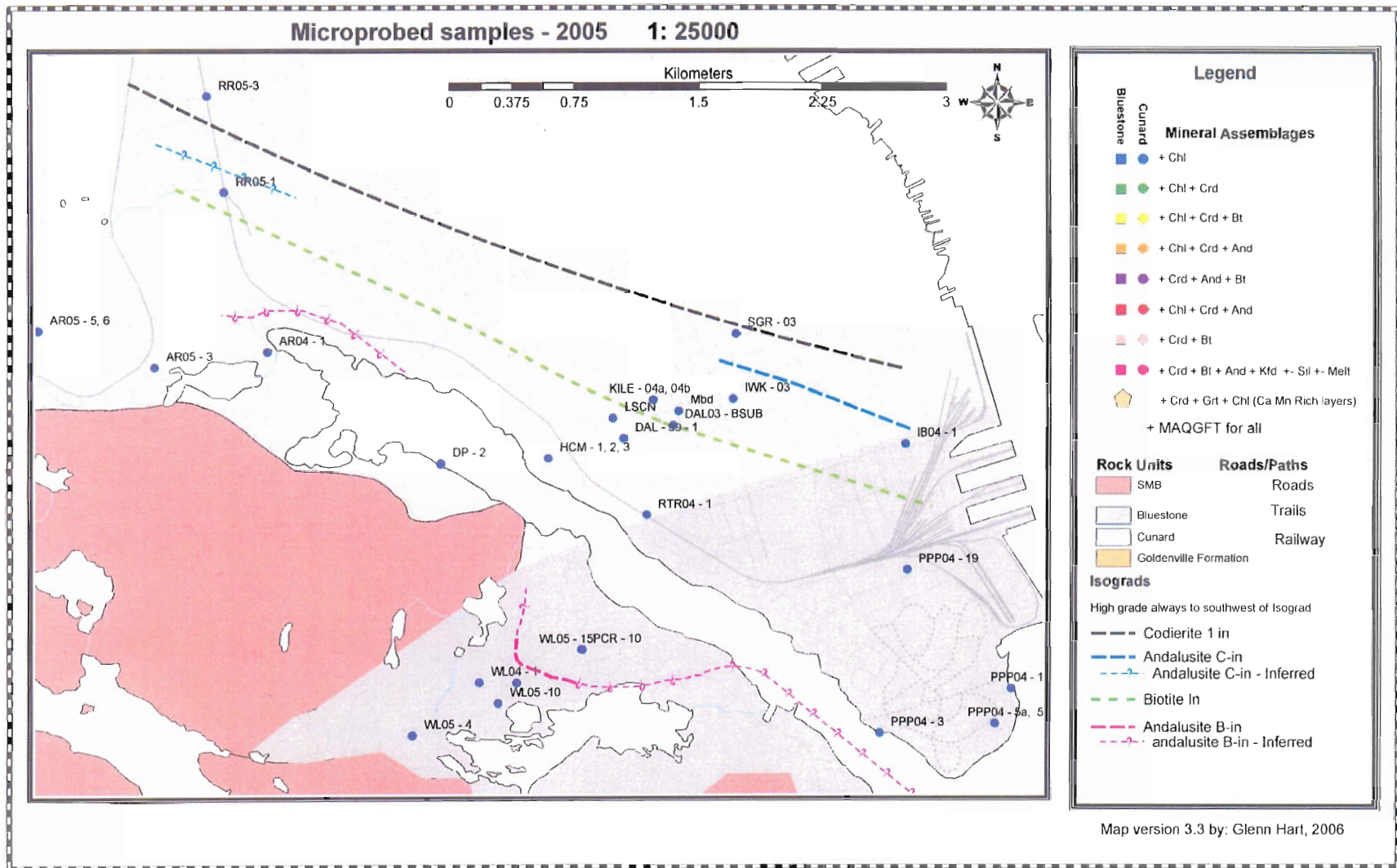


Fig C2: Showing sample locations which have been analyzed by microprobe for this study.

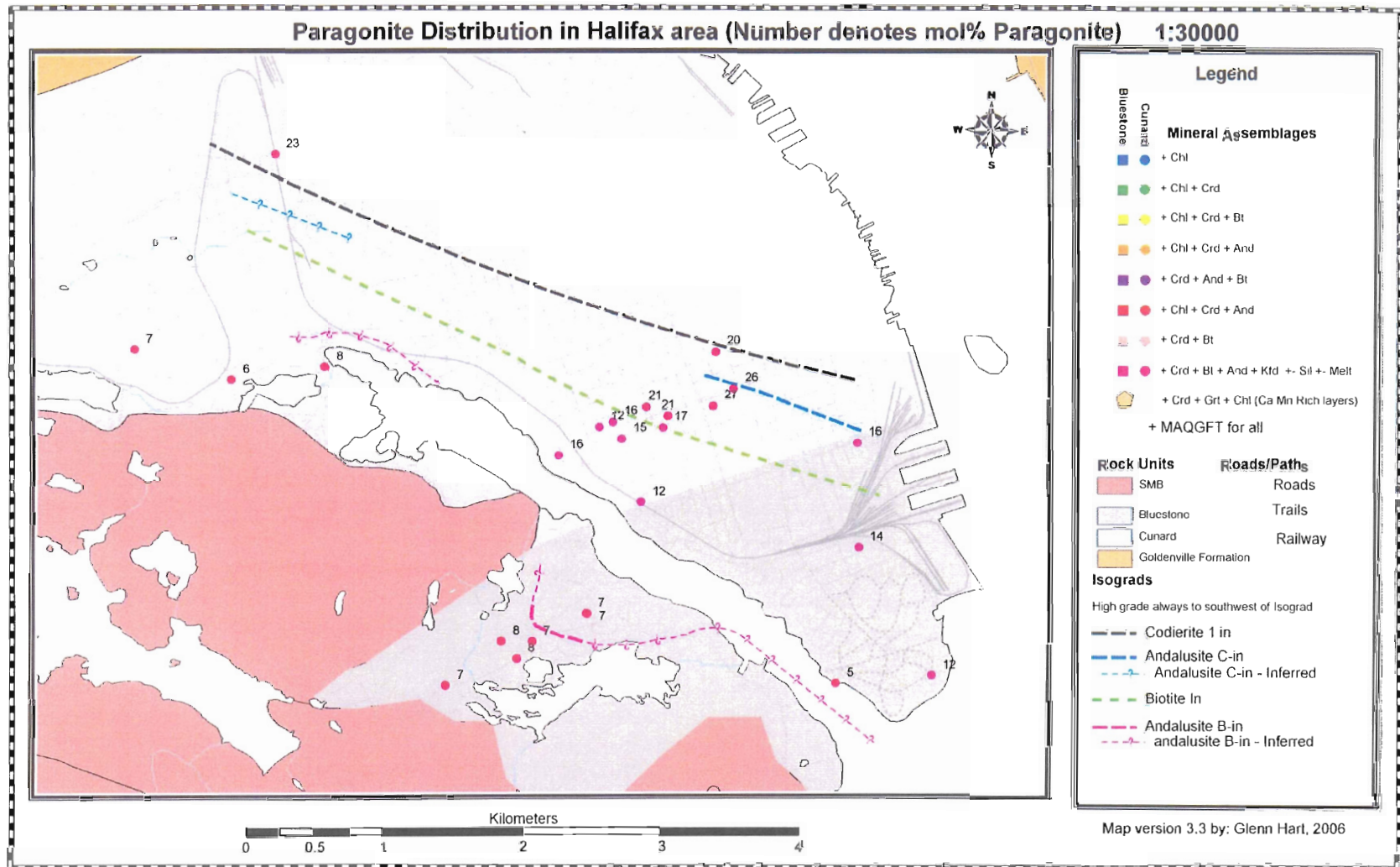


Fig C3: Mol% paragonite (in white mica) distribution in study area. Decrease in mol% Pa in Cunard Member samples proximal to contact. Lesser amounts in Bluestone member samples.

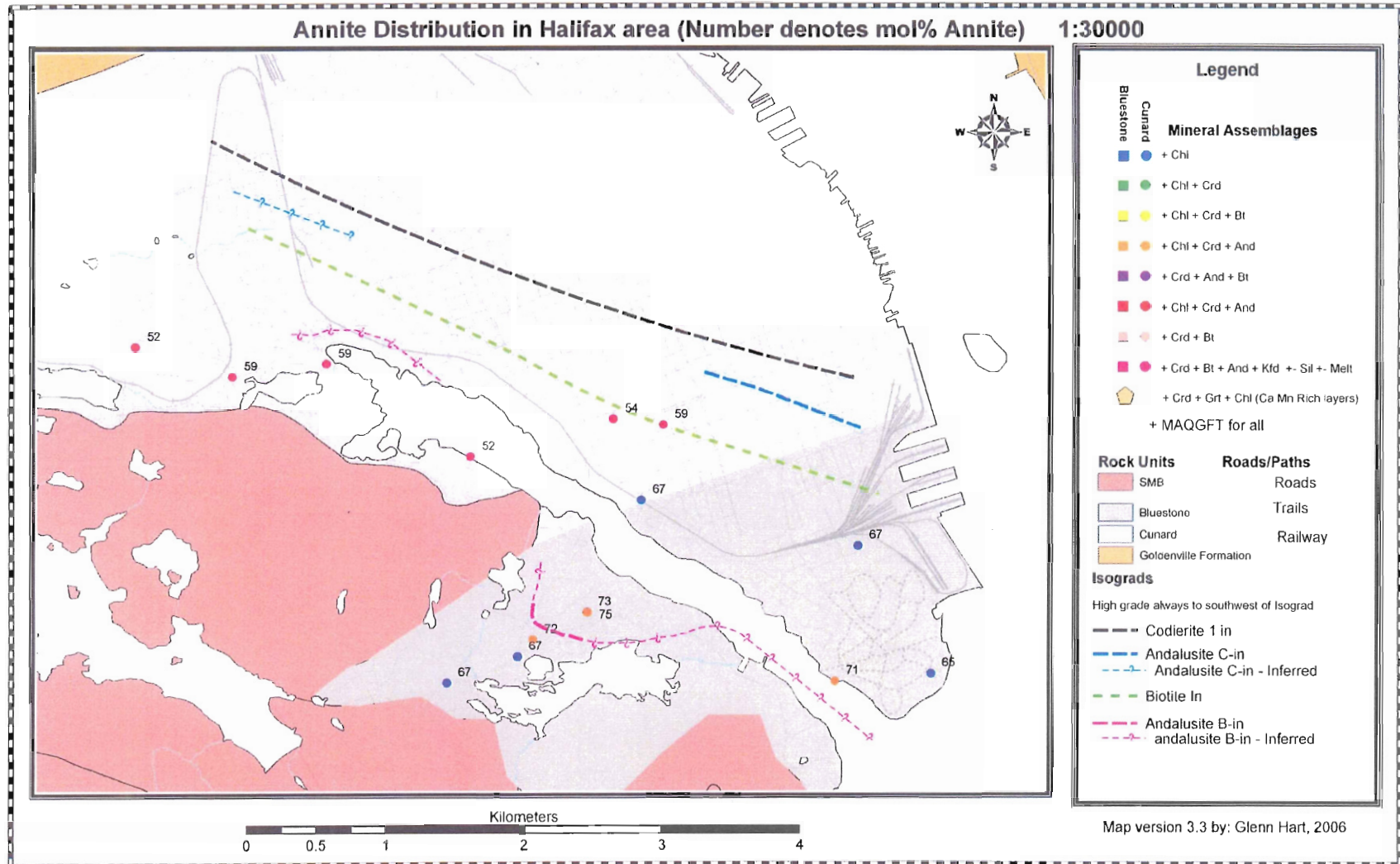


Fig C.4: X_{ann} (annite) content (in biotite) distribution in study area.

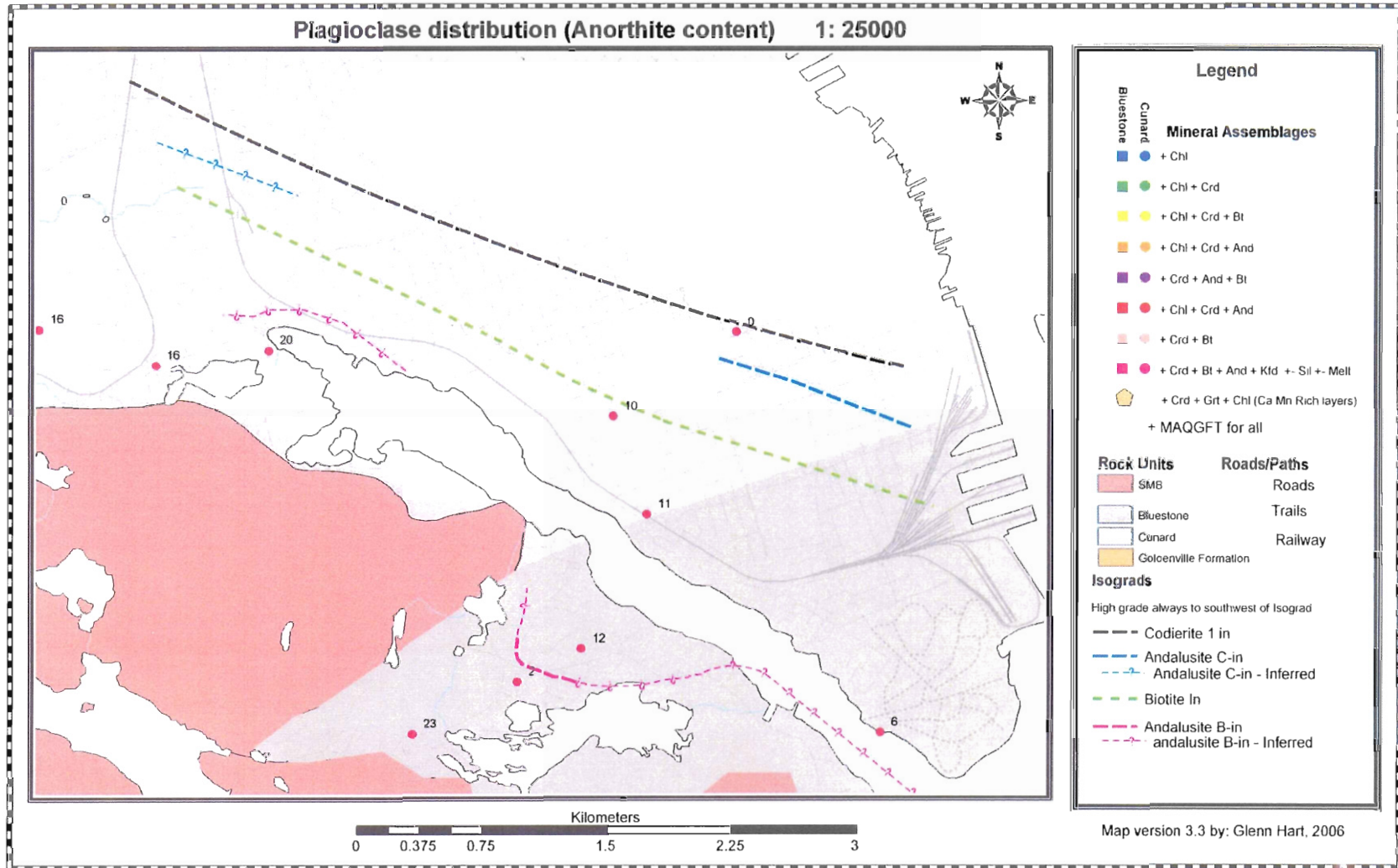


Fig C.5: Plagioclase distribution in study area. Sorted by % anorthite